Leveraging Enzyme Excretion Systems for the Cell-Free Synthesis of Lactic Acid

A Technical Report presented to the faculty of
the School of Engineering and Applied Science
University of Virginia

by

Collin Marino
Clare Cocker
Ethan Coleman
Gavin Estrella

On my honor as a student, I have neither given nor received
unauthorized aid on this assignment.

Clare Cocker, Ethan Coleman, Gavin Estrella, Collin Marino

Techinical advisor: Eric W. Anderson, Department of Chemical Engineering

May 10, 2024

Contents

1 Executive Summary

One promising way to optimize lies in the application of cell-free synthesis, a novel approach where the biological machinery typically confined within cells is extracted and used to directly convert feedstocks into end products. This departure from traditional methods has the potential to significantly enhance both efficiency and yield.

This report explores the feasibility of leveraging cell-free synthesis to produce lactic acid on a manufacturing scale. Lactic acid was selected due to its expansive market applicability, spanning pharmaceuticals, cosmetics, food and beverage, and biodegradable plastics.

Here, we designed an industrial-scale process to determine the effectiveness of lactic acid production using cell-free synthesis. This process is split into three sections: upstream unit operations, cell-free reactor, and downstream unit operations.

Upstream unit operations make the enzymes necessary to produce lactic acid. First, a seed train makes enough *B. subtillis* to inoculate nine 10,000-liter bioreactors. Once inoculated, these reactors will produce the necessary enzymes for the lactic acid. The cell-free reactor utilizes the enzymes from the upstream section and glucose to produce lactic acid. The temperature and pH of the reactors are controlled to ensure the optimal conditions of 50 degrees Celsius and a pH of 7. The cell-free reactor produces 25 million kilograms of lactic acid annually.

Once made, the lactic acid is sent to the last section of the process, the downstream unit operations. The first unit operation is the nanofiltration membrane system of 4 membranes used to recover enzymes. Recycled water is added to the feed of each membrane to keep the enzyme concentration low and prevent viscosity problems. The retentate stream of the membranes is sent through a different membrane to concentrate it for the cell-free reactor. The permeate streams of the nanofiltration system are sent to the next unit operation, the flash drum.

The flash drum uses 183 MW to vaporize some of the water in the product stream. The vapor from the flash drum is condensed and sent to the nanofiltration membrane system. The liquid from the flash drum's bottom is combined with sulfuric acid to lower its pH. This causes some of the sodium that was added in the cell-free reactor to precipitate as solid sodium bisulfate.

The product stream is sent through a sedimentation tank to remove this solid. This removes all of the sodium bisulfate that was created.

Afterward, the product stream is sent through a liquid-liquid extractor to remove byproducts that were created by the enzymes in the cell-free reactor. The extractor uses an organic solvent mixture of 12% trioctylamine and 88% octanol and recovers 97% of the lactic acid. The stream leaving out of the bottom of the extractor is treated and disposed of as waste. The stream leaving out of the top of the extractor is sent to the last set of unit operations, the three-column distillation cascade. The first column removes water, the second column removes octanol, and the third column removes trioctylamine. The removed octanol and trioctylamine are recycled back into the liquid-liquid extractor. The distillate of the third column is the final product, resulting in 23 million kilograms of lactic acid annually for the entire process.

This process has a total capital investment ($365 million). The total capital investment is spread over a two-year start-up period. Each year, 23 million kilograms of lactic acid are produced at $11.12 per kilogram. This creates a revenue of $253 million. The annual operating costs accumulate to $95 million for a gross income of $158 million each year. Over a plant life of twenty years, $2.1 billion dollars are accumulated at an IRR of 25%. Based on a multitude of factors including the novelty of the process, several key physical questions, and a preferred IRR of 40%, this project is economically not viable.

The main causes of this process's insufficiency are the large capital costs of the filter membranes in the downstream processing, along with the high power requirement of the downstream processing. The root cause of both costs is the low concentration of lactate at the outlet of the cell-free reactor. We do not recommend purifying enzymes on-site and feeding them directly into a cell-free reactor, as described in our process. Instead, immobilized enzyme technologies may be a much better way to leverage cell-free synthesis for future designs. Altogether, cell-free synthesis still remains a promising field that has the potential to revolutionize biomanufacturing in the decades to come. However, as of now, there are still many challenges that need to be overcome before widespread cell-free synthesis can be made feasible.

2 Introduction

2.1 Motivation and Background

Many industries are dependent on large quantities of biocommodities to continuously run their biochemical processes. Biocommodities, the cheap raw materials essential for almost every chemical and biochemical process, are inexpensive compared to high-value products. The cost is heavily reliant on the feedstock cost which accounts for 30 percent to 70 percent of production expenses.[1] One of the most versatile biocommodities in the current market is lactic acid which has applications in the pharmaceutical, cosmetic, food and beverage, and biodegradable plastics industries.[2] All of these industries are vital to standard products in American life. This already sophisticated market is expected to grow at a rapid rate. Lactic acid production was projected as a 3.5 billion dollar industry in 2022 and is projected to double by 2031 allowing for a well-designed, cheap production process to crack into the market.[3]

One of the cutting-edge methods to cheaply produce biocommodities is cell-free biocatalysis. Cell-free biotransformation is the use of several enzymes to create catalytic networks outside of microbial organisms for the production of biochemical products. Cell-free biotransformation was shown to increase product yield, improve process flexibility, and hasten reaction rate which will decrease the time required to produce commodities like lactic acid.[1] These enzymes are also recyclable without the downside of cell glucose consumption.[4] Results from anaerobic cell catalysis experimentation find that 10 percent of the feedstock is lost from the feed stream with more unconverted feedstock being consumed in recycle streams.[1] By removing cell consumption of feedstock in both the initial and recycled streams, the cost is decreased as the efficiency increases making cell-free catalysis a viable alternative to cell fermentation. Cell-free biotransformation also decreases the number of waste products because of enzyme pathway selectivity, if enzyme selection is effectively performed.[1]

The production of lactic acid still faces several constraints, the chief among them is waste production.[5] Waste production is accompanied by environmental restrictions that severely reduce allowable production and increase the cost compared to less sustainable and traditional alterna-

tives.[5] Cell-free biotransformations should reduce these lactic acid side product concerns, but complete elimination is not a reasonable expectation. Cell-free biotransformations also have less data than traditional cell fermentations.[1] Additional data may need to be gathered in this project to develop an efficient process that mitigates the side products and waste accumulating in lactic acid production. The aim of cell-free production of lactic acid is to reduce the cost of pure lactic acid mass manufacture so that we reduce the price of various medical, food, and plastic alternative products that consumers use daily.

2.2 Product Uses

The lactic acid (LA) market has a high demand for products in many industries such as food, cosmetics, and biopolymers.[2] Each industry has its requirements for the grade of LA it utilizes, thus the purity of lactic acid determines its market. For example, polymer-grade LA requires a high purity, 99 weight percent, product to be used in the polymerization of polylactic acid (PLA), whereas food-grade LA for applications in food acidification and antimicrobial packaging only requires an 88 weight percent product.[6] With 85 percent of the LA market demand stemming from the food industry, targeting the production of 88 weight percent LA will have the largest space for profitablilty.[2] The Food and Drug Administration recognizes LA as a generally recognized as safe (GRAS) product when produced from fermentation, thus it will be easy to adhere to regulations on the final food-grade product.[7]

2.3 Plant Capacity

Our process will produce 36 million kilograms of 88-weight percent lactic acid solution annually. This is about 1.4 times what is normally produced by an industrial plant (about 26 million kilograms per year).[8] There are three reasons for choosing this production scale. The first reason is that there are previous studies that have analyzed lactic acid production at this scale.[3,8,9] These studies contain data that we can use in our design and help inform decisions in the future. The second reason is that we want to determine if cell-free synthesis can be done at an industrial scale. By showing that we can economically produce this much lactic acid, we will be able to demonstrate the viability of cell-free synthesis to fermentation processes like the production of lactic acid. However, the novelty of this process is in the cell-free synthesis, allowing for

fewer purification steps to maintain standard purity as well as having greater yield per batch of enzymes as they are not limited by the cell's growth in fermentation as is standard now. The third reason is profitability. Lactic acid is a relatively cheap product compared to the amount of resources required to produce it, making it less profitable at smaller scales.[8] Because of this, lactic acid must be produced at an industrial scale, which is why our process produces so much lactic acid.

3 Discussion

In the following discussion, the design choices behind the proposed process will be described.

Figure 1: Overall process block flow diagram.

The process is separated into 3 sections, the upstream, cell-free reactor, and downstream processes as summarized in the following block flow diagram, Figure 1. A full process flow diagram can be found in Appendix A1 and A2. Additionally, notes on the nomenclature used in the process diagrams can be found in Appendix A3.

3.1 Upstream

3.1.1 Enzyme Production

3.1.1.1 Cell Acquisition

The process begins with the fermentation of *Bacillus subtilis* to produce enzymes needed for the subsequent cell-free reactor. To achieve most efficiently, the strain of *B. subtilis* we aim to use requires manipulation via advanced synthetic biology. However, this is out of the scope of our design. The bioreactor design assumes synthetic biologists will be able to provide a starter culture consisting of the following characteristics:

- The genes encoding each of our enzymes will be inserted into the DNA of our bacteria, coding to produce each enzyme in the correct ratio and conformation needed for the cell-free pathway.

- The enzymes produced during fermentation will be excreted using the CITase pathway.[10] This enables enzymes to be released into the surrounding media, removing the need for a cell lysis unit operation for enzyme harvesting.
- The bacteria will have been engineered to not need an inducer to begin producing our target enzymes.
- Our co-factor, NAD+, will be co-exported from the bacteria alongside our enzyme, in the necessary ratio for the enzyme pathway.

3.1.1.2 Growth Kinetics

B. subtilis has been studied under various growth conditions and has been used to produce a range of products. We will utilize a model based on the work of Stamenković-Stojanović et al.[11,12] The fermentation was carried out under the following conditions: 37°C, 10 g/L glucose, 8 g/L nutrient broth. It is worth noting that while the model selected had the most complete kinetic data, there is other promising research describing alternative growth mediums of interest. One medium of particular interest is sugar cane bagasse due to its cost-effectiveness as a cheap waste product.[13]

The growth curve from Stamenković-Stojanović et al.'s work[11] was fit to the equation 1 using the least squares method to approximate its shape. The final values for the parameters were A=6.198 [g/L], k=0.008 [1/hr], and n=2.079, where $X(t)_{fit}$ is cell mass concentration [g/L] and t is time [h]. These values do not represent a physical property but provide an equation for *B. subtilis's* growth under these conditions. The fit captured the shape of the growth curve fairly well as seen in Figure 2, despite r^2 being only 0.45.

$$\mathrm{X_{fit}}(t) = A(1 - e^{-kt^n}) \tag{1}$$

Protein production had a theoretical maximum estimated from Kawabata et al.'s work,[10] demonstrating that protein excretion systems can produce up to 80 g/L of protein. However, to ensure a balanced material balance, the actual estimated amount of protein produced was determined by optimization based on CO_2 production as described in Appendix A5.

Table 1: Kinetic Parameters for *B. subtilis*. Xo is initial cell concentration, Po is initial protein concentration, $Y_{X/S}$ is biomass to substrate yield, $Y_{P/S}$ is protein to substrate yield, and $\mu_{\max}$ is the maximum growth rate. Additionally, X, S, and P is the cell, substrate, and protein product concentrations, respectively.

Parameter	Xo $\frac{g}{L}$	So $\frac{g}{L}$	Po $\frac{g}{L}$	$Y_{X/S}$ $\frac{g}{g}$	$Y_{P/S}$ $\frac{g}{g}$	$\mu_{\max}$ $\frac{1}{h}$	K_s $\frac{g}{L}$	K_i $\frac{g}{L}$
Value	0.35	10	0	0.78	0.73	0.273	2.325362	2.537149

Next, using the fit equation and the following kinetic parameters in table 1 calculated from Stamenković-Stojanović et al.'s work,[11] cell growth (X), substrate consumption (S) were fit to model the fermentation. The method of least squares was used again to solve for optimal K_s and K_i values, as they were not reported in the literature. The equations used were as follows with Y being yield coefficients, K_s being the saturation constant, and K_i being the inhibitory constant:

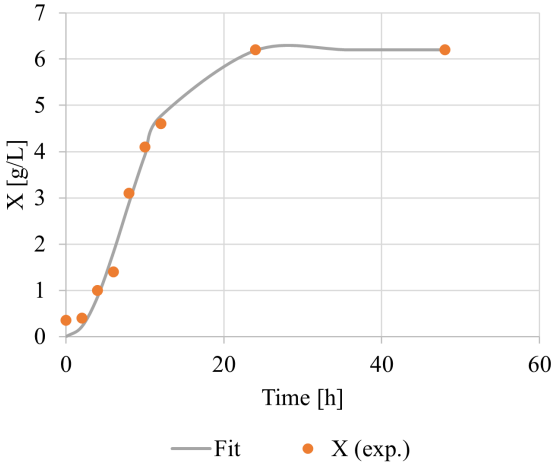

Figure 2: Experimental values from Stamenković-Stojanović et al.'s work[11] compared to the fit equation 1.

$$\mathrm{t}_n = \ln\left(\frac{\frac{x_{(n-1)}}{x_n}}{\mu}\right) + t_{(n-1)} \tag{2}$$

$$\mathrm{X} = Y_{\frac{X}{S}}(S_0 - S_n) + X_0 \tag{3}$$

$$\mathrm{P} = Y_{\frac{P}{S}}(S_0 - S_n) \tag{4}$$

$$\mu_n = \frac{\mu_{max} S_n}{K_s + S_n} \ln\left(\frac{S_n}{K_i}\right) \tag{5}$$

Note that equation 5, for μ is not a typical Monod equation. Adding the natural log allowed for the agreement with the substrate limitation reported in the model study. K_i and K_s were optimized to 2.54 g/L and 2.33 g/L respectively. The resulting growth curve is in Figure 3.

At this glucose concentration, the degree of enzyme production would not be sustainable for our process. Therefore, the concentration was increased from 10 g/L to 80 g/L. This required

the k_La to be scaled from the literature value of 45 1/hr.[12] Using the worst-case scenario for oxygen consumption (where the oxygen uptake rate, OUR_{max}, is equal to the oxygen transfer rate, OTR), we back-calculated the biomass to oxygen consumption ratio, $Y_{O_2/S}$. Using this and the new maximum biomass concentration produced from 80 g/L of glucose, the k_La was scaled from 45 1/hr to 177 1/hr as calculated in Appendix A6.

Media was handled uniquely in this design. Realistically, media is required for growth and production of protein in microbes. However, the initial mass balance completed for biomass growth did not incorporate the impact of media on growth, rather it depended solely on the presence of the substrate glucose. Adding media into the overall mass balance of the upstream, specifically around the production bioreactor, the additional mass was ”converted” to biomass. This material balance edit is outlined in Appendix A5. Additionally, all media was assumed to be completely consumed in the bioreactor. This assumption should be revisited as media realistically is not fully consumed and would be present in downstream purification. It is likely a buffer exchange unit would need to be added to remove additional media before entering the cell-free reactor, though with the current assumption, this is out of scope.

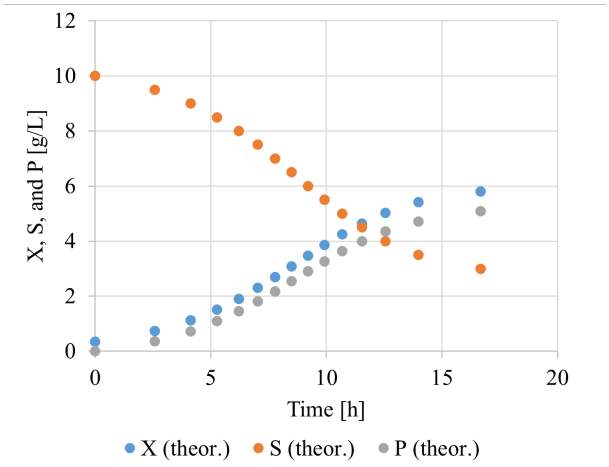

Figure 3: Summary of modeled *B. subtilis* based on Stamenković-Stojanović et al.’s work,[11] where in 16.67 hours, the cell density reached 5.81 g/L, consuming 70% of the available glucose, and yielding 5.08 g/L of enzyme. Further growth metrics are available in Appendix A4.

The actual concentration of media will be 1:1 with respect to glucose, so 80 g/L of media. The makeup of this media will be similar to the difco sporulation medium (DSM) used in Stamenković-Stojanović et al.’s work.[12] The full composition is outlined in Appendix A7, though it is mainly beef extract, yeast extract, peptone, and NaCl as well as some trace salts.

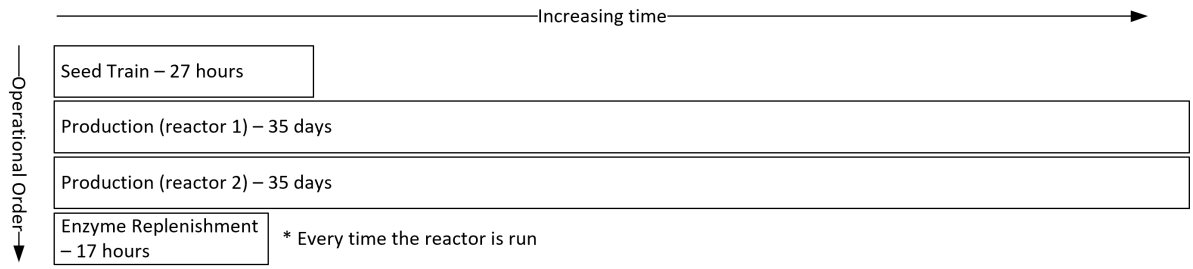

Figure 4: Overview of upstream bioreactor process.

3.1.1.3 Bioreactor Cascade Production of Enzyme

The cell-free reactor requires 150 g/L of bulk enzyme, therefore *B. subtilis* will be fermented in a series of bioreactors to provide enough enzyme mass to fill the cell-free reactor to the set concentration. However, the bioreactors create a dilute solution that requires concentration to reach the desired set point. Figure 4 provides a summary of this series of bioreactors that will be described below. The design equations utilized in the bioreactor design are outlined in Appendix A8. Additionally, a full process flow diagram for the upstream portion of this process (both fermentation and purification) can be found in Appendix A1.

3.1.1.4 Seed Train

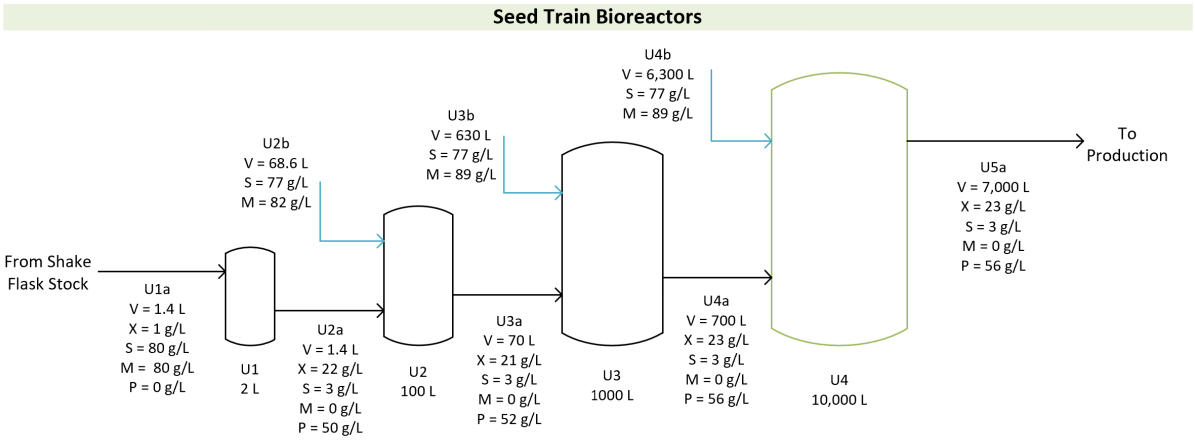

Figure 5: Process flow diagram for the seed train with concentrations of cells, glucose, media, and enzymatic product denoted as X, S, M, and P respectively. The streams at the top of the reactors increase the volume of liquid within the reactor, diluting the input stream and creating space for the cells to proliferate.

The first step in the upstream process will consist of four bioreactors making up the seed train to produce enough biomass to inoculate multiple 10,000 L production scale reactors. This

will only occur once a year before the process start-up. The bioreactor order will be small (U1), medium (U2), large (U3), and production scale (U4) at 2, 100, 1,000, and 10,000 L respectively. Each reactor will have 80 g/L of glucose as substrate and is designed to reach the target k_La of 177 1/hr. The specific design of each reactor is outlined in Table 2 with the reactor dimensions following the specifications in 6. All reactors will only be filled to 70% working volume to account for head space in the reactor. The reactor will be kept at 37°C and a pH of 7, though the pH is not predicted to change significantly, thus no design of pH control has been included. Air will be supplied as opposed to pure oxygen. The reactors are also designed with only one Rushton impeller for mixing and are equipped with 4-baffles. Moving farther along in the seed train to larger reactors, the cell-dense media of the previous reactor will be diluted with a solution of media, water, and glucose as denoted in the additional streams in Figure 5. The seed train step will take a total of 26.2 hours and will be conducted in batch mode.

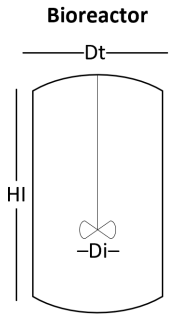

Figure 6: Generalized dimension variables for bioreactor design.

3.1.1.5 Enzyme Production Cycles

With enough cell biomass created to inoculate a large-scale fermentation, a series of fermentations will be carried out for 35 days to produce the enzyme needed for the cell-free reactor. This stage will only occur during start-up once a year and will be carried out twice to provide for the two cell-free reactors that will run in parallel. The series is made up of nine 10,000 L reactors (U4 and U5.2-9). Eight (U5.2-9) will be used strictly for enzyme production and will feed into later purification steps, while one reactor (U4) will be used as a culture reactor that will re-inoculate the other eight reactors after being held temporarily in a storage tank, S5.

Each run of the 9 reactors is considered a cycle yielding 440 kg of enzymes per cycle per reactor for a total of 3,516 kg of enzyme. It takes 101 cycles over 36 days to fill one cell-free reactor with 355,102 kg of enzyme. Plant start-up requires 2 filled cell-free reactors, which is accomplished via 202 cycles over 72 days yielding a total of 710,204 kg of enzyme. Each cycle time includes 5.6 hours of fermentation time and 3 hours of processing time between cycles for cleaning and refilling of the reactors. The 10,000 L bioreactors share the same design as the

Table 2: Design specifications for all upstream bioreactors. The design equations used to specify these equations can be found in Appendix A8.

Equipment	Identifier	Volume	Working Volume	Tank Diameter	Tank Height	Tank Area	Impeller Diameter	Mixing Rotation	Oxygen Transfer Coefficient	Air Flow	Agitation Power	Batch Time
		V [L]	Vw [L]	Dt [m]	HI [m]	At [m^2]	Di [m]	N [RPM]	kLa [1/hr]	Qg [vvm]	Pg [W]	t [hr]
2 L Bioreactor	U1	2	1.4	0.14	0.14	0.01	0.05	1,050	176.8	0.007	3.7	6.83
100 L Bioreactor	U2	100	70	0.25	0.25	0.05	0.08	600	176.8	0.014	14.3	7.82
1,000 L Bioreactor	U3	1,000	700	1.08	1.08	0.92	0.36	250	176.8	0.037	1,581	5.84
10,000 L Bioreactor	U4	10,000	7,000	2.34	2.34	4.28	0.78	200	176.8	2.994	37,565	5.58
10,000 L Bioreactor	U5.2-9	10,000	7,000	2.34	2.34	4.28	0.78	200	176.8	2.994	37,565	5.58

production-scale reactor and this stage's overview is outlined in Figure 7 and Table 2.

The three hours between cycles will drain out spent broth, spray clean and drain the reactor, sterilize the growth medium, and load in the inoculum. The first 60 minutes will drain the fully reacted reactors into the centrifuge as the desired separation will be conducted in one hour. Next, for 20 minutes, spray devices will wash the inside of the reactor, satisfying a clean-in-place design.[14] The design of this cleaning step is out of the scope of this design. After that 30 minutes will be dedicated to loading water and solids into the reactor, solids being media powder and glucose from storage silos. These silos will accommodate 4 weeks or 79 cycles worth of solids, estimated to be about 340,648 kg of glucose or 218,545 L. With this estimate, four 100 m^3 silos will house the glucose and nutrient broth powders, 2 for each substance. To deliver the solids to the fermenters, each will be equipped with 10 ft screw conveyors that can be easily maneuvered and connected to the desired reactor. For ease of process description, the glucose and media will be described in the blue "water" streams, not the screw conveyor streams in the process flow diagram and stream tables. This is due to the variable flowrates that the screw conveyors use.

Once the water and solids have been introduced to the reactors they will be mixed and heated to sterilization. The Center for Disease Control recommends sterilizing for "4 minutes at 132°C".[15] So, assuming a well-mixed heating of the reactor via built-in electric heaters, to reach 132°C from room temperature in 30 minutes, will require 1,596 kW of power via equation 6.[16] Cooling the reactor from 132°C to the working temperature of 37°C will take approximately 31 minutes according to equation 7 using water in a cooling jacket, included in the purchased vessel.[17] After

the reactor has cooled, approximately 8 minutes remain between cycles for flexibility.

$$\text{k}W = \frac{M \cdot Cp \cdot (T_2 - T_1)}{t \cdot 3,600 \cdot 1,000} \tag{6}$$

Equation 6 variables: M is the weight of media, glucose, and water [kg]. C_p is the specific heat of water [J/kg C]. T_1 and T_2 are the initial and final temperatures of the fluid [C]. The t is the time to heat the reactor [hr]. This equation solves for kW which is wattage.

$$\theta = \ln\left(\frac{T_1 - t_1}{T_2 - t_1}\right)\left(\frac{M \cdot C_p}{U \cdot A}\right)\left(\frac{1}{3,600}\right) \tag{7}$$

Equation 7 variables: The t_1 is the temperature of the cooling fluid [C]. T_1 and T_2 are the initial and final temperatures of the fluid [C]. U is the overall heat transfer coefficient of the coolant (water in a jacketed reactor) [W/m^2C], estimated to be 1,000 W/m^2C.[17] A is the heat exchange area of the coolant [m^2]. M is the weight of media, glucose, and water [kg]. C_p is the specific heat of the fluid [J/kg C]. θ is the time required to cool down the tank [hr].

During the fermentation, the temperature is maintained at 37°C. To account for this heat, we accounted for 4 factors: 1) heat contributed by agitation in equation 9, 2) heat contributed from microbe growth in equation 8, 3) heat loss due to evaporation in equation 10, and 4) heat loss due to convection cooling of the fermenter in equation 11. During one fermentation, the $Q_{agitation}$ provided 37.6 kW, the Q_{growth} provided 2.4 kW, the $Q_{evaporation}$ removed 14.8 kW, and the $Q_{tankloss}$ removed 26.2 kW, leaving essentially negligible net heat accumulation. This assumption of balanced heating and cooling would need to be validated with heat transfer coefficient measurements of the cell broth and tank to ensure heat requirements are met in later studies. A glycol coolant system could be installed if the heat is no longer negligible.

$$\text{Q}_{growth} = 0.00014 \cdot OUR \cdot V_w \tag{8}$$

Equation 8 variables: OUR is the maximum oxygen utilization rate [mmol O_2 / L hr]. The 0.00014 factor converts the mmol O_2/hr to kJ/s.[18] V_w is the working volume of the reactor [L].

Q_{growth} is the heat produced from cell growth [kW].[18]

$$\mathrm{Q}_{agitation} = \frac{P_g}{1,000} \tag{9}$$

Equation 9 variables: P_g is the power required to aerate the gassed fluid [W].[18] P_g is obtained during bioreactor design, as explained in Appendix A8. $Q_{agitation}$ is the heat produced due to agitation [kW].

$$\mathrm{Q}_{evaporation} = -\dot{M_g} \cdot \dot{X_{H_20}} \cdot \Delta H \tag{10}$$

Equation 10 variables: Evaporation removes heat, so the equation is negative. $\dot{M_g}$ is the molar flowrate of supplemented air [mol_{air}/s]. X_{H_20} is the saturation mole fraction [mol_{H_2O}/mol_{air}] of water at 37 C, which is equal to 6.2%. ΔH is the enthalpy of vaporization [kJ/mol_{H_2O}], which is 40.65 kJ/mol_{H_2O}. $Q_{evaporation}$ is the heat loss due to evaporation [kW].

$$\mathrm{Q}_{tankloss} = -A \cdot h_c \cdot \Delta T \tag{11}$$

Equation 11 variables: Heat loss through the tank walls removes heat, so the equation is negative. A is the surface area of the tank [m^2]. h_c is the convective heat transfer coefficient of the tank [kW/m^2K], which for free convection of air is estimated as 0.06 kW/m^2K.[19] ΔT is the difference in temperature between the broth inside (310 K/37 C) and the air outside the tank (293 K/20 C) [K]. $Q_{tankloss}$ is the heat loss due to convection outside the tank [kW].

3.1.1.6 Enzyme Replenishment During Normal Operation

During normal operation, it is expected that roughly 2% of the bulk enzyme (about 4,500 kg of enzyme per reaction) will need to be replaced after each cell-free reaction due to degradation of the enzymes. Accounting for this loss, an enzyme "make-up" stage will be conducted in parallel with the cell-free reactor. Using the same cycle design as described above, two cycles will be run to resupply the lost 4,500 kg of enzyme. With each cycle taking 5.6 hours and 3 hours allotted for cleaning and filling, it will take just over 17 hours to replenish the enzymes during normal operation. This leaves roughly 5 hours for purification before the next cell-free reaction begins. Each cycle will also require an input of 4,312 kg of glucose.

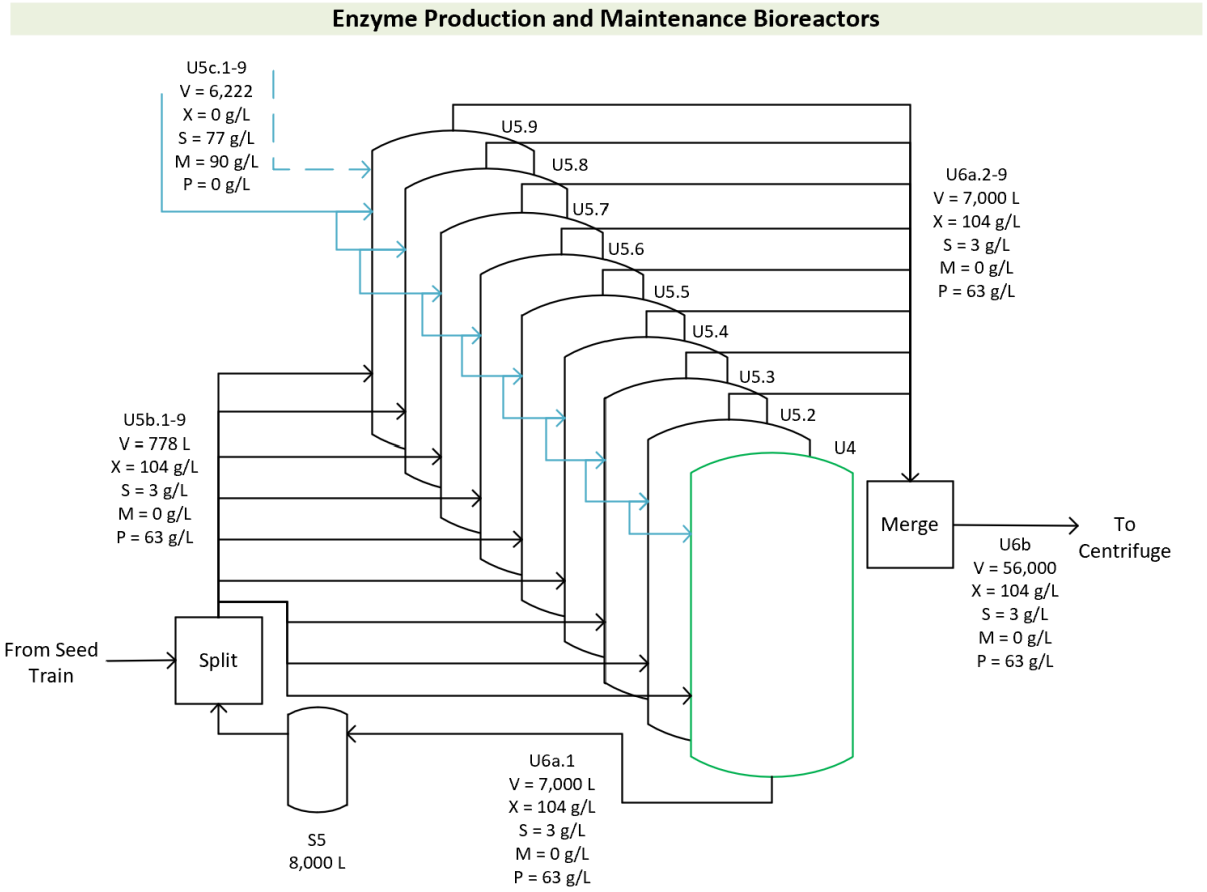

Figure 7: Process flow diagram for the production reactors during plant start-up and normal plant operation (replenishment). Again the streams at the top of the reactors increase the volume of liquid within the reactor, diluting the input stream and creating space for the cells to proliferate. Cells, glucose, media, and enzymatic product concentrations are denoted as X, S, M, and P respectively. Note the division of the inoculation streams into the other reactors and the mixing of the output enzyme streams before continuing to the purification steps.

These replenishment cycles cannot be directly added into the cell-free reactor as the reactor will either be busy converting glucose to lactic acid or draining downstream. To keep the process continuous, these cycles will be temporarily stored in a storage tank, CF3, which will also hold enzyme recycle streams until a cell-free reactor is free to be filled.

3.1.2 Purification

3.1.2.1 Disk Stack Centrifuge

Next, the outlet stream of the production bioreactor must be purified to remove the cells from the enzyme product. By utilizing the excretion system *B. subtilis* and assuming its optimization, there should be minimal contaminants in the resulting supernatant stream. The outlet stream, U6b, will have a flowrate of 56,000 L/hr, so a disk stack centrifuge (U6) will separate these components. Disk stack centrifuges were selected to allow for the high throughput necessary. The centrifuge is designed with inner and outer radii of 0.45 and 0.50 m respectively. The half-cone angle is 45 degrees and there will be 50 stacks in the centrifuge.

Using these design parameters the following design was calculated: a sigma value of $8.1x10^{-6}$ m/s, a required angular velocity of 894.5 RPM, and a power input of 37.53 kW (see Appendix A10 for design equations). The output streams of this centrifuge were determined by assuming an 85% v/v cell composition in the sludge stream. Additionally, it was assumed that the concentration of enzymes and glucose would remain the same in all streams. The final separation of the inlet streams is described in Figure 8, resulting in a 63.7% enzyme yield in the supernatant stream. The cellular waste sludge from the centrifuge will be taken to S6, which is an incinerator. The design of this device is out of the scope of this project. However, once the sludge is burnt, it will be removed as solid waste.

It is worth noting that the complete removal of cellular waste is an ideal assumption, while not completely realistic. In the future design of this process, additional polishing steps to remove fermentation contaminants should be considered. Additionally, the assumption of treating the sludge as a liquid should be reevaluated as the density of the cells will likely have it behave more like a very viscous solution. Finally, the enzyme solution will likely contain small molecules and other enzymes, which may need to be further purified before continuing to the cell-free

reactor.

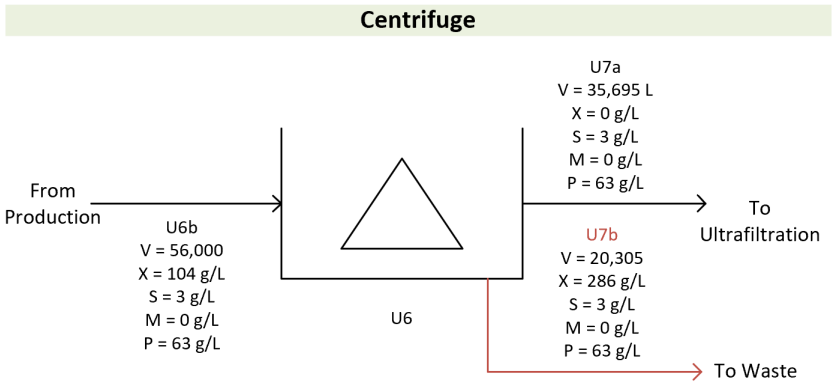

Figure 8: Process flow diagram for the centrifuge. The red line is the ”sludge” that will be removed and treated as waste. The top outlet stream will continue to the next stage in purification. Further breakdown of the streams can be found in Appendix A3

3.1.2.2 Ultrafiltration

The output from the centrifuge will have a lower concentration of protein than will be used in the cell-free reactor. To account for this, the protein-containing stream, U7a, will be condensed from 63 g/L to 176 g/L of bulk enzymes using an ultrafiltration membrane (U7). The actual concentration in the cell-free reactor is 150 g/L, but the addition of water and glucose will dilute this stream as it enters the reactor, so a higher concentration is required. The membrane will have a molecular weight cut-off of 150-300 Da as all target enzymes have a larger molecular weight. This will enable the assumption of complete rejection of the enzymes ($\sigma_p = 1$) while allowing water to not be rejected at all ($\sigma_w = 0$). Additionally, these streams will contain glucose, which will have the rejection coefficient of $\sigma_g = 0.185$.[20] The membranes utilized by our process are linearly scaled from the membranes designed by Alexandri et al.[20] In their work, they designed a 1.7 m^2 membrane for a batch volume of 113.5 L. The batch volume through our membrane will be 35,695 L, which linearly scales the membrane area to 534.64 m^2. The resulting separated flowrates were calculated using the design equation 12. The final flowrates are outlined in Figure 9. The concentration factor (CF) for the enzymes is 3.02, the CF for glucose is 1.23, the permeate flux is 66.76 L/m^2hr, and the differential pressure is 3 bar. The feed pressure in stream U7a is 30 bar, and the retentate (stream U8a) and permeate (stream U8b) pressure is 27 bar in each. The system is then depressurized back to atmospheric pressure when released into storage vessels. Further stream details for the ultrafiltration unit can be found in

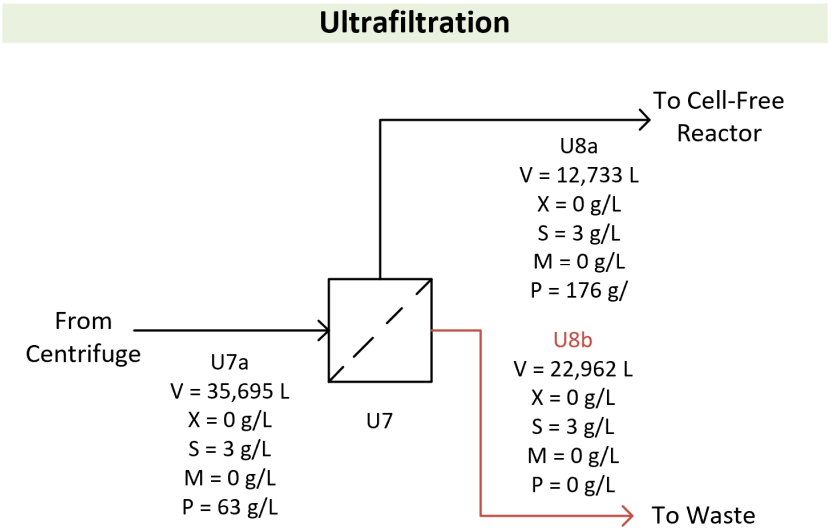

Figure 9: The process flow diagram for the ultrafiltration unit. U8a is the retentate (concentrated proteins) and U8b in red is the permeate (excess solution).

Appendix A4. Following ultrafiltration, the separated enzymes will be held in a storage tank before entering the cell-free reactor.

$$\frac{C}{C_0} = (CF)^{\sigma_p} = \left(\frac{V_0}{V}\right)^{\sigma_p} ; \; V_{U8b} = V_{U7a} - V \tag{12}$$

Equation 12 variables: C is the final desired concentration of enzymes and C_0 is the initial concentration of enzymes [g/L]. cF is the concentration factor of the enzymes. σ_p is the partition coefficient for the enzymes. V is the final solution volume to achieve the desired concentration factor and V_0 is the initial volume of the input solution [L]. Additionally, the secondary equation is a volume balance around the ultrafiltration unit (where V is V_{U8a}).

3.1.2.3 Potential Upstream Improvements

It is worth noting that the upstream portion in its current state is not fully optimized. Most of the aforementioned assumptions would benefit from additional experimentation to confirm their validity. Also, all fermentations were operated as a true batch operation. In the future, utilizing a fed-batch operation could increase the cell growth and, thus, the production capabilities of the fermentations. This could reduce the need for multiple production-scale bioreactors. Additionally, all reactors will have their temperature maintained via electric heaters and cooled by a water jacket. With more design, a more efficient heating and cooling regimen could be designed

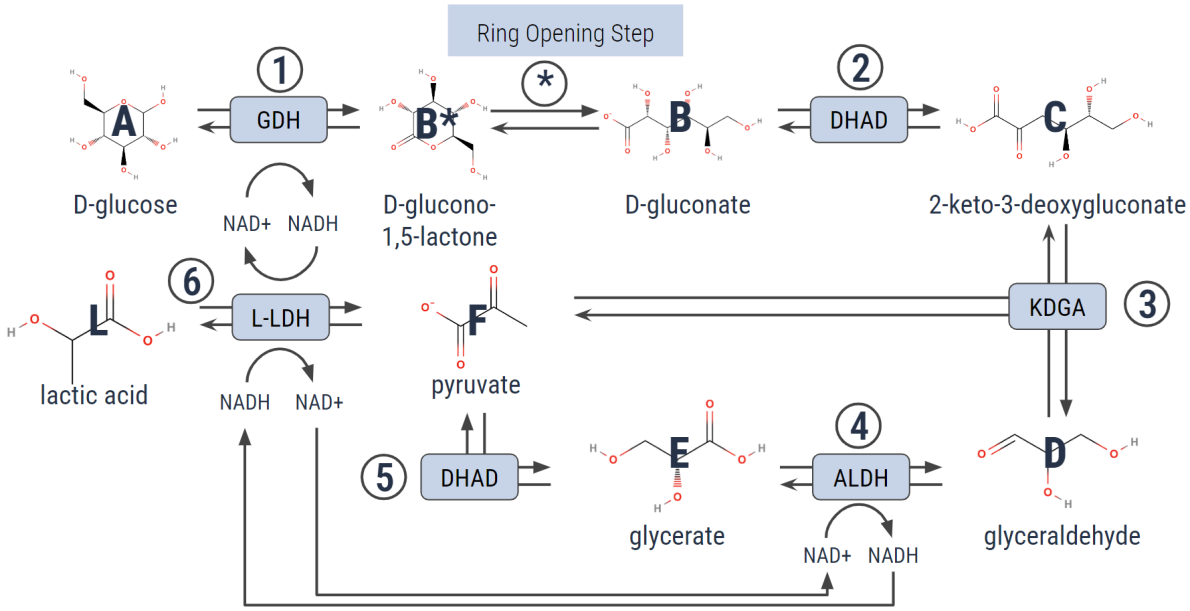

Figure 10: Enzymatic pathway overview. The main reactor in this lactic acid plant is a cell-free reactor that uses 5 enzymes, GDH, DHAD, KDGA, ALDH, and L-LDH to catalyze the seven-step conversion from D-Glucose to L-Lactate. Each compound in the pathway is given its own letter, and each enzyme-catalyzed step is given its own number. The step between 1 and 2 is referred to with an asterisk to denote that it is the only non-catalyzed step in the pathway.[21]

using cooling water and steam from other parts of the process.

3.2 Cell-Free Reactor

3.2.1 Reactor Kinetics

To make predictions about the efficacy of various reactor configurations, a kinetic model was developed based on the reaction pathway shown in Figure 10. The kinetic description of this pathway is shown in Equations 13 through 29.

In equations 13 - 29 all capital K parameters of the form K_{iA} represent the Michaelis-Menten parameter of species A in step i. Similarly, all parameters of the form $k_{cat,i}$ represent the k_{cat} value of the enzyme-catalyzed reaction step i. Finally, square brackets denote the concentration of a species. The lettering convention of the species and the numbering convention of steps is consistent with Figure 10. These equations were derived primarily from Michaelis-Menten and Ping-Pong kinetics[22,23] with the only exceptions being equations 24, 25 and 28. However, in all cases following reversible Ping-Pong kinetics, a simplified version of the mechanism was used,

in which case the reverse steps were approximated as one-directional Ping-Pong kinetics in both directions, as opposed to the more formal definition commonly used in the literature.[23] This simplifying assumption was necessary to reduce the number of parameters needed for each reaction step. Additionally, the resulting kinetic equations derived under this assumption reduce to the same form as the true bidirectional ping-pong mechanism when either the forward or reverse direction is dominating. Because the concentrations of intermediates throughout the pathway are found to be very low in experimental studies,[21] this assumption is justified. Additionally, some of the reverse reactions were neglected altogether, as experimental data indicate that the build-up of the intermediates that would undergo these reverse reactions is negligible throughout a batch reaction. As such, only equations 23,24,28 and 29 were treated as reversible.

As mentioned, the kinetics that govern the equations 24, 25, and 28 were not modeled using standard enzyme kinetics. The kinetic step described in Equation 24 is not enzyme-catalyzed, as it describes a spontaneous ring-opening ester hydrolysis. Existing experimental data show that this reaction follows pseudo-first-order kinetics with a known rate constant.[24] Finally, equations 25 and 28 were derived from a custom kinetic mechanism following a derivation similar to that of traditional Michaelis-Menten kinetics, but which incorporates the fact that Steps 2 and 5 in the reaction pathway are catalyzed by the same enzyme. As such, species E and F inhibit reaction 2 while species B inhibits reaction 5. The full derivation of this mechanism is shown in Appendix Figure A11.

$$\frac{\partial[A]}{\partial t} = -r_1 \tag{13}$$

$$\frac{\partial[B*]}{\partial t} = r_1 - r_* \tag{14}$$

$$\frac{\partial[B]}{\partial t} = r_* - r_2 \tag{15}$$

$$\frac{\partial[C]}{\partial t} = r_2 - r_3 \tag{16}$$

$$\frac{\partial[D]}{\partial t} = r_3 - r_4 \tag{17}$$

$$\frac{\partial[E]}{\partial t} = r_4 - r_5 \tag{18}$$

$$\frac{\partial[F]}{\partial t} = r_3 + r_5 - r_6 \tag{19}$$

$$\frac{\partial[L]}{\partial t} = r_6 \tag{20}$$

$$\frac{\partial[NAD]}{\partial t} = r_1 + r_4 - r_6 \tag{21}$$

$$\frac{\partial[NADH]}{\partial t} = -r_1 - r_4 + r_6 \tag{22}$$

$$r_1 = \left(\frac{k_{cat,1}[A][NAD]}{K_{1A}[NAD] + K_{1NAD}[A] + [A][NAD]} - \frac{k_{cat,-1}[B*][NADH]}{K_{-1B*}[NADH] + K_{-1NADH}[B*] + [B*][NADH]}\right)[GDH]_0 \tag{23}$$

$$r_* = k_*[B*] - k_{-*}[B] \tag{24}$$

$$r_2 = \left(\frac{k_{cat,2}K_{5E}K_{-5F}[B]}{K_{5E}K_{-5F}[B] + K_{2B}K_{-5F}[E] + K_{2B}K_{5E}[F] + K_{2B}K_{5E}K_{-5F}}\right)[DHAD]_0 \tag{25}$$

$$r_3 = \left(\frac{k_{cat,3}[C]}{K_{3C} + [C]}\right)[KDGA]_0 \tag{26}$$

$$r_4 = \left(\frac{k_{cat,4}[D][NAD]}{K_{4D}[NAD] + K_{4NAD}[D] + [D][NAD]}\right)[ALDH]_0 \tag{27}$$

$$r_5 = \left(\frac{K_{2B}(k_{cat,5}K_{-5F}[E] - k_{cat,-5}K_{5E}[F])}{K_{5E}K_{-5F}[B] + K_{2B}K_{-5F}[E] + K_{2B}K_{5E}[F] + K_{2B}K_{5E}K_{-5F}}\right)[DHAD]_0 \tag{28}$$

$$r_6 = \left(\frac{k_{cat,6}[F][NADH]}{K_{6F}[NADH] + K_{6NADH}[F] + [F][NADH]} - \frac{k_{cat,-6}[L][NAD]}{K_{-6L}[NAD] + K_{-6NAD}[L] + [L][NAD]}\right)[LLDH]_0 \tag{29}$$

3.2.2 Kinetic Parameters

Together, equations 13 through 29 require 25 independent kinetic parameters, many of which can be derived from enzyme assays that have been reported in the existing literature. However, these parameters only provide ball-park estimates of the true parameters, as they are highly dependent on the temperature and pH at which they were measured. Moreover, many of the values reported are given as simple Michaelis-Menten parameters; however, for the two-substrate reactions, these will only be effective Michaelis-Menten and are not the same as the ones needed in equations 13 through 29. Fortunately, the true parameters can be approximated from the effective Michaelis-Menten parameters if the conditions of the assay are known. This process is described in Appendix A12. Unfortunately, even with these calculations, some of the necessary parameters did not exist in the literature, so two pre-trained neural networks known as MLAGO and TurNuP were used to predict them from enzyme and substrate sequence data.[25,26] All of these values and their source of origin are given in Table 3. However, both the predicted and the literature values are expected to have substantial error and, therefore, they still cannot be used directly. To fix this, least-squares regression was used to fit the model parameters to transient data from an existing article detailing this cell-free pathway.[21] This was done by writing an objective function that numerically solved the system for a given set of parameters and

computed the sum of squares against this numerical solution and the experimental data points. This objective function was then optimized using the Nelder-Mead algorithm, where the starting points were generated from the ML-predicted and literature values. Finally, to reduce the size of the parameter space for this optimization and to include more experimental data in the model, enzyme activity measurements recorded at pH 7 and 50°C were used to relate the k_{cat} values of Steps 1, 2, 3, 4, 5 and 6 to their associated K values. This reduced the number of fitting parameters by six. The equivalence relationships used are shown in equations A1 and A2. The final regressed parameters are also shown in Table 3 along with the initial values.

3.2.3 Model Considerations and Insights

It is worth noting that the model developed in the above two sections, and the conclusions drawn from it are not perfect. Having developed this complex model, it is clear that the main rate-limiting step in the cell-free pathway seems to be the recycling of the coenzyme throughout the catalytic cycle. This also explains in part why the predictions made by the model based solely on the literature parameters predict a much faster conversion as shown in Figure 11, as the literature data lack detailed descriptions for the NAD-based Michaelis-Menten parameters. As such, the pre-regression model is incapable of modeling the kinetic slowdown that results from low concentrations of NAD. Furthermore, this also highlights one of the key flaws in this overall approach to lactic acid production. Regardless of the initial concentration of NAD and NADH, the concentration of one of these coenzymes will be pushed to almost zero because of the lack of regulatory processes. In other words, even if you start with a 50/50 mix of NAD and NADH, the NAD will be quickly consumed in the first step by GDH. This will in turn cause the rate of glucose catalysis to go to almost zero until a molecule of lactate is produced, which regenerates the NAD. However, this results in the production of very low concentrations of NAD which keeps the overall rate of glucose catalysis very low and limits the overall pathway kinetics.

As a result, this limits the volumetric lactic acid production rate to the point where extremely large cell-free reactors are needed to reach the desired mass production rate of 1.5 kg/s of lactic acid. These reactors also produce fairly low concentrations of lactate, which results in large volumes of water in the downstream processes. As such, fixing this issue has the potential to

Table 3: Model Parameters with Initial and Fit Values.

Model Parameter	Initial Value	Fit Value	Relative Change	Initial Value Source
$k_{cat,1}$ (h^{-1})	284372.000000	83643.000000	-0.71	Lit.[27] & MLAGO[26]
$k_{cat,-1}$ (h^{-1})	0.00000	1.810210		Arbitrary Value
k_{*} (h^{-1})	9.00000	Not Regressed		Literature[24]
k_{-*} (h^{-1})	0.00005	Not Regressed		Free energy
$k_{cat,2}$ (h^{-1})	154.80000	358.300000	1.31	Literature[28]
$k_{cat,3}$ (h^{-1})	23724.00000	2354.750000	-0.90	TurNuP[25]
$k_{cat,4}$ (h^{-1})	78840.00000	4646.100000	-0.94	TurNuP[25]
$k_{cat,5}$ (h^{-1})	183.60000	28.713900	-0.84	Literature[28]
$k_{cat,-5}$ (h^{-1})	0.00000	4.601920		Arbitrary Value
$k_{cat,6}$ (h^{-1})	1706184.00000	213607.000000	-0.87	TurNuP[25]
$k_{cat,-6}$ (h^{-1})	1954476.00000	1049074.675013	-0.46	TurNuP[25]
K_{1A} (mM)	1.58195	1.517450	-0.04	Lit. & MLAGO[26]
K_{1NAD} (mM)	0.54636	3.394000	5.21	MLAGO[26]
K_{-1B*} (mM)	0.00000	1.442910		Arbitrary Value
K_{-1NADH} (mM)	0.00000	1.260630		Arbitrary Value
K_{5E} (mM)	0.23000	0.006710	-0.97	Literature[28]
K_{-5F} (mM)	0.00000	0.000000		Arbitrary Value
K_{2B} (mM)	0.18000	0.099180	-0.45	Literature[28]
K_{3C} (mM)	0.47673	0.116190	-0.76	MLAGO[26]
K_{4D} (mM)	0.04960	1.026360	19.69	MLAGO[26]
K_{4NAD} (mM)	0.03366	0.832960	23.75	MLAGO[26]
K_{6F} (mM)	3.70000	0.000003	-1.00	Literature[29]
K_{6NADH} (mM)	0.03000	0.011433	-0.62	Literature[29]
K_{-6L} (mM)	410.00000	219.270000	-0.47	Literature[29]
K_{-6NAD} (mM)	0.09000	0.010001	-0.89	Literature[29]

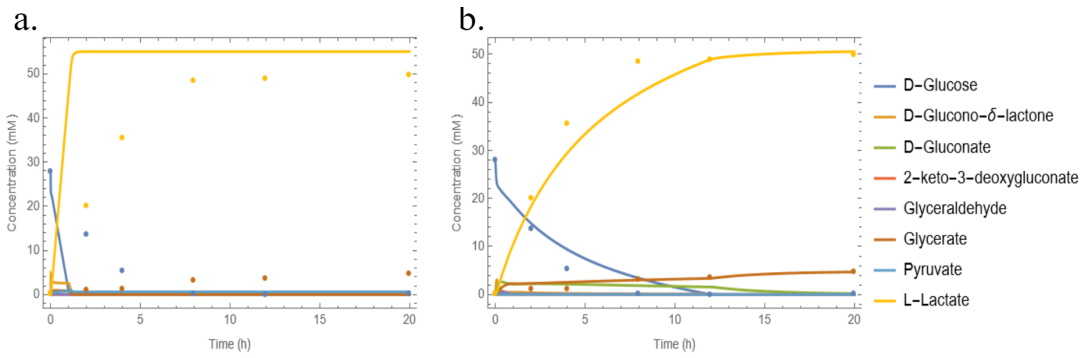

Figure 11: Comparing kinetic model to experimental data. **a.** Model predictions using initial parameters. **b.** Model predictions using regressed parameters. The solid lines represent the model predictions while the dots represent the experimentally measured values[21]

make this process significantly more economical.

The main reason why this is not an issue for cellular processes is that living cells have complex feedback networks that tightly regulate their concentrations of cytoplasmic coenzymes.[30–32] As such, this provides one potential solution for the cell-free case, whereby the addition of other NAD/NADH-utilizing enzymes could decrease the sensitivity of the system to coenzyme imbalances.

However, perhaps a more promising approach would be to better tune the ratios of enzymes in the cell-free process. Some approaches have been taken to do this experimentally by matching enzyme activities,[21] however optimizing this computationally with a more rigorous kinetic model would likely lead to better conclusions. Unfortunately, the kinetic model presented here likely has too much error in the parameter estimates to be used for such a degree of fine-tuning. To avoid this, a two-fold approach is recommended. First, a simplified kinetic model is recommended, which assumes that the conversion of D-gluconate to pyruvate and glycerate happens much faster than the other steps in the process, allowing this conversion to be modeled as instantaneous. Furthermore, this simplified model should implement a pseudo-steady-state approximation, in which it is assumed that the L-Lactate, pyruvate, and glycerate are in direct thermodynamic equilibrium. Finally, modeling of each equilibrium step should be done directly using first-order kinetics, where the substrates bind the proteins directly and the binding coefficients and k_{cat} values are modeled directly and reversibly. In this way, no assumptions are made about the coenzyme-dependent binding steps in this model, which the rough model devised herein shows are the most significant kinetic steps in the process.

The downside of this approach is that there is no good way to estimate the parameters of this model from those of the literature. As such, more experiments would be needed to show the concentrations of pathway intermediates over the course of the reaction, as was done to obtain the data points shown in Figure 11. These experiments would need to be performed at different enzyme and coenzyme concentrations. A new objective function could then be made to fit all of this data to the simplified kinetic model, and estimates of all new parameters could be obtained to yield a much more accurate model. Finally, the ratios of GDH and L-LDH in the new model

could be fine-tuned computationally to find the ratios that maintain a constant NAD/NADH ratio and therefore maximize the production rate.

Nevertheless, with the limitations of the model in mind, it was possible to predict the volume requirement of the reactor and the optimal enzyme ratios needed to reach an outlet lactic acid concentration of 55 g/L after 22.5 hours. The final reactor volume was found to be 1500 m^3 and the optimal enzyme concentrations of GDH, DHAD, KDGA, ALDH and LLDH were found to be 25.33 mg/ml, 55.06 mg/ml, 0.76 mg/ml, 66.9 mg/ml and 1.95 mg/ml (totaling to 150 mg/mL total enzyme). In addition, the reactor requires a total NAD/NADH concentration of 24 g/L, where the ratio does not matter as long as some NAD+ is present, since an equilibrium concentration between the two is reached almost instantaneously.

3.2.4 Reactor Geometry, Mixing and pH Control

The model developed in sections 3.2.1 and 3.2.2 was used to predict the optimal conditions for a cell-free reactor. The primary design specification for this reactor was that it should be able to produce 1.5 kg/s of lactate. The biggest design constraint in scaling up the reactor was enzyme concentration. At concentrations greater than 150 mg/mL total protein in solution, the viscosity of most protein solutions tends to leave the linear region described by Einstein's Viscosity Equation.[33–35] After this point, the viscosity of most protein solutions increases exponentially[34] with increasing protein concentration, which would cause considerable problems with pumping, diffusion, and heat transfer. As such, 150 mg/mL was used as the upper bound on the acceptable total protein concentration in the reactor. This still allowed for the individual ratios of the enzymes to be tuned using the kinetic model subject to this constraint, along with tuning the feed glucose concentration. The selected enzyme concentrations were: 25.33 mg/mL GDH, 55.06 mg/mL DHAD, 0.76 mg/mL KDGA, 66.90 mg/mL ALDH, and 1.95 mg/mL LLDH.

Additionally, while less problematic, another constraint was the expected amount of coenzyme (NAD/NADH) that would be present in the reactor. The coenzyme will be cotransported out of the *B. subtilis* with the enzymes and as such the final concentration of the coenzyme is dependent on the concentration of the enzymes GDH, ALDH, and LLDH. Under this cotransport assumption, we can write the expected concentration of NAD and NADH as a function of

the enzymes as shown in Equations 30 and 31.

$$[NAD] = \frac{[NAD]_{cell}}{K_{1NAD} + [NAD]_{cell}}[GDH]_0 + \frac{[NAD]_{cell}}{K_{4NAD} + [NAD]_{cell}}[ALDH]_0 + \frac{[NAD]_{cell}}{K_{-6NAD} + [NAD]_{cell}}[LLDH]_0 \quad (30)$$

$$[NADH] = \frac{[NADH]_{cell}}{K_{-1NADH} + [NADH]_{cell}}[GDH]_0 + \frac{[NADH]_{cell}}{K_{-4NADH} + [NADH]_{cell}}[ALDH]_0 + \frac{[NADH]_{cell}}{K_{6NADH} + [NADH]_{cell}}[LLDH]_0 \quad (31)$$

The derivations of these equations are shown in Appendix Figure A14. Unfortunately, using this NAD concentration alone was not enough to design a reactor of a reasonable size capable of hitting the 1.5 kg/s production rate under the 150 mg/mL enzyme concentration constraint. As such, it was assumed that 15 times the values produced by equations 30 and 31 would be present in the reactor. To simplify the modeling in the upstream process, it was assumed that the NAD always co-transports with the enzymes in every step at the required ratios, and so, aside from the kinetic modeling, no mention of NAD or NADH is seen in the other sections. Instead, the mass of coenzyme in any mass flow is assumed to be part of the total enzyme mass flow. This means that it is assumed that the upstream bioreactor also produces enough NAD and NADH to keep the cell-free reactor running properly. In any future work, this assumption needs to be considered in more detail and in the worst case, could result in the need for another bioreactor in the plant whose sole purpose is the production of NAD. To make matters worse, there is also some evidence that NAD may degrade with time in the cell-free reactor and the associated recycle loop over time.[36] This serves as another crucial area for future work.

Nevertheless, with these NAD assumptions and within the 150 mg/mL enzyme constraint, it was possible to design a reactor to achieve the target yield. This was done by numerically solving another constrained optimization problem on the fit kinetic model, where the individual enzyme concentrations were varied along with the feed concentration, and the net production rate was maximized. This constrained optimization was performed once again using the Nelder-Mead algorithm.

After running this optimization, a reactor with a volume of 1500 m^3 was found to be the smallest reactor capable of reaching the 1.5 kg / s production goal under the enzyme limitation of 150 mg/mL. After finding the optimal reactor volume, the next step was to design the mixing and thermal control for the reactor. Due to the large size of the reactor, it was decided that

jet mixing would be the most reasonable approach. To design such a jet-mixing system the following design equations were used.[37]

$$\theta_{99} = 3\frac{z^2}{UD} \tag{32}$$

$$\theta_z = \theta_{99}\frac{ln\left(\frac{100-z}{100}\right)}{ln\left(0.01\right)} \tag{33}$$

$$P = \frac{1}{2}q\rho U^2 \tag{34}$$

In order for these empirical equations to hold, it was also ensured that the following were true:

- The tank depth-to-width ratio was between 0.2 and 3.
- The tank volume of 1,500 m^3 is between 0.2 and 12,000 m^3.
- The momentum characterization, $\frac{UD}{Z}$, of the mixing is between 0.013 and 0.14 m/s.
- The nozzle diameter characterization, $\frac{Z}{D}$, is between 86 and 750.
- The Reynolds number of the flow through the jet nozzle is greater than 10,000.

In the above, Z represents the length of the jet path in jet mixing (that is, the distance from the jet to the edge of the tank), θ_z is the time it takes for the tank to reach a homogeneity of z%, U is the velocity of the fluid in the jet nozzle, D is the diameter of the jet nozzle, q is the volumetric flow rate through the nozzle, ρ is the density of the fluid in the reactor and P is the power delivered to the reactor through the jet stream.

The primary design consideration for the mixing system was to allow the mixing to homogenize the reactor faster than any pH changes could occur; this way caustic could be added to the jet stream to neutralize any pH disturbances caused by the production of carboxylic acids from the glucose feed. From the mechanism shown in Figure 10 it is seen that the rate of acid production is approximately equal to the negative rate of glucose consumption since the acids are made in the lactone ring opening step which is the rate limited by the glucose consumption. Using the

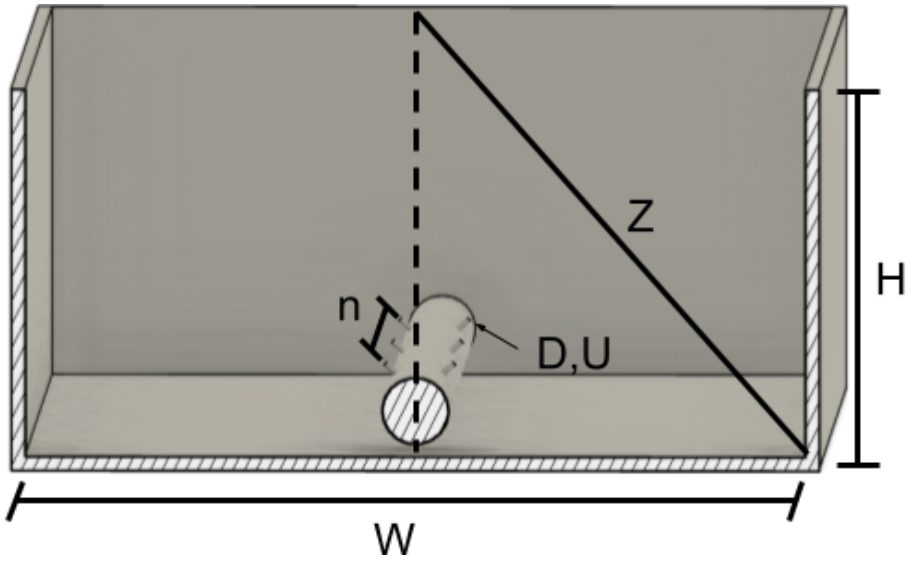

Figure 13: Cross section of the cell-free reactor geometry highlighting the key values used to design the jet mixing system. H and W are the respective width and height of the reactor interior, Z is the jet mixing path length, n is the number of jet nozzles present (n=6 in this example image), D is the diameter of each jet nozzle, and U is the fluid velocity in each jet nozzle. The final values of these parameters can be found in Table 4

kinetic model described in sections 3.2.1 and 3.2.2, the average acid production rate was found to be 31.4 mM/h as shown in Figure 12. Based on this rate, it would take 36 seconds for a pH swing of 3 to occur in the reactor, which is around the acceptable limit based on the usable pH ranges of the enzymes present in the cell-free reactor.[38–41] If one wishes to restore the reactor to a state of around 76% homogeneity in this time, that value of θ_{99} must be 115 seconds according to equation 33. With this constraint in mind, equation 34 was re-parameterized in terms of the reactor's volume, width, height, and jet fluid velocity. The constraints on the semiempirical model were then re-parameterized in the same way, to create a 3D region in the phase space spanned by the reactor's width, height, and jet fluid velocity. During this reparametrization, it was also assumed that the reactor could be modeled as n smaller reactors where n was the number of jets present. A diagram showing the geometric meaning of the key values in the jet mixing system is shown in Figure 13. After reparametrization, the following design constraints are shown in equations 35-39.

$$\frac{\rho U D}{\eta} > 10,000 \tag{35}$$

$$0.2 < \frac{2H}{W} < 3 \tag{36}$$

$$0.013 < \frac{\text{UD}}{Z} < 0.14 \tag{37}$$

$$86 < \frac{Z}{D} < 750 \tag{38}$$

$$\theta_{99} = 115s \tag{39}$$

The product of the height and width of the reactor was then maximized to effectively minimize the plant footprint of the reactor within these constraints given the fixed reactor volume of 1500 cubic meters. The resulting dimensions were a width of approximately 7.6 m and a height of approximately 3.8 m, and a reactor length of 52 m. The power requirement of the jet pump was then minimized under the above constraints and the additional constraint that the resulting reactor length remains below the minimal footprint value of 52 m. The functional form of the pumping power in terms of the optimization parameters is shown in equation 40.

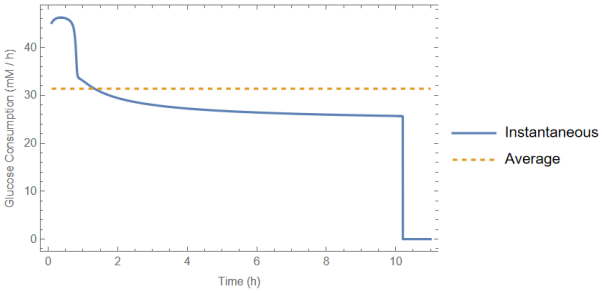

Figure 12: Glucose consumption rate in the cell-free reactor. The average consumption rate was used to approximate the rate of pH change in the reactor to serve as a design constraint for the cell-free reactor's jet mixing system.

$$P \propto \frac{D^2 U^3 V_R}{H W^2} \tag{40}$$

Here P is the power added to the fluid by the pump, V_R is the volume of the reactor, and all other parameters are described in Figure 13. This optimization yielded the final reactor dimensions that are presented in table 4 along with all other properties of the final cell-free reactor design. Final mass balences around the reactor are shown in Table A13.

Table 4: Cell-free reactor geometry. The parameters are consistent with the ones described in Figure 13.

Reactor Property	Value	Units
Volume (V_R)	1500	m^3
Width (W)	8.5	m
Height (H)	4	m
Length (L)	54	m
Mixing Power (P)	70	kW
Jet Nozzle Diameter (D)	2.469	in
Jet Fluid Velocity (U)	12	m/s
Mixing Flow Rate (q)	3469	m^3/h
Number of Jets (n)	26	

3.2.5 Protein Solution Density and Viscosity Models

It should also be noted that, for the Reynolds number and pumping power to be correctly computed, a model was needed for the density and viscosity of the concentrated protein solutions. It is known that one of the primary driving forces for viscosity in concentrated protein solutions is molecular crowding.[33,34,42] As a result, some key parameters needed to make accurate predictions are the effective volumes occupied by the proteins in the solution. To obtain rough estimates, software known as HullRad[43] was used to find the intrinsic viscosities of each protein based on their 3D structures, providing a way to predict protein volume from concentration. Protein structures were taken from their associated protein data bank files, since all pathway enzymes, aside from DHAD, had been previously crystallized. For DHAD, a predicted structure was calculated using AlphaFold2 through Neurosnap, assuming a tetrameric structure.[44–48] The alpha-fold structure classifications can be seen in Table A5, and the structure with the highest ranking is shown in Figure A13. The raw HullRad results can all be found in Table A6. After the intrinsic viscosities for each protein were obtained, they were used to calculate the concentration of a pure hemoglobin solution that would have the same protein volume using equation 41.

$$C_{eff} = \frac{1}{[\eta_{HG}]} \sum_i [\eta_i] C_i \tag{41}$$

Here C_{eff} is the effective mass concentration of a hemoglobin solution having the same protein volume, $[\eta_{HG}]$ is the intrinsic viscosity of hemoglobin (which was found to be 3.436 mL/g through HullRad), $[\eta_i]$ is the intrinsic viscosity of enzyme i in the solution and C_i is the mass

concentration of enzyme i in the solution. After finding this effective concentration, the viscosity of the solution was estimated from existing data that reported the viscosity of hemoglobin as a function of enzyme concentration.[42] Finally, to account for changes in temperature on viscosity, equation 42 was used.

$$\eta = \eta_0 \frac{\eta_{HG}}{\eta_{ref}} \tag{42}$$

Here η is the temperature-corrected viscosity, η_0 is the viscosity of the solution in the absence of proteins at the desired temperature, η_{HG} is the viscosity of a pure hemoglobin solution at the concentration given by equation 41, and η_{ref} is the viscosity of the pure solvent used in experimental measurements of the hemoglobin viscosity (which was taken to be the viscosity of pure water at 37°C and 1 atm). Using this model, the viscosity in the reactor was assumed to be 1.8 cP at the 50°C temperature of the reactor.

It is important to note that this model assumes that all of the proteins in the solution are globular proteins with properties similar to hemoglobin and that all of the proteins in the solution behave as perfect spheres with similar radii. For the enzymes used in the cell-free reactor, these assumptions are likely acceptable, but it should be noted that this model has yet to be experimentally validated. Nevertheless, it likely provides a decent approximation of the viscosity of the final protein solution, as it is logically consistent with existing theories.[44–48]

The densities of the solution were computed in a similar way using the partial specific volumes provided by HullRad (also shown in Table A6). These values were used in equation 43

$$\rho = \sum_i C_i + \rho_S \left(1 - \sum_i \bar{V}_i C_i\right) \tag{43}$$

Here $\bar{V}_i$ is the partial specific volume of protein i provided by HullRad, C_i is the mass concentration of protein i in the solution, and ρ_S is the density of the solution in the absence of proteins. The derivation of equation 43 is shown in Figure A15. Using this equation, the density of the fluid in the cell-free reactor was found to be 1026.88 kg/m^3.

3.2.6 Temperature Control

Aspen Plus was used to model the average heat duty of the cell-free reactor. A simplified model was made using the RStoic reactor block in Aspen assuming a 100% conversion of D-glucose and sodium hydroxide to sodium lactate and water. The NaOH was fed to the RStoich block as a 30% (by weight) solution and the glucose was fed as a 6% (by weight) solution to reflect the initial glucose concentration in the reactor. The flow rates were given as 5.69 and 60.97 m^3/h so that one hour of simulation time corresponds to one batch and both feeds were supplied at 24°C and 1 atm. This resulted in a heat duty of 555 kW for the RStoic block in the model, meaning that one batch requires 555 kWh of net heat input. However, as it has been designed, it is not assumed that the reactor is physically insulated, and so heat transfer to the surroundings must also be considered. The plant will be built just outside of Detroit, Michigan (more details are provided in Section 4.5). Weather reports show that typical wind speeds are around 18 mph and that average low temperatures are around 18 °C in the winter months.[49] Using these values, it can be estimated that 460 kW of convective heat transfer will occur across the large faces of the reactor. Details of this calculation are shown in Figure A16. Adding the additional heat duty resulting from the 555 kWh net enthalpy change, a total heat duty of around 485 kW is expected. This heating will need to be controlled digitally and it will be assumed that the necessary heat transfer can be achieved by placing a heat exchanger in the jet mixing recycle stream, as shown in Figure 14. To provide a conservative upper bound, a 555 kW heater will be used.

3.2.7 Final Reactor Design

The process flow diagram for the cell-free reactors is shown in Figure 14. To allow for the near-continuous production of lactic acid, two cell-free reactors will be run in parallel. In this way, one reactor can be drained by downstream operations, while the other produces lactic acid. As such, all downstream operations can be performed continuously. A more detailed summary of the final cell-free reactor block can be found in Section 4.1.0.2

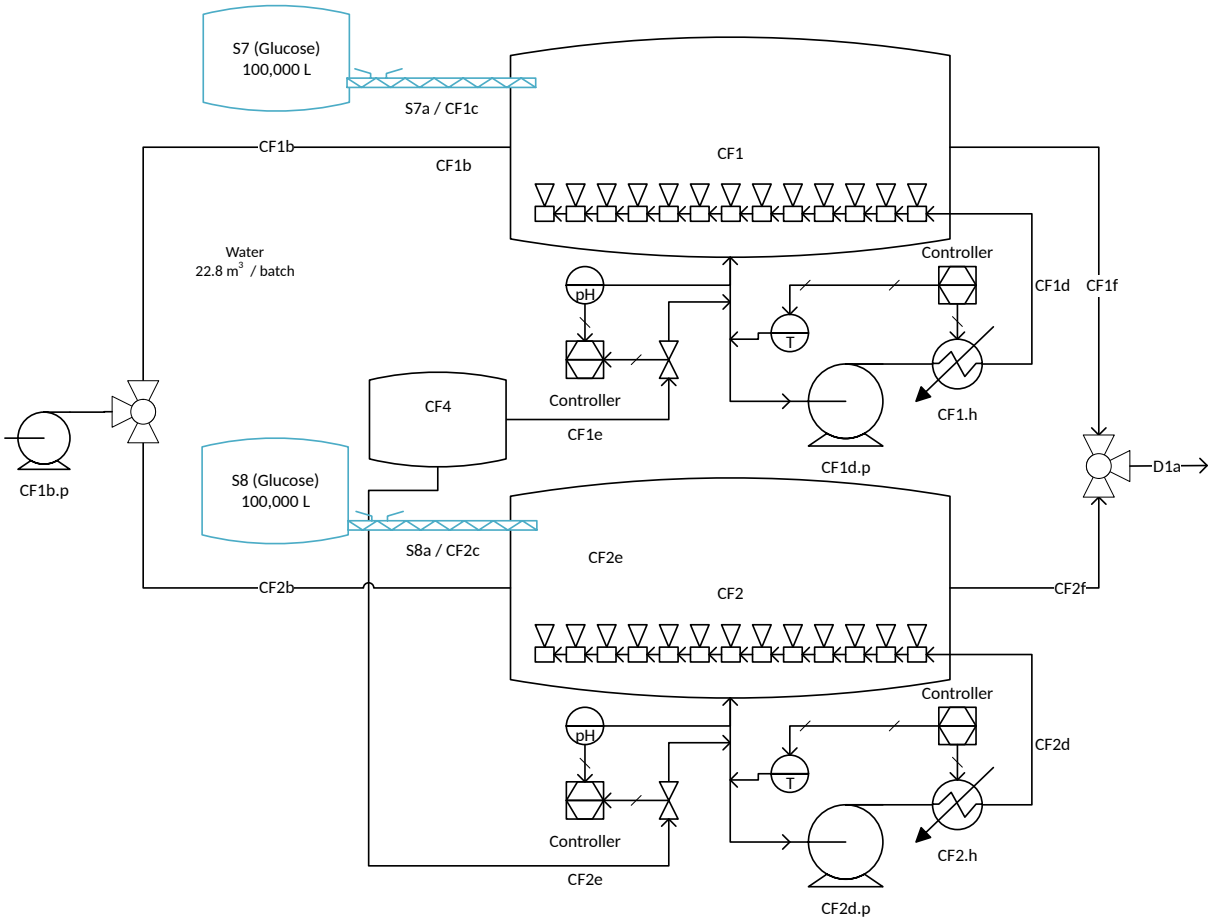

Figure 14: Process flow diagram of the cell-free reactors and their associated auxiliary equipment. The mass flows for each inlet and outlet stream can be found in Table A13.

3.3 Downstream

3.3.1 Nanofiltration Membrane System

3.3.1.1 Nanofiltration Membrane Purpose

The product from the cell-free reactor is sent through several nanofiltration membranes. The main purpose of this unit operation is to separate the protein from the product stream and recycle it back into the cell-free reactor. This is to save money on producing more enzymes and ensure the product does not contain any enzyme contaminants.

3.3.1.2 Membrane Filter Theory

Each membrane filter's design parameters were determined using the following theory. First, the lactic acid rejection coefficient is needed. This allows us to determine how much lactic acid stays in the retentate and how much leaves in the permeate. Our membrane filters' lactic

acid rejection coefficient is 0.125.[20] Second, the membrane area must be defined. This was calculated by scaling up the membrane area from the basis paper. The area we will utilize for our membrane filters is 44600 m^2. These values allow us to calculate the parameters for the rest of the membrane filter. The first parameter determined was the final lactic acid concentration of the permeate streams. This was done using the following steps. First, a system of equations was defined.

$$\frac{C}{C_0} = (CF)^{\sigma-1} \tag{44}$$

Equation 44 variables: CF is the concentration factor of the membrane, C_0 is the feed concentration, C is the permeate concentration, and sigma is the rejection coefficient.

$$Q_P = \frac{Q_F}{CF} \tag{45}$$

Equation 45 variables: Q_P is the volumetric permeate flow rate, Q_F is the volumetric feed flow rate, and CF is the concentration factor.

$$Q_R = Q_F - Q_P \tag{46}$$

Equation 46 variables: Q_P is the volumetric permeate flow rate, Q_F is the volumetric feed flow rate, and Q_R is the volumetric retentate flow rate.

$$u_p = \frac{Q_P - Q_F}{A} \tag{47}$$

Equation 47 variables: Q_P is the volumetric permeate flow rate, Q_F is the volumetric feed flow rate, A is the membrane area, and u_p is the average permeate flux.

Equation 44 calculates the concentration factor, determining how much lactic acid leaves in the permeate. Equation 45 calculates the permeate flow rate. Equation 46 calculates the retentate flow rate. Second, a target must be defined. The target is to hit a protein concentration of 150 mg/ml in the retentate stream for all four stages. Finally, an independent variable must

also be defined. For these calculations, the independent variable will be the final lactic acid concentration. After these steps, the final lactic acid concentration varies through trial and error until the target retentate protein concentration is reached. This is done for all four stages to find their flow rates and concentrations. The second parameter that was determined was the average permeate flux. This was calculated using Equation 47.

3.3.1.3 Nanofiltration Membrane System Design

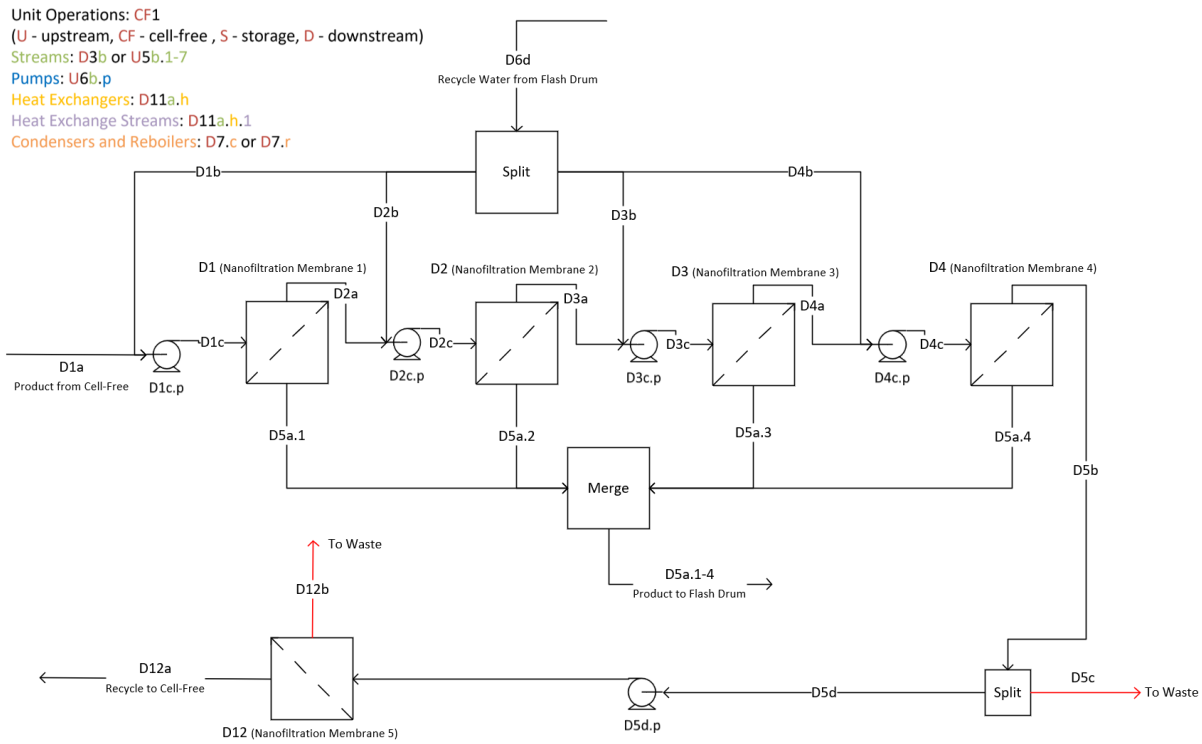

Figure 15: Process Flow Diagram for the Nanofiltration Membrane System

The overall mass balance of the system is shown in Table 5 to Table 9. Each nanofiltration membrane will have a membrane area of 44625 m^2 and an average permeate flux of 1.473 $L/m^2/hr$. They will operate at a pressure of 30 bar and have a pressure drop of 3 bar.[20] This pressure is needed to achieve the required separation and permeate flux for our process. Figure 15 shows the nanofiltration system. As shown in the figure, four different membrane filters will be used. The feed stream (D1a) is directly from the output of the cell-free reactor and includes the byproduct intermediates and the proteins used to create the lactic acid. This feed combines with recycled makeup water (D1b) from the next unit operation, the flash drum. The purpose of this is to reduce the concentration of protein and prevent the filter from clogging.

Table 5: Overall Mass Balance for Nanofiltration Membrane (D1)

Mass [kg/hr]	D1a	D1b	D1c	D2a	D5a.1
Water	65777	65777	131554	65742	65814
Glycerate	170	0.0249	170	85.0	85.1
Glyceraldehyde	17.7	0.474	18.2	9.08	9.09
D-Gluconate	14.6	0	14.6	7.30	7.30
L-Lactate	3588	124	3712	1687	2025
Protein	9867	0	9867	9867	0
Glucose	0.21	0	0.210	0.105	0.105
Na^+	1037	0	1037	519	518
Total	80472	65901	146373	77916	68459

Table 6: Overall Mass Balance for Nanofiltration Membrane (D2)

Mass [kg/hr]	D2a	D2b	D2c	D3a	D5a.2
Water	65742	65812	131554	65740	65816
Glycerate	85.0	0.0249	85.0	42.5	42.5
Glyceraldehyde	9.08	0.474	9.56	4.78	4.78
D-Gluconate	7.30	0	7.30	3.65	3.65
L-Lactate	1687	124	1811	824	989
Protein	9867	0	9867	9867	0
Glucose	0.105	0	0.105	0.0524	0.0525
Na^+	519	0	519	259	259
Total	77916	65936	143853	76741	67115

Table 7: Overall Mass Balance for Nanofiltration Membrane (D3)

Mass [kg/hr]	D3a	D3b	D3c	D4a	D5a.3
Water	65740	65814	131554	65734	65820
Glycerate	42.5	0.0249	42.5	21.2	21.3
Glyceraldehyde	4.78	0.474	5.25	2.62	2.63
D-Gluconate	3.65	0	3.65	1.82	1.82
L-Lactate	824	124	948	432	517
Protein	9867	0	9867	9867	0
Glucose	0.0524	0	0.052443	0.0262	0.0262
Na^+	259	0	259	130	129
Total	76741	65938	142679	76189	66492

Table 8: Overall Mass Balance for Nanofiltration Membrane (D4)

Mass [kg/hr]	D4a	D4b	D4c	D5b	D5a.4
Water	65734	65820	131554	55960	75595
Glycerate	21.2	0.0249	21.3	9.04	12.22
Glyceraldehyde	2.62	0.474	3.10	1.32	1.78
D-Gluconate	1.82	0	1.82	0.775	1.05
L-Lactate	432	124	556	288	266
Protein	9867	0	9867	9867	0
Glucose	0.0262	0	0.026204	0.0111	0.0151
Na^+	130	0	130	55.0	74.4
Total	76189	65944	142133	66181	75950

Table 9: Overall Mass Balance for Nanofiltration Membrane (D12)

Mass [kg/hr]	D5b	D5c	D5d	D12a	D12b
Water	55960	1,117	54,843	45,270	9,573
Glycerate	9.04	0.180	8.86	7.31	1.55
Glyceraldehyde	1.32	0.03	1.27	1.05	0.222
D-Gluconate	0.775	0	0.770	0.634	0.134
L-Lactate	288	6	282	221	61.2
Protein	9867	197	9,670	9,670	0
Glucose	0.0111	0	0.01	0.00905	0.00191
Na^+	55	1.1	54	45	9.4
Total	66181	1322	64859	55214	9645

It also increases the system's recovery, as less lactic acid is lost. The permeate streams (D5a.1 - D5a.4) that are going to the flash drum contain no protein. This is because the pores in the filter are much smaller than the proteins, meaning that none of them get through to the permeate stream. The lactic acid recovery of the nanofiltration membrane system is 93%.

The retentate stream (D5b) of the fourth nanofiltration membrane (D4) is split into two streams: a purge stream (D5c) and a recycle stream (D5d). This can be seen in Figure 15. The purge stream is there to remove degraded enzymes from the process. The recycle stream is sent to another nanofiltration membrane to concentrate the proteins further. This is because extra water is added to the cell-free reactor through the sodium hydroxide solution, which means a higher feed concentration of protein is needed to hit the target concentration in the reactor. The membrane has an area of 18530 m^2 and an average permeate flow rate of 2.443 $L/m^2/hr$. The permeate stream (D12b) is treated and disposed of as waste. The retentate stream (D12a) is sent to a tank for temporary storage before it is fed into the cell-free reactor.

3.3.2 Flash Drum

3.3.2.1 Flash Drum Purpose

A flash drum is required to concentrate the lactic acid product stream and recover makeup water for the nanofiltration membrane system. The main reason why this unit operation is in

place is because of the amount of water leaving the membrane filters. The liquid-liquid extractor (LLE) and distillation cascade require more resources to treat more water. For the LLE, more solvents will be needed. More energy will be needed for the distillation. There will be larger economic costs in both cases, meaning the water should be separated from the product. The flash drum can perform this separation, making it an integral part of our process.

3.3.2.2 Flash Drum Design

This unit operation was simulated and designed in ASPEN Plus. The liquid volume of the flash drum is 107 m^3. The diameter is 7.16 meters, and the tangent-to-tangent height is 3.66 meters. The design gauge pressure is 2.43 barg. The design temperature is 150 degrees Celsius, and the operating temperature is 122 degrees Celsius. The flash drum will be made out of stainless steel.

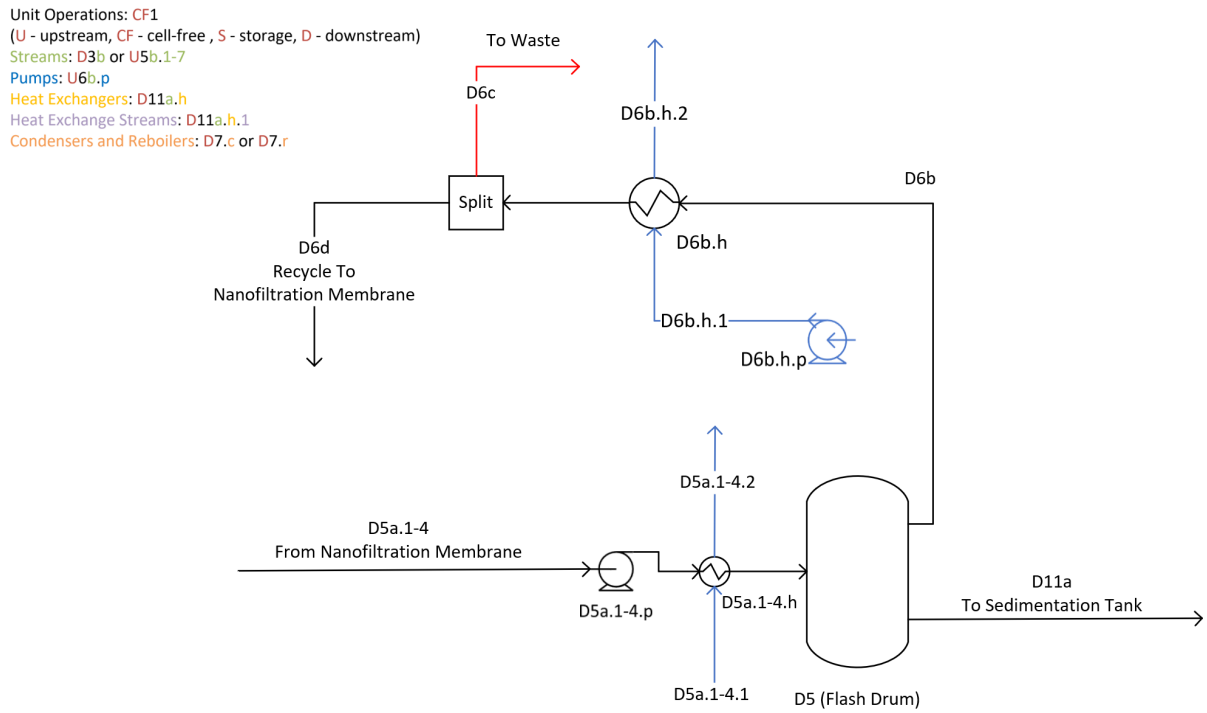

Figure 16: Process Flow Diagram for Flash Drum

The overall mass balance around the flash drum is shown in Table 10, and the process flow diagram of this process can be seen in Figure 16. Before entering the flash drum, the feed (D5a.1-4) must be depressurized to 2.03 bar. This ensures that the flash drum works properly and gets the desired separation. Afterward, it gets sent through a heat exchanger that utilizes steam. The main purpose of this heat exchanger is to give the feed stream enough energy so

Table 10: Overall Mass Balance for Flash Drum (D5)

Mass [kg/hr]	D5a.1-4	D6b	D6c	D6d	D11a
Water	273,046	264,683	1,460	263,223	8,363
Glycerate	161	0	0	0.1	161
Glyceraldehyde	18.2	1.91	0.01	1.90	16.3
D-Gluconate	13.9	0	0	0	13.9
L-Lactate	3,797	499	2.70	497	3298
Glucose	0.270	0	0	0	0.270
Na^+	982	0	0	0	982
Total	278018	265184	1463	263722	12834

that when it is put through the flash drum, the separation is adiabatic. This effectively serves to power the flash drum. A heat exchanger powered by steam is used instead of electricity because it is much cheaper and more efficient. The temperature of the flash drum is at 102 degrees Celsius. This temperature is high enough that it allows most of the water to be recovered as water vapor. A lower temperature would prevent separation, while a much higher temperature would result in all of the water going out the top of the flash drum. The distillate (D6b) is then condensed into water and cooled to 50 degrees Celsius through a heat exchanger. The distillate is then split into a recycle stream (D6d) and a waste stream (D6c). The flash drum recovers more water than is needed to dilute the nanofiltration feed streams. The recycle stream leaving the flash drum's top has some lactic acid. However, because it is being recycled back into the nanofiltration membrane, most of the lactic acid stream will be recovered, increasing the overall yield of the process. As discussed later, the waste stream is sent to a treatment plant for disposal. The product stream (D11a) leaving the bottom of the flash contains 33 times less water than the feed and recovers a large amount of lactic acid. Some intermediate byproducts are still present, but those will be removed thoroughly in the later downstream unit operations. The product stream will go to the next step in the process, the sedimentation tank. The flash drum has an 87% recovery.

3.3.3 Sedimentation Tank

3.3.3.1 Sedimentation Purpose

The pH of the product stream must be lowered before the product goes through the liquid-liquid extractor. This is to increase the effectiveness of the LLE and protonate the lactic acid. The lactic acid coming out of the cell-free reactor is deprotonated. For the product to be in the specified form, a proton must be added to the lactic acid to make it protonated. These requirements are fulfilled by adding sulfuric acid to the product stream.

One side effect of adding sulfuric acid is the creation of a sodium bisulfate (NaHSO4) byproduct. Sodium ions are present in the product stream due to the use of sodium hydroxide in the cell-free reactor. The sodium ions (Na+) can bond with the bisulfate (HSO4-) ions formed from the protonation of lactic acid to make sodium bisulfate. The sodium bisulfate would not be an issue if the amount were under the solubility limit. However, enough sodium ions are present to result in an amount much greater than the solubility limit. Because of this, solid particles of sodium bisulfate start to form. These particles will interfere with the rest of the downstream process, as they can accumulate in places like the distillation column trays. As a result, they must be removed before the next downstream unit operation. The sedimentation tank can remove the solid sodium bisulfate, which is why it has been added to the process.

3.3.3.2 Sedimentation Design

The following steps must be taken to design the sedimentation tank. The first step is to determine the settling speed of a sodium bisulfate particle. This was determined by using equation 48.[50]

$$V_S = 8.925 \cdot \frac{\sqrt{1 + 95 \cdot \frac{\rho_s - \rho}{\rho}} - 1}{d} \tag{48}$$

Equation 48 variables: V_S is the settling velocity (m/s), ρ_s is the density of sodium bisulfate (kg/m^3), ρ is the density of water (kg/m^3), and d is the diameter of a sodium bisulfate particle (m).

Sodium bisulfate has a particle diameter of 0.74 mm and a density of 2435 kg/m^3.[51,52] This results in a settling speed of 0.000333 m/s. The second step is to initialize certain design specifications. In this case, the depth, the detention time, and the weir loading rate will be 3.5 meters, 4 hours, and 186 m^2/day, respectively. This is because they are within the range of typical values for industrial rectangular sedimentation tanks.[53] The third step is to input the initialized design specifications and the flow rate coming into the sedimentation tank into equations 49 to 54.[53]

$$V = Qt \tag{49}$$

Equation 49 variables: V is the volume of the sedimentation tank, Q is the volumetric flow rate, and t is the detention time.

$$A = \frac{V}{d} \tag{50}$$

Equation 50 variables: A is the area of the sedimentation tank floor, V is the volume of the tank, and d is the depth of the tank.

$$W = \sqrt{\frac{V}{4d}} \tag{51}$$

Equation 51 variables: W is the width of the sedimentation tank, V is the volume of the tank, and d is the depth of the tank.

$$L = 4W \tag{52}$$

Equation 52 variables: W is the width of the sedimentation tank and L is the length of the tank.

$$u = \frac{Q}{d * W} \tag{53}$$

Equation 53 variables: u is the flowthrough velocity, Q is the volumetric flow rate, d is the depth

of the sedimentation tank, and W is the width of the tank.

$$L_W = \frac{Q}{W.L.} \tag{54}$$

Equation 54 variables: L_W is the length of the sedimentation tank weir, Q is the volumetric flow rate, and W.L. is the weir loading factor.

The final design specifications are as follows. The tank is 6.18 meters long, 1.55 meters wide, and 3.5 meters deep. The volume of the sedimentation tank is 33.45 m^3 and the surface area is 9.56 m^2. The flow-through velocity is 0.000429 m/s. The weir length is 1.07 meters. To ensure all sodium bisulfate particles get removed, the maximum height the particle will fall over the tank's length must be determined.[54] This can be done using equation 55. For this sedimentation tank, the particle's maximum height it can fall is 4.79 meters. This is higher than the tank's actual depth, meaning that all of the particles will settle at the bottom before the end of the tank.

$$h = V_S \cdot \frac{L}{u} \tag{55}$$

Equation 55 variables: h is the settling height, V_S is the settling speed, L is the length of the sedimentation tank, and u is the flowthrough velocity.

The overall mass balance around the sedimentation tank is shown in Table 11 and the process flow diagram in Figure 17. The feed (D11a) coming into the sedimentation tank will be combined with sulfuric acid (D11b). This saturates the stream with sodium bisulfate and results in solid sodium bisulfate. The solid stream (D11c) coming out of the bottom of the sedimentation tank will contain all the undissolved sodium bisulfate and some water. The treatment of this stream will be discussed in a later section. The product stream (D11d) will be sent to the liquid-liquid extractor for further purification.

3.3.4 Liquid-Liquid Extractor (LLE)

3.3.4.1 LLE Purpose

After the sedimentation tank, the product stream is processed through a liquid-liquid extractor.

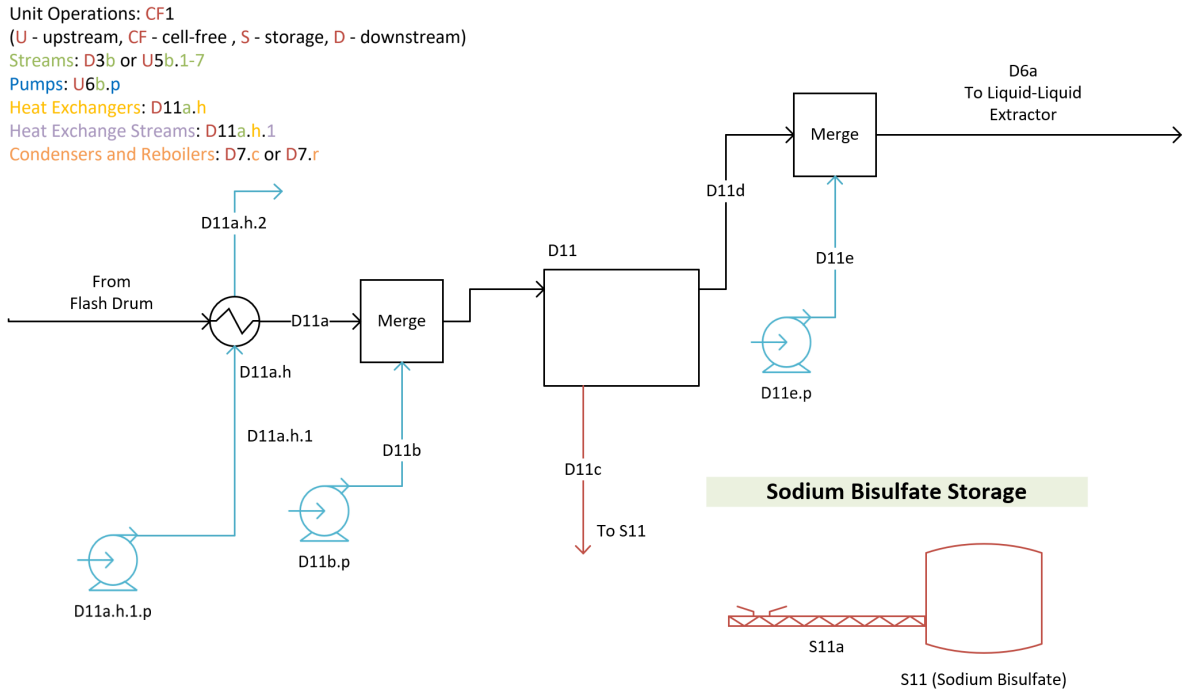

Figure 17: Process Flow Diagram for Sedimentation Tank

Table 11: Overall Mass Balance for Sedimentation Tank (D11)

Mass [kg/hr]	D11a	D11b	D11c	D11d	D11e	D6a
Water	8,363	0	302	8,062	302	8,363
Glycerate	161	0	0	0	0	0.0
Glyceraldhyde	16.3	0	0	16.3	0	16.3
D-Gluconate	13.9	0	0	0	0	0.00
Lactate	3298	0	0	0	0	0.00
Glyceric Acid	0	0	0	162	0	162
D-Gluconic Acid	0	0	0	14.0	0	14.0
Lactic Acid	0	0	0	3335	0	3335
Glucose	0.27	0	0	0.270	0	0.270
Na^+	982	0	0	653	0	653
Sulfuric Acid	0	3590	0	0	0	0
$Bisulfate^-$	0	0	0	1907	0	1907
Sodium Bisulfate	0	0	2011	0	0	0
Total	12834	3590	2313	14151	302	14452

There are two reasons for this. The first is to separate some intermediate byproducts from the lactic acid. This will let us reach the target purity for our final product. The second reason is to reduce the amount of solid waste produced. One of the main methods of lactic acid recovery is precipitation, which produces solid waste in the form of gypsum.[55] Gypsum requires a lot of treatment before it can be disposed of, increasing the unit operation cost. A liquid-liquid extractor will be used to reduce costs as an alternative to precipitation.

3.3.4.2 LLE Theory

Two phases exist inside the extractor: an aqueous phase and an organic phase. For this process, the aqueous phase of the extractor is water, while the organic phase is a mixture of trioctylamine (TOA) and octanol. This mixture is used because it extracts a significant amount of lactic acid.[56] This unit operation was modeled using ASPEN Plus. For the LLE model to work, a distribution coefficient is required. The distribution coefficient determines how much of a specific chemical is in the aqueous and organic phases. For this process, the distribution coefficient will be 5, meaning the organic phase has five times more lactic acid than the aqueous phase.[56]

3.3.4.3 LLE Design

A sensitivity analysis was performed in Aspen to determine the number of stages and solvent flow rate needed for optimal lactic acid recovery. This resulted in 15 stages and a total solvent flow rate of 5000 kilograms per hour for the LLE. After determining these parameters, the column diameter was determined. First, several assumptions were made: the continuous phase is the feed coming into the top of the LLE, the dispersed phase is the organic product coming out of the top of the LLE, and the column will operate at 50% of flooding.[57] Then, several design parameters were established from Aspen: the mass flow rate of the continuous phase is 14390 kg/hr, the mass flow rate of the dispersed phase is 11600 kg/hr, the density of the continuous phase is 968 kg/m^3, and the density of the dispersed phase is 1251 kg/m^3. The following are also some physical properties that are used to determine the column diameter: the viscosity of the continuous phase[58] is 0.00089 $Pa \cdot s$ and the interfacial tension between the organic and aqueous phase is 8.52 dyn/cm.[59] Using these assumptions, design parameters, and

physical properties lets us calculate the column diameter using the equations 56 to 60.[57]

$$\frac{U_D}{U_C} = \frac{m_D}{m_C} \cdot \frac{\rho_C}{\rho_D} \tag{56}$$

Equation 56 variables: $\frac{U_D}{U_C}$ is the superficial velocity ratio, m_D is the mass flow rate of the dispersed phase, m_C is the mass flow rate of the continuous phase, ρ_C is the density of the continuous phase, and ρ_D is the density of the dispersed phase.

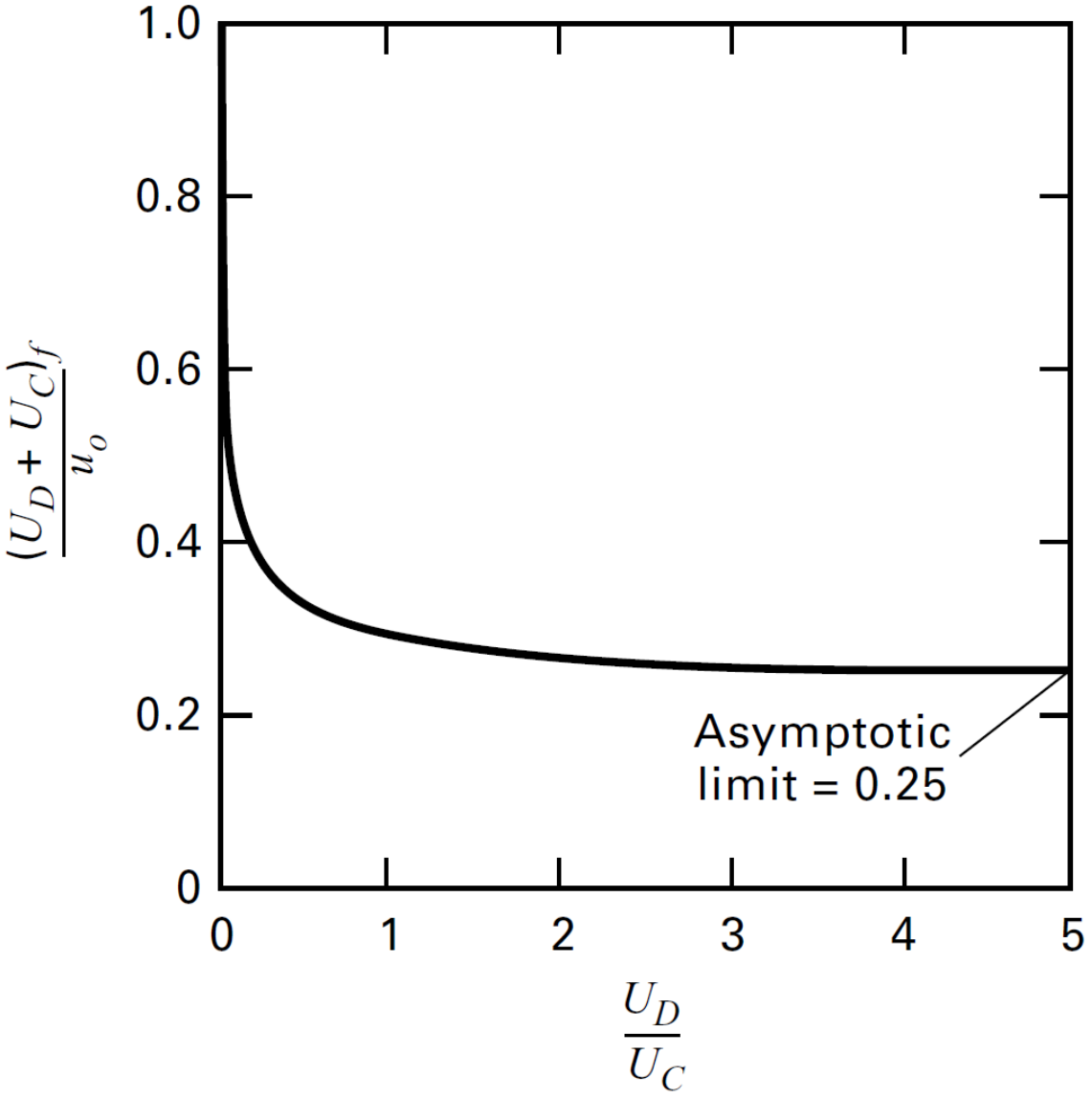

Figure 18: $\frac{(U_D+U_C)_f}{u_0}$ vs $\frac{U_D}{U_C}$ from Seader et al. (2010).[57] This graph is used to determine $\frac{(U_D+U_C)_f}{u_0}$ for equation 58.

$$u_0 = \frac{0.01\sigma \cdot (\rho_C - \rho_D)}{\mu_C \rho_C} \tag{57}$$

Equation 57 variables: u_0 is the velocity of a dispersed droplet, σ is the interfacial tension between the organic and aqueous phase, μ_C is the viscosity of the continuous phase, ρ_C is the density of the continuous phase, and ρ_D is the density of the dispersed phase.

$$(U_D + U_C)_{50\% offlooding} = 0.5 \cdot \frac{(U_D + U_C)_f}{u_0} \cdot u_0 \tag{58}$$

Equation 58 variables: $(U_D + U_C)_{50\% offlooding}$ is the total superficial velocity when the column is operating at 50% of the flooding capacity, $(U_D + U_C)_f$ is the total superficial velocity when the column is flooding, and u_0 is the velocity of a dispersed droplet.

$$A = \frac{\frac{m_C}{\rho_C} + \frac{m_D}{\rho_D}}{(U_D + U_C)_{50\% offlooding}} \tag{59}$$

Equation 59 variables: A is the cross-sectional area of the column, $(U_D + U_C)_{50\% offlooding}$ is the total superficial velocity when the column is operating at 50% of the flooding capacity, m_D is the mass flow rate of the dispersed phase, m_C is the mass flow rate of the continuous phase, ρ_C is the density of the continuous phase, and ρ_D is the density of the dispersed phase.

$$D = \sqrt{\frac{4A}{\pi}} \tag{60}$$

Equation 60 variables: D is the diameter of the column, and A is the column's cross-sectional area. After the column diameter was determined, the column height was calculated using the following equations.[57,60]

$$HETS = \frac{HETS}{D_T^{1/3}} \cdot D^{1/3} \tag{61}$$

Equation 61 variables: HETS is the height of a theoretical equilibrium stage and D is the diameter of the column.

$$H = HETS \cdot N \tag{62}$$

Equation 62 variables: HETS is the height of a theoretical equilibrium stage, N is the number of stages in the column, and H is the height of the column.

The final design specifications are as follows. The column will have 15 stages, a diameter of

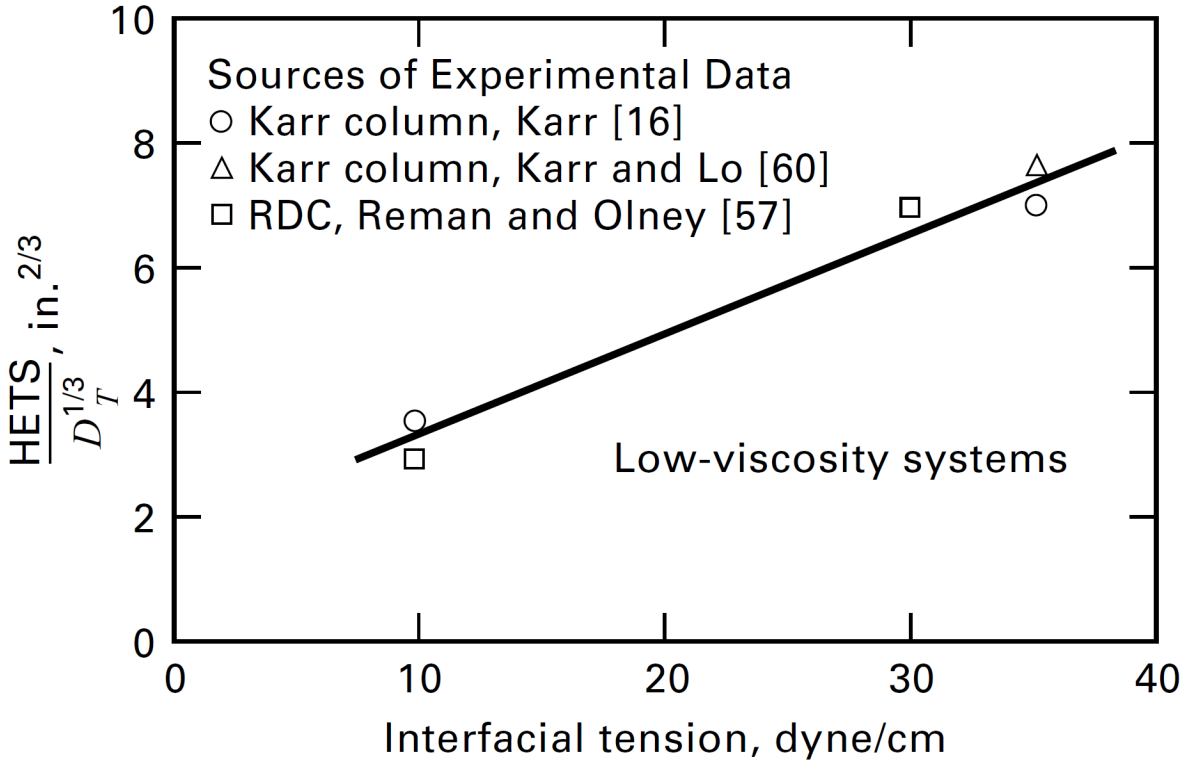

Figure 19: $\frac{HETS}{D_T^{1/3}}$ vs Interfacial Tension from Seader et al. (2010).[57] This graph is used to determine $\frac{HETS}{D_T^{1/3}}$ for equation 61.

Table 12: Overall Mass Balance for Liquid-Liquid Extractor (D6)

Mass [kg/hr]	D6a	D6e	D6f	D7a	D7b
Water	8,363	0	24.9	3,263	5,126
Glyceric acid	162	0	0.440	135	27.5
Glyceraldhyde	16.3	0	0.520	13.9	2.90
D-Gluconic acid	14.0	0	0	13.1	0.9
Lactic Acid	3335	0	7.25	3228	114
Glucose	0.270	0	0	0.140	0.140
Trioctylamine	0	42.7	557	557	42.7
Octanol	0	7.42	4393	4397	3.31
Na^+	653	0	0	0	653
Sulfuric Acid	0	0	0	0	0
$Bisulfate^-$	1,907	0	0	0	1907
Total	14452	50	4983	11607	7878

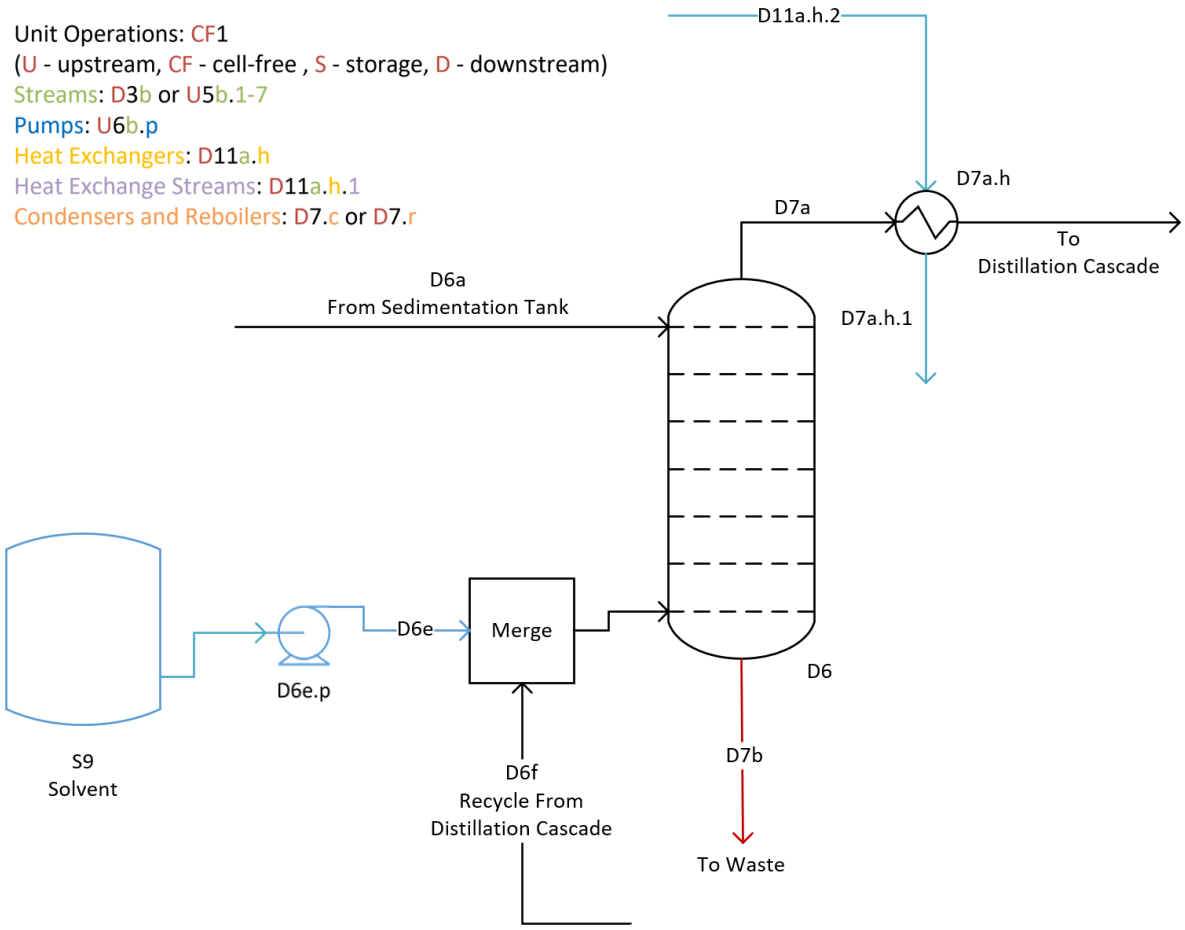

Figure 20: Process Flow Diagram for the Liquid-Liquid Extractor

1.57 meters, and a height of 4.97 meters. It will be made out of stainless steel. The process flow diagram of this unit operation is shown in Figure 20, and the overall mass balance is shown in Table 12. The feed stream (D6a) coming into the liquid-liquid extractor has a pH of 1.5. This pH results in the highest distribution coefficient.[56] The lower pH prevents TOA from entering the aqueous phase and protonates the lactic acid. The solvent stream being fed is about 12% TOA, which is the composition that has the highest distribution coefficient with the least amount of TOA required.[56] The solvent stream (D6e) will mix with the recycle stream (D6f) from the distillation cascade before being fed into the liquid-liquid extractor. The product stream (D7a) coming out of the top of the extractor will go into the distillation cascade. This stream has a significant intermediate byproduct, but the distillation cascade will separate most of it from the lactic acid. The waste stream (D7b) leaving the bottom of the extractor will be treated at the facility due to the need to neutralize the stream's sulfuric acid, organic chemicals, and sodium bisulfate. All sulfuric acid, bisulfate ions, and sodium ions will be assumed to be left in the waste stream (aqueous phase) due to their acidity and high polarity.[61] The process had a lactic acid recovery of 97%.

3.3.5 Distillation Cascade

The final separation process resulting in our lactic acid product is a distillation cascade containing three distillation columns and a decanter. This cascade allows the recycling of nearly one hundred percent of the octanol and trioctylamine used in the liquid-liquid extractor while removing most of the water produced and fed in earlier stages of the production process. The result is a 95.6 percent purity lactic acid stream with the remaining 4.4 percent of the product consisting of glycerate, gluconate, and glucose. There are a few technical issues that would need to be addressed prior to plant construction, namely lower than atmospheric pressures in all of the columns, but these issues were necessary to meet separation goals while maintaining low reboiler temperatures. As seen in Figure 21, the cascade first separates out the wastewater stream (stream D10a) in the first column (D7) and the decanter (D10). Then the cascade separates and recycles all of the octanol in the second column (D8) and ends in the third column (D9) with the separation and recycling of trioctylamine. The modeling, sizing, and costing of this part of the process were completed in ASPEN Plus v14 using NRTL properties under Vapor-Liquid-Liquid

Equilibrium. Two ASPEN Plus files were used, one with the correct components used to determine the correct material balances, column internal conditions (pressure, stage temperatures, number of stages) and another used to size and price the unit operations and their ancillary systems where materials in notably small quantities with missing properties in ASPEN Plus were approximated as chemicals that left the system at the same location (glyceraldehyde as water and glycerate, glucose, and gluconate as lactic acid).

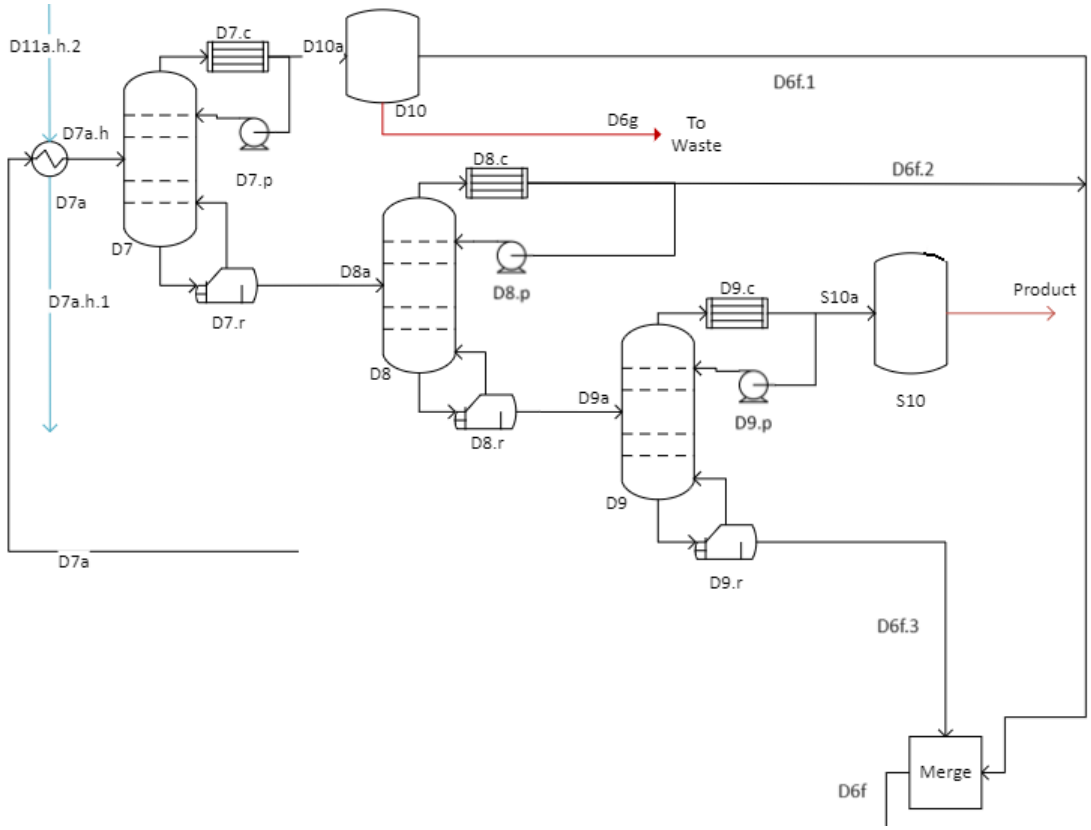

Figure 21: Process Flow Diagram of the Distillation Cascade

There were a set of design criteria and chemical properties that shaped the design of each column within the cascade. The first property is the decomposition temperature of lactic acid at 185°C. This limited the operating temperatures within the column to less than 185°C which could be met by decreasing the column pressure or reducing the distillate to feed ratio. The lower pressures of the columns were all used to reduce the heat duty of the reboilers and condensers as well as lower the lower-stage temperatures. The main drive during design was the separation of water and the organic extraction chemicals from each other and from the final lactic acid product. All of these materials had higher decomposition temperatures in solution (higher than 215°C)

than lactic acid and therefore were not temperature-limiting chemicals. The other chemicals within the process, glycerate, glucose, and gluconate, left the column with the lactic acid product stream and glyceraldehyde left with the wastewater stream were not of decomposition concern because they were not necessary for the product or being recycled.

The second design criterion was to model all condensers as total condensers which allowed all of the vapor coming out the top of the columns to be treated as two liquid streams (distillate and reflux streams). This allowed these streams to be recycled without needing to consider multiple phases being present in each stream except in the case of the water separation column (D7) which had an octanol and a water liquid phase which resulted in a decanter (D10) being used to separate the two phases. The condensers were all treated as shell and tube heat exchangers when being sized. Additionally, the reboilers were all treated as kettle reboilers which allowed them to be approximated as shell and tube heat exchangers when being sized as well. The steam streams going into the reboiler were made consistent at one hundred and sixty-five psig which heated them to approximately 250°C and left the reboilers at 240°C. This was the temperature needed to efficiently heat the third column (D9) and was also used to heat the second column reboiler (D9.r). This is the upper end of steam pressure and temperature used in industry and represents a potential area of optimization. The first column reboiler (D7.r) is heated at one hundred psig. All of the condensers used cooling water entering the heat exchangers at 30°C and exiting the heat exchangers at 45°C based on industry standards.

These columns were designed as sieve tray columns instead of packed columns or bubble trays for several reasons. Tray columns provide clear heights, and the tray separation times the number of trays, compared to packed columns which require a more complex set of calculations making their performance less predictable.[62] Plate columns are also less prone to back mixing and provide more positive contact between liquid and vapor streams by repeating mixing and separation. Most importantly, plate columns reduce the probability of flooding which is an issue at high liquid loads.[62] All three columns have high liquid loads throughout the column in this cascade. This was deemed more advantageous than the reduced pressure drop provided by packed columns during vacuum distillation or by the cheaper operation cost at smaller diameters. Sieve trays were chosen because they are more efficient than bubble trays[62] and because they

serve as the ASPEN default simplifying calculations. The weeping issue, the worst aspect of sieve trays, is mitigated by the high vapor flow rate through the tray perforations which should maintain efficiency over a similarly sized bubble-tray.[62] Trays were spaced at 0.6096 meters for all of the columns because it is the industry standard and allows for easier cleaning.[63] Based on the composition of the streams flowing through these unit operations, all of the equipment is made of stainless steel in order to reduce acidic damage or excessively fast chemical buildup.

The final major assumption that remained consistent throughout all three distillation columns was that each column could be approximated between fifty and sixty percent efficiency based on industrial estimates.[64] Typical distillation columns operating below atmospheric pressure, as is the case with all of the distillation columns in this cascade, have listed efficiencies between forty and fifty percent for bubble-tray columns. This is much lower than at atmospheric pressure because the contact time between vapor and liquid at each stage is shortened.[62] Given that this cascade functions with sieve trays, which have slightly better efficiencies than bubble trays, efficiencies between fifty and sixty percent were used to estimate the number of actual trays needed to meet the separation specifications.

All of the recycle streams are recombined and fed through a heat exchanger (D6f.h) and then a pump (D6f.p). The heat exchanger lowers the combined recycle stream (stream D6f) from 125.4℃ to 22℃ in order to match the organic separation chemical flow temperature entering the LLE. The cooling water used in D6f.h required a temperature of 15℃ to reach 22℃ as needed in the LLE. The pump raises the stream pressure from one tenth of an atmosphere to one atmosphere which is the LLE operating pressure. Both of these unit operations are addressed in the ancillary equipment section.

3.3.5.1 Column 1 (D7): Wastewater Separation from Lactic Acid

The first column separates out the entire quantity of water through the distillate and feeds a ninety percent water stream, ten percent octanol stream, and trace amounts of glyceraldehyde into the decanter (D10) for further separation. The remaining components from the feed stream (D7a), including the product lactic acid, flow out the bottoms (D8a). The material balance of the water separation column is shown in Table A7. The removal of water is treated as the highest

priority aspect of this step, so other factors were sacrificed in order to meet the separation goals.

While water only comprises 28 mass percent of the feed stream, it comprises seventy-one molar percent of the feed into D7. This consideration set a high molar distillate to feed ratio for the column. Octanol and lactic acid made up the majority of the remaining mass and molar flow in the feed. As seen in Table A7, the wastewater stream (stream D10a), exiting the condenser (D7.c) and heading to the decanter (D10), is composed of ninety mass percent water and ten mass percent octanol. Because water is a waste product of this process, the amount of octanol in this stream poses a potentially high replacement cost. This separation issue is solved by feeding stream D10a into a decanter. Lactic acid comprises forty percent, octanol comprises fifty-one percent, and trioctylamine comprises seven percent of the mass flowing from the reboiler (D7.r) into D8 for further separation.

The pressure of the column was set at one-tenth of an atmosphere. To remove all of the water from the bottom stream (stream D8a), a distillate-to-feed ratio of 0.725 was used. The reflux ratio that resulted in the most separation between octanol and water was fifteen. The feed stage was set at stage ten. All of these values were found by varying their values in ASPEN until the stream separation was maximized at the set pressure and number of stages. In order to get a 9:1 mass ratio of water to octanol, an ideal number of stages was calculated using Equation 63 where the relative volatility between the light and heavy key components was found using vapor pressures at the temperature of the bottom stage of the column. The work in Figure A17 shows that eleven is the ideal number of stages. The total vapor pressures are sourced from NIST with octanol and water being treated as the heavy and light key components respectively because they were the hardest two chemicals to separate. With an estimated efficiency of fifty-five percent based on the industrial standards and assumptions discussed, the actual number of twenty stages or eighteen trays.

$$n_{\text{min}} + 1 = \frac{\log\left(\frac{x_{\text{LK,D}}}{x_{\text{HK,D}}} \cdot \frac{x_{\text{HK,B}}}{x_{\text{LK,B}}}\right)}{\log(\alpha)} \tag{63}$$

The column height was found using Equation 64, which takes the number of trays multiplied

by the standard height between trays (0.6096 meters). That resulted in D7 being 10.97 meters tall.

$$\text{Height} = (\text{tray spacing}) \times (\text{Number of Trays}) = 0.6096 \times N \tag{64}$$

The diameter was found using a five-step process from Wankat's *Separation Process Engineering*. First, the flow parameter was calculated using Equation 65 where vapor density, (ρ_v), was found using a derivation of the ideal gas law, Equation 66, and the liquid density, (ρ_l), was found using Equation 67.

$$F_{\text{lv}} = \left(\frac{W_{\text{l}}}{W_{\text{v}}}\right)\left(\frac{\rho_{\text{v}}}{\rho_{\text{l}}}\right)^{\frac{1}{2}} \tag{65}$$

Where W_l is the liquid mass flow rate in kg/h and W_v is the vapor mass flow rate in kg/h.

$$\rho_v = \frac{P \cdot MW}{R \cdot T} \tag{66}$$

Where P is the column pressure in atmospheres, MW is the molecular weight in kg/mol, R is the gas constant in $\frac{\text{m}^3\cdot\text{atm}}{\text{mol}\cdot\text{K}}$, and T is temperature in Kelvin.

$$\rho_l = (\text{specific gravity}) \times (\text{density of water}) = (SG) \times (1000) \tag{67}$$

Because the flows at the top of the column are composed almost entirely of octanol, all of the chemical-specific parameters were approximated as octanol. The liquid-vapor ratios, temperatures, pressures, and initial liquid and vapor flow rates were approximated using values from the center trays in each section as listed in the stream profiles section of ASPEN Plus. The mass flow rate ratios were then approximated as the liquid-vapor flow ratios because the chemical composition of both the liquid and vapor flows is almost completely octanol. The flow parameter was then used in conjunction with the twenty-four-inch tray spacing to determine the capacity factor for flooding using Figure 22.

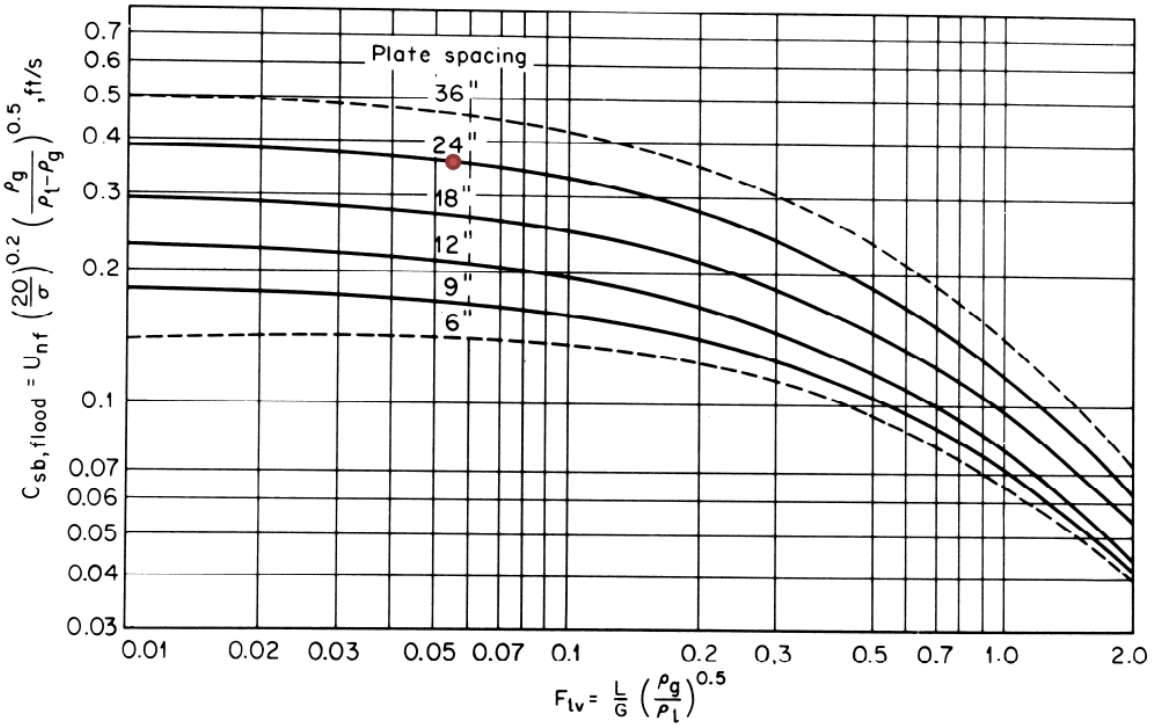

Figure 22: Capacity factor for flooding of sieve trays from Fair and Matthews (1958)

The third step is to use the found capacity factor for flooding to determine the flooding velocity with Equation 68.

$$u_{\text{flood}} = C_{\text{sb,f}} \left(\frac{\sigma}{20}\right)^{\frac{1}{5}} \left(\frac{\rho_{\text{l}} - \rho_{\text{v}}}{\rho_{\text{v}}}\right)^{\frac{1}{2}} \tag{68}$$

Where u_{flood} is flooding velocity in ft/s and (σ) is surface tension in dynes.

The surface tension was again approximated as the dominant component in the stream profile, octanol. The fourth step is to determine the vapor flow rate using Equation 69.

$$V = \frac{D}{1 - \frac{L}{V}} \tag{69}$$

Where V is the Vapor Molar Flow Rate, L is the Liquid Molar Flow Rate, and D is the Distillate Molar Flow Rate, all in mol/h.

The distillate value was taken as the distillate flow rate in the ASPEN stream table. The diameter of the top and bottom sections of the column was finally found using Equation 70.

$$\text{Dia} = \left(\frac{4V \cdot \text{MW}}{\pi \cdot \eta \cdot \rho_v \cdot 0.8 \cdot u_{\text{flood}}} \right)^{\frac{1}{2}} \tag{70}$$

Where (η) is stage efficiency and Dia is the column diameter in meters.

The flooding fraction was assumed as 0.8.[65] The column efficiency was assumed to be the section efficiency. The top section was found to be 12.2 meters in diameter and the bottom section was found to be 9.25 meters in diameter. The complete set of calculations can be found in Table A8 labeled as Column 1. However, many of the assumptions laid out in finding these diameters were not the most accurate assumptions, so the diameters were recalculated using the column internals feature of ASPEN Plus. It was found that the diameters calculated in ASPEN Plus were within half a meter of each other, so instead of simulating the diameters for independent sections, the one diameter was simulated for the entire column to reduce the initial fixed cost of the column. This diameter was found to be 10.73 meters and was used as the official diameter for further sizing and cost estimations.

The condenser (D7.c) had a distillate outlet temperature of 58.1°C and a heat duty of 35340 kilowatts. The design as a shell and tube heat exchanger was completed by ASPEN Plus. The heat exchange area was 889 square meters. The tubes were 0.0254 meters in outer diameter and 6.096 meters in length. The tubes were spaced 0.03175 meters apart in a triangular configuration. There were 1828 tubes in the condenser and an expected inner shell diameter of 1.43 meters which is at the upper limit of commercially manufactured heat exchangers.[66] Sizing data can be found in Table A9 under C1-Condenser. The reflux pump (D7.p) was treated as a centrifugal pump with an efficiency of 0.7. The material flowing through the pump had a specific gravity of 0.942, between water and octanol, and a flow rate of 1128 liters per minute. The reflux pump was designed to meet a reflux rate of 2768 kilomoles per hour and has a differential pressure of one atmosphere per the ASPEN simulation. This reflux pump requires 35.16 kilowatts to operate.

The reboiler (D7.r) had a bottom outlet temperature of 155.4°C and a heat duty of 36017 kilowatts. The design as a shell and tube heat exchanger was completed by ASPEN Plus. The heat exchange area was 4976 square meters. The tubes were 0.0254 meters in outer diameter

and 6.096 meters in length. The tubes were spaced 0.03175 meters apart in a triangular configuration. This reboiler uses 100 psig steam to maintain the reboiler operating temperature. There were 10229 tubes in the reboiler and an expected inner shell diameter of 1.85 meters which is outside the upper limit of commercially manufactured heat exchangers and would require a specially made design.[66] Sizing data can be found in Table A9 under C1-Reboiler. Both the condenser and reboiler sizes being outside or at the upper limit of commercial heat exchanger design means that the cost of these pieces of equipment far exceeds not only the cost of all other heat exchangers in the cascade combined but also the cost of any of the distillation towers.

3.3.5.2 Column 2 (D8): Octanol Recycle Separation from Lactic Acid

The second column separates out the remaining quantity of octanol through the distillate and feeds a 99.8 percent octanol stream with trace amounts of lactic acid and glycerate into a recycle stream (stream D6f.2) entering the recycle stream mixer. The remaining components from the feed stream, including the product lactic acid and trioctylamine, flow out the bottoms. The material balance of the octanol separation column is shown in Table A10. The removal of octanol is treated as the priority aspect of this step, so other factors were sacrificed in order to meet the separation goals.

Octanol comprises fifty-one mass percent of the feed stream and forty-five molar percent of the feed into D8. This consideration set the molar distillate to feed ratio for the column at 0.447. Lactic acid made up forty percent, trioctylamine comprised seven percent, and glycerate comprised two percent of the mass flows in the feed. As seen in Table A10, the octanol recycle stream (stream D2f.2), exiting the condenser (D8.c) and heading to the recycle stream mixer, is composed of 99.8 mass percent octanol and 0.2 mass percent lactic acid. This process recycles nearly all of the octanol passing through distillation back into the LLE. Lactic acid comprises eighty-two percent, trioctylamine comprises fourteen percent, and glycerate comprises about four percent of the mass flowing from the reboiler (D8.r) into D9 for further separation.

The pressure of the column was set at one-tenth of an atmosphere. To remove all of the octanol from the bottoms stream (stream D9a), a distillate-to-feed ratio of 0.447 was used. The reflux ratio that resulted in the most separation between octanol and water was six. The feed stage was

set at stage eighteen. All of these values were found by varying their values in ASPEN until the stream separation was maximized at the set pressure and number of stages. To get a 998:2 mass ratio of octanol to lactic acid in the distillate, an ideal number of stages was calculated using Equation 63 where the relative volatility between the light and heavy key components was found using vapor pressures at the temperature of the bottom stage of the column. The work in Figure A18 shows that twenty-six is the ideal number of stages. The total vapor pressure of octanol was sourced from NIST and the total vapor pressure of lactic acid was sourced from ChemBook. Octanol was treated as the light key component and lactic acid was treated as the heavy key component because they had the closest relative volatilities. With an estimated efficiency of fifty-five percent based on the industrial standards and assumptions discussed, the actual number of stages was forty-nine or forty-seven trays.

The column height was found using Equation 64, which takes the number of trays multiplied by the standard height between trays (0.6096 meters). That resulted in D8 being 28.65 meters tall. The diameter was found using a five-step process from Wankat's *Separation Process Engineering* as described in Section 3.3.5.1.

Because the flows at the top of the column are composed almost entirely of octanol, all of the chemical-specific parameters were approximated as octanol for the top section. Because the bottom streams of the column were composed almost entirely of lactic acid, all of the chemical-specific parameters were approximated as lactic acid for the bottom section. The top section was found to be 2.55 meters in diameter and the bottom section was found to be 2.64 meters in diameter. The complete set of calculations can be found in Table A8 labeled as Column 2. However, many of the assumptions laid out in finding these diameters were not the most accurate assumptions, so the diameters were recalculated using the column internals feature of ASPEN Plus. It was found that the diameters calculated in ASPEN Plus were within half a meter of each other, so instead of simulating the diameters for independent sections, the one diameter was simulated for the entire column to reduce the initial fixed cost of the column. This diameter was found to be 3.04 meters and was used as the official diameter for further sizing and cost estimations.

The condenser (D8.c) had a distillate outlet temperature of 142.6℃ and a heat duty of 3382 kilowatts. The design of a shell and tube heat exchanger was completed by ASPEN Plus. The heat exchange area was 40.7 square meters. The tubes were 0.0254 meters in outer diameter and 6.096 meters in length. The tubes were spaced 0.03175 meters apart in a triangular configuration. There were 84 tubes in the condenser and an expected inner shell diameter of 0.67 meters which is within the range of conventionally manufactured heat exchangers.[66] Sizing data can be found in Table A9 under C2-Condenser. The reflux pump (D8.p) was treated as a centrifugal pump with an efficiency of 0.7. The material flowing through the pump had a specific gravity of 0.728, around the specific gravity of octanol at one-tenth of an atmosphere, and a flow rate of 715 liters per minute. The reflux pump was designed to meet a reflux rate of 187 kilomoles per hour and has a differential pressure of one atmosphere. This reflux pump requires 28.74 kilowatts to operate.

The reboiler (D8.r) had a bottoms outlet temperature of 171.1℃ and a heat duty of 3384 kilowatts. The design as a shell and tube heat exchanger was completed by ASPEN Plus. The heat exchange area was 414 square meters. The tubes were 0.0254 meters in outer diameter and 6.096 meters in length. The tubes were spaced 0.03175 meters apart in a triangular configuration. This reboiler uses 165 psig steam to maintain the reboiler operating temperature. There were 852 tubes in the reboiler and an expected inner shell diameter of 1.23 meters which is within the range of conventional manufactured heat exchangers.[66] Sizing data can be found in Table A9 under C2-Reboiler.

3.3.5.3 Column 3 (D9): Trioctylamine Recycle Separation from Lactic Acid

The third column separates out the entire quantity of trioctylamine through the bottoms and feeds a 99.8 percent water stream and trace amounts of glycerate and lactic acid into the recycle stream (stream D6f.3) mixer for recycling into the LLE. The remaining components from the feed stream make up the product and flow out of the bottoms (S10a) into the product storage tank (S10). The material balance of the trioctylamine separation column is shown in Table A11. The removal of trioctylamine is treated as the highest priority aspect of this step, so other factors were sacrificed in order to meet the separation goals.

Trioctylamine comprises fourteen mass percent of the feed stream and comprises four molar percent of the feed into D9. This consideration set a high molar distillate to feed ratio for the column. Lactic acid made up the majority of the mass and molar flows in the feed. As seen in Table A11, the trioctylamine recycle stream (stream D6f.3), exiting the reboiler (D9.r) and heading to the recycle stream mixer, is composed of 99.8 mass percent trioctylamine with trace amounts of glycerate and lactic acid. This process recycles all of the trioctylamine passing through distillation back into the LLE. Lactic acid comprises 95.6 percent and glycerate (along with glucose and gluconate) comprises about 4.4 percent of the mass flowing from the condenser (D9.c) into S10 as the final purified product.

The pressure of the column was set at one-tenth of an atmosphere. To remove all of the trioctylamine from the product stream (stream S10a), a distillate-to-feed ratio of 0.959 was used. The reflux ratio that resulted in the most separation between octanol and water was five. The feed stage was set at stage ten. All of these values were found by varying their values in ASPEN until the stream separation was maximized at the set pressure and number of stages. To get a 991:1 mass ratio of trioctylamine to lactic acid in the bottoms, an ideal number of stages was calculated using Equation 63 where the relative volatility between the light and heavy key components was found using vapor pressures at the temperature of the bottom stage of the column. The work in Figure A19 shows that thirteen is the ideal number of stages. The total vapor pressure of trioctylamine was sourced from EChemi and the total vapor pressure of lactic acid was sourced from ChemBook. Lactic acid was treated as the light key component and trioctylamine was treated as the heavy key component because they were the most important materials to separate. With an estimated efficiency of fifty-five percent based on the industrial standards and assumptions discussed, the actual number of stages was twenty-four or twenty-two trays.

The column height was found using Equation 64, which takes the number of trays multiplied by the standard height between trays (0.6096 meters). That resulted in D9 being 13.41 meters tall. The diameter was found using a five-step process from Wankat's *Separation Process Engineering* as described in section 3.3.5.1.

The top section was found to be 2.45 meters in diameter and the bottom section was found to be 2.80 meters in diameter. The complete set of calculations can be found in Table A8 labeled as Column 3. However, many of the assumptions laid out in finding these diameters were not the most accurate assumptions, so the diameters were recalculated using the column internals feature of ASPEN Plus. It was found that the diameters calculated in ASPEN Plus were within half a meter of each other, so instead of simulating the diameters for independent sections, the one diameter was simulated for the entire column in order to reduce the initial fixed cost of the column. This diameter was found to be 2.85 meters and was used as the official diameter for further sizing and cost estimations.

The condenser (D9.c) had a distillate outlet temperature of 102.6°C and a heat duty of 4773 kilowatts. The design as a shell and tube heat exchanger was completed by ASPEN Plus. The heat exchange area was 24.3 square meters. The tubes were 0.0254 meters in outer diameter and 6.096 meters in length. The tubes were spaced 0.03175 meters apart in a triangular configuration. There were 50 tubes in the condenser and an expected inner shell diameter of 0.54 meters which is within the range of conventionally manufactured heat exchangers.[66] Sizing data can be found in Table A9 under C3-Condenser. The reflux pump (D9.p) was treated as a centrifugal pump with an efficiency of 0.7. The material flowing through the pump had a specific gravity of 0.817, around the specific gravity of lactic acid at one-tenth of an atmosphere, and a flow rate of 112 liters per minute. The reflux pump was designed to meet a reflux rate of 185 kilomoles per hour and has a differential pressure of one atmosphere. This reflux pump requires 23.85 kilowatts to operate.

The reboiler (D9.r) had a bottoms outlet temperature of 182.2°C and a heat duty of 4588 kilowatts. The design as a shell and tube heat exchanger was completed by ASPEN Plus. The heat exchange area was 244 square meters. The tubes were 0.0254 meters in outer diameter and 6.096 meters in length. The tubes were spaced 0.03175 meters apart in a triangular configuration. This reboiler uses 165 psig steam to maintain the reboiler operating temperature. There were 502 tubes in the reboiler and an expected inner shell diameter of 1.11 meters which is within the range of conventional manufactured heat exchangers.[66] Sizing data can be found in Table A9 under C3-Reboiler.

3.3.5.4 Decanter (D10): Wastewater Separation from Octanol Recycle

The decanter (D10) separates most of the wastewater from the octanol leaving the condenser of the first column (D7.c) and feeds a ninety-three percent octanol and a seven percent water stream into the recycle stream (stream D6f.1) mixer for recycling into the LLE. The remaining components from the feed stream are treated as wastewater and flow out the bottom of the decanter (stream D6g) to be treated. The material balance of the decanter is shown in Table A12. The recovery of octanol is treated as the highest priority aspect of this unit, so other factors were sacrificed in order to meet the separation goals. Temperature and pressure were varied to maximize the water-octanol separation.

Water comprises ninety mass percent of the feed stream and comprises 98.4 molar percent of the feed into D10. Octanol comprises 9.5 percent and glyceraldehyde comprises 0.5 percent of the mass flow rate in the feed. As seen in Table A12, the octanol recycle stream (stream D6f.1), exiting the top of the decanter (D9.r) and heading to the recycle stream mixer, is composed of ninety-three mass percent octanol and seven mass percent water. This process recycles nearly all of the octanol loss to wastewater in stream D10a back into the LLE. Water comprises 99.5 percent and glyceraldehyde comprises 0.5 percent of the mass flowing from the bottom of the decanter as a waste stream.

The pressure of this vessel was set at one-tenth of an atmosphere and an operating temperature of 115°C to separate the octanol and water mixture. One-tenth of an atmosphere is used to maximize the octanol-water separation and minimize octanol loss into the wastewater stream. The decanter requires 247 kilowatts to meet the operating temperature. ASPEN Plus completed the sizing and costing of this vessel. It has a 2402-liter volume. The decanter is 0.91 meters in diameter and 3.66 meters tangent to the tangent height.

3.3.5.5 Potential Improvements in the Distillation Cascade

A summary of the cascade parameters can be seen in Table 13. This cascade is not fully optimized as suggested by the consistent pressure through the columns. This is driven in large part by two factors, a high degree of separation between components in all three columns and maintaining column temperatures below 185°C to prevent the decomposition of lactic acid. This

Table 13: Distillation Cascade Operating and Design Parameters

Unit Operation	Unit Name	Temperature (°C)	Pressure (bar)	Size	Heat Duty (kW)
Water Separation Column	D7	58-155	0.101	D = 10.72m H = 10.97m	N/A
D7 Condenser	D7.c	58	0.101	A = 889sqm	35,659
D7 Reboiler	D7.r	155	0.101	A = 4976sqm	36,346
Octanol Separation Column	D8	142-171	0.101	D = 3.04m H = 28.65m	N/A
D8 Condenser	D8.c	142	0.101	A = 40.7sqm	3,511
D8 Reboiler	D8.r	171	0.101	A = 414sqm	3,513
TOA Separation Column	D9	103-182	0.101	D = 2.85m H = 13.41m	N/A
D9 Condenser	D9.c	103	0.101	A = 24.3sqm	3,962
D9 Reboiler	D9.r	182	0.101	A = 244sqm	4,596
Decanter	D10	115	0.101	D = 0.91m H = 3.66m	247

limited column optimization and resulted in 0.1 atmosphere being the pressure used in each column. Using lower than atmospheric pressures in the cascade increased column cost significantly because it increased the number of trays in the (and therefore the heights of the) columns by a factor of 2 compared to atmospheric pressure columns.[64] Doubling the efficiency and halving the number of stages as in atmospheric conditions would decrease the price of each tower by 30% to 40%. These pressures could be increased if the separation purities of the distillate and bottoms streams were reduced. To accomplish that, the recycle stream or the product stream would have to be less pure which would levy additional expenses for either solvent replenishment and waste disposal or a lower product revenue driven by a lower price point respectively.

The other major cost was the removal of water which resulted in a massive condenser and reboiler in the water separation column (D7). The reboiler has the highest individual utility cost each year due to the heat duty needed to maintain the separation purities in each stream. Decreasing the distillate purity within this column or finding a way to remove more water earlier in the process at a cheaper rate would reduce the necessary heat duty and significantly reduce annual utility expenses.

Another optimization consideration is the large diameter (10.73m) of the water separation column (D7) which is approximately equal to its height (10.97m). The large diameter of the column, relative to its height, is the result of maximizing the vapor flow rate which is extremely

high due to the high flow rates entering the column paired with the high degree of separation. It is also the result of reducing the column energy demands which reduces the reboiler duty and cost of this utility. To solve this problem, multiple columns could be used, the degree of separation could be reduced, or the reboiler utility cost being lowered would allow for the column diameter to shrink and reduce the expense of D7.

The limiting factor in this process is the decomposition temperature of lactic acid which limits the column specifications when operating with high separation goals. Keeping this limitation in mind while optimizing these factors and adjusting column design is necessary to maintain realism in this design.

3.4 Ancillary Equipment

3.4.1 Pump Design

For the enzyme bioreactors upstream, there will be two main uses of pumps: one for draining end-of-fermentation broth and the second for supplying water to the reactors at the beginning of the fermentation. These will have varying power capacities and will be stainless steel centrifugal pumps. Pumps U2a.p, U3a.p, U4a.p, and U5a.p will pump fermentation broth from U2 to U3, U3 to U4, U4 to the production bioreactors (U4 and U5.2-9), respectively. Pumps U6a.p1 and S3.p will pump the recycled inoculation broth back into the production bioreactors. Pumps U2b.p, U3b.p, U3b.p, and U5c.p will pump water into bioreactors U2, U3, U4, and U5.2-9, respectively.

Pump U6b.p will take the merged production fermentation broth to the disk stack centrifuge. Pump U7b.p will take the waste sludge to the incinerator and U7a.p will take the supernatant to the ultrafiltration membrane. Pump U8b.p will take the wastewater to be disposed and U8a.p will take the concentrated protein to the cell-free storage tank.

Details of these pumps including the flowrate through them and their annual power can be found in Table 19 in Section 4.3.4. The accompanying visual for the upstream ancillary equipment can be found in Appendix A1.

For the nanofiltration membrane system (D1 to D4) shown in Figure 23, the following cen-

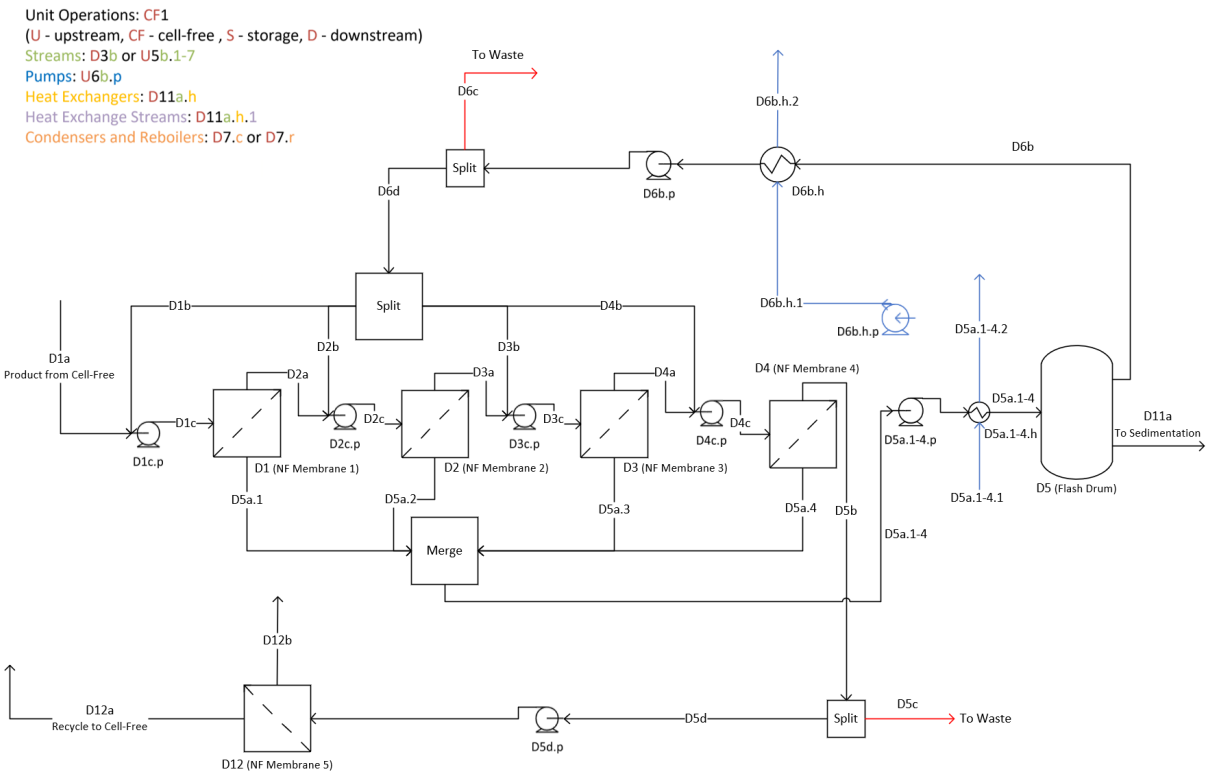

Figure 23: Process Flow Diagram of Nanofiltration System and Flash Drum

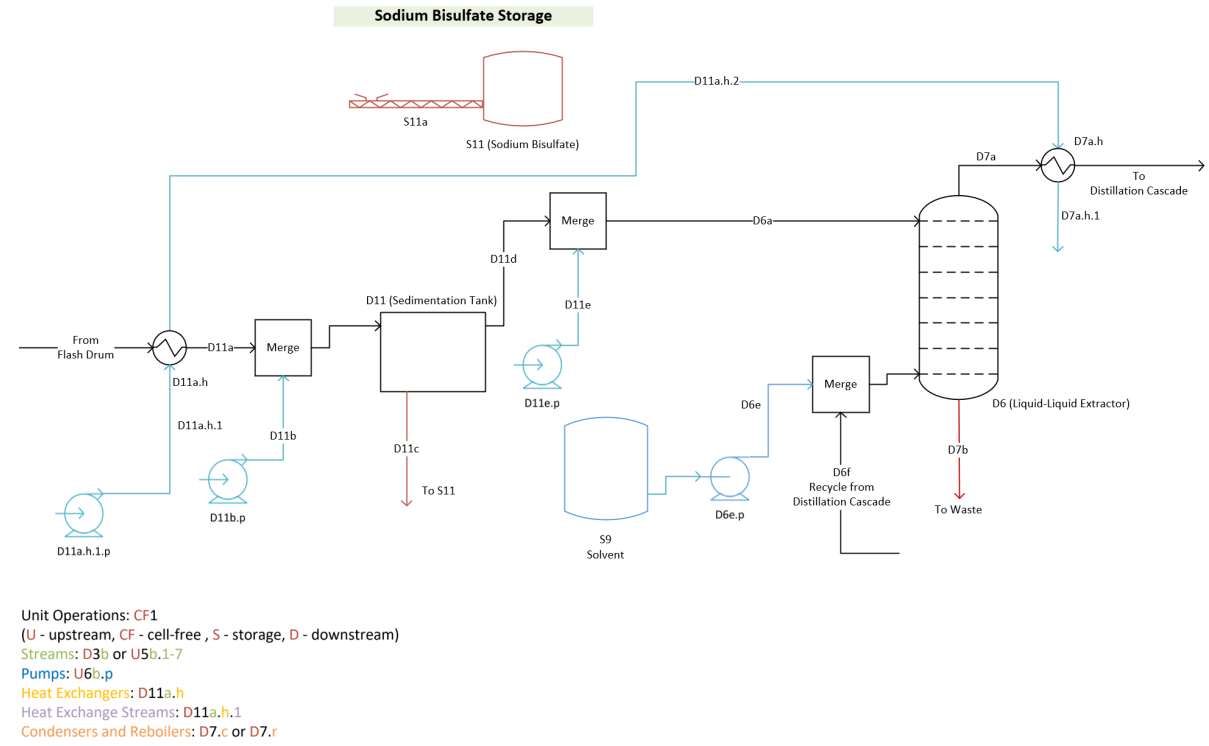

Figure 24: Process Flow Diagram of Sedimentation Tank and Liquid-Liquid Extractor

trifugal pumps will pressurize and transport a unit's feed streams: D1c.p, D2c.p, D3c.p, and D4c.p. Each pump will pressurize its respective stream to 30 bar for the nanofiltration membranes.

For the additional nanofiltration membrane (D12), one turbine and one centrifugal pump will be utilized. The pump, D5d.p, will pressurize stream D5d to 30 bar for the nanofiltration membrane. The turbine, D12a.p, will depressurize the stream D12a from 27 bar to 1 bar.

For the flash drum (D5), one turbine and one centrifugal pump is used. The turbine, D5a.1-4.p, will depressurize the stream D5a.1-4 from 27 bar to 2.03 bar. The centrifugal pump, D6b.h.p, will be used to transport cooling water into a heat exchanger (D6b.h).

For the sedimentation tank (D11), three pumps will be used: D11a.h.1.p, D11b.p, and D11e.p. Pump D11a.h.1.p will be used to transport cooling water into two heat exchangers (D11a.h and D7a.h). Pump D11b.p will be used to transport sulfuric acid to the sedimentation tank. Pump D11e.p will be used to transport makeup water to the liquid-liquid extractor.

For the liquid-liquid extractor (D6), one pump will be used. This pump, D6e.p, will be used to transport the solvent mixture of octanol and trioctylamine into the liquid-liquid extractor. Another centrifugal pump, D6f.p will be used in the recycle stream (stream D6f) from the distillation cascade to raise the stream pressure from 0.1 atm to 1 atm.

All pumps are outlined in Table 19 in Section 4.3.4.

3.4.2 Tank and Miscellaneous Equipment Design

In the upstream portion of the plant, 4 silos will be used to house 4 weeks of raw materials. Each tank will be 10,000 L, tanks S1 and S2 will contain glucose, and tanks S3 and S4 will contain media. Additionally, each silo will be equipped with a 10 ft screw conveyor to deliver solid media and glucose into the fermentation bioreactors, called S1a, S2a, S3a, and S4a. There will also be a temporary holding tank for the inoculation broth that is 8,000 L, called S5. Linking the upstream and cell-free reactor portion of the process, there will be a 150,000 L holding tank to house enzyme between cell-free reactions, called CF3.

In the downstream portion of the plant, 3 tanks will be used to store 4 weeks' worth of raw

materials. Tank S9 will store the needed solvent mixture for the liquid-liquid extractor. Tank S10 will store the lactic acid product. Tank S11 will store the sodium bisulfate byproduct. A screw conveyor (S11a) that has a power of 0.25 kW will be used to transport the sodium bisulfate from the sedimentation tank to tank S11.[67]

All tanks and other miscellaneous equipment are outlined in Section 4.3.4.

3.4.3 Heat Exchangers

All heat exchangers are modeled in ASPEN Plus for the following unit operations. For the flash drum (D5), two heat exchangers will be utilized: D5a.1-4.h and D6b.h. D5a.1-4.h is a shell and tube heat exchanger used to heat the stream D5a.1-4 from 50 degrees Celsius to 122 degrees Celsius. This will provide enough energy to the stream so that the flash drum will operate adiabatically. D5a.1-4.h will have a heat transfer area of 3244 m^2, one tube pass, and one shell pass. The tube will have a design pressure of 7.72 barg, a design temperature of 218 degrees Celsius, and an operating temperature of 122 degrees Celsius. The tube will be 6.096 meters long, with a pitch of 0.03175 meters and an outside diameter of 0.0254 meters. The shell will have a design pressure of 12.09 barg, a design temperature of 218 degrees Celsius, and an operating temperature of 190 degrees Celsius. D6b.h is a shell and tube heat exchanger that cools the stream D6b from 102 degrees Celsius to 50 degrees Celsius. This will condense the distillate steam into water used for the nanofiltration membranes. D6b.h will have a heat transfer area of 3079 m^2, one tube pass, and one shell pass. The tube will have a design pressure of 1 barg, a design temperature of 130 degrees Celsius, and an operating temperature of 33 degrees Celsius. The tube will be 6.096 meters long, with a pitch of 0.03175 meters and an outside diameter of 0.0254 meters. The shell will have a design pressure of 1 barg, a design temperature of 130 degrees Celsius, and an operating temperature of 102 degrees Celsius.

For the sedimentation tank (D11), one heat exchanger will be used: D11a.h. D11a.h is a shell and tube heat exchanger that uses cooling water to cool the stream D11a from 102 degrees Celsius to 33 degrees Celsius. D11a.h will have a heat transfer area of 111 m^2, one tube pass, and one shell pass. The tube will have a design pressure of 1 barg, a design temperature of 130 degrees Celsius, and an operating temperature of 93 degrees Celsius. The tube will be 6.096

meters long, with a pitch of 0.03175 meters and an outside diameter of 0.0254 meters. The shell will have a design pressure of 1 barg, a design temperature of 130 degrees Celsius, and an operating temperature of 1902 degrees Celsius.

One heat exchanger will be used for the liquid-liquid extractor (D6): D7a.h. D7a.h is a shell and tube heat exchanger that will heat the stream D7a from 33 to 53 degrees Celsius, the required feed stream temperature for the first distillation column. D7a.h will have a heat transfer area of 6.36 m^2, one tube pass, and one shell pass. The tube will have a design pressure of 0.0210 barg, a design temperature of 121 degrees Celsius, and an operating temperature of 93.3 degrees Celsius. The tube will be 6.096 meters long, with a pitch of 0.03175 meters and an outside diameter of 0.0254 meters. The shell will have a design pressure of 0.0210 barg, a design temperature of 121 degrees Celsius, and an operating temperature of 53 degrees Celsius.

Another heat exchanger, D6f.h, cools the recycle stream (stream D6f) into the LLE from the distillation cascade. D6f is a shell and tube heat exchanger used to cool stream D6f from 125 degrees Celsius to 22 degrees Celsius, the operating temperature for the LLE. D6f.h will have a heat transfer area of 29.18 m^2, one tube pass, and one shell pass. The tubes will have a design pressure of 0.02 barg, a design temperature of 153 degrees Celsius, and an operating temperature of 100 degrees Celsius. The tube will be 6.096 meters long, with a pitch of 0.03175 meters and a tube outer diameter of 0.0254 meters. The shell will have a design pressure of 0.02 barg, a design temperature of 154 degrees Celsius, and an operating temperature of 125 degrees Celsius. The shell's inner diameter is 0.58m with 60 tubes.

3.5 Waste Disposal

Most of the waste streams from the process will be treated onsite. This includes neutralizing acidic and basic components in stream D7b and deactivating enzymes and other bacterial components in streams U8b and D5c. The design of the equipment needed to treat the waste is out of our scope. Once treated, the following waste streams will be sent to a municipal wastewater facility: U8b, D5c, D12b, D7b, and D6g. The disposal costs associated with these waste streams can be found in Figure A28 to Figure A29. The sodium bisulfate stream (D11c) is treated differently than the other waste streams. This is because it is an inert solid that is not

significantly valuable. As a result, it is not economical to sell it as a product, and it does not require treatment. Because of this, the plant will throw it away in a landfill for $50 per ton.[68]

In the upstream portion of the process, specifically in stream U7b, a cell slurry will leave the process as waste out of the disk stack centrifuge. This stream contains genetically modified organisms and will require processing before being discarded. U7b will first be incinerated to remove this environmental biohazard to kill all viable cells. While this incinerator's design is out of this project's scope, the equipment cost will be included in the plant's cost. The ash from the incinerated cells will be disposed of as solid waste through a contract waste management company. Other routes to explore in the future for this waste stream could include harvesting the cells for use as a cheap nutrient source or as fuel for an anaerobic digester to decrease heat cost downstream.

4 Final Design

4.1 Unit Operation Summary

4.1.0.1 Upstream

The process starts with a bioreactor seed train to produce *B. subtilis* in quantities to innoculate production scale bioreactors. All streams and equipment mentioned are depicted in Appendix A1. The seed train will start with a 2 L reactor (U1) filled with cells, media, water, and glucose by hand (U1a). The cells will be retrieved from a synthetic biology lab where the master cell bank is kept. The following bioreactor, U2, will increase in volume (to 100 L) and will have water pumped (U2b.p) in. Also, a set of screw conveyors (S1a, S2a, S3a, and S4a) will be connected to the reactor to add media and glucose from storage silos (S1, S2, S3, and S4). The reactor will then be heated up and sterilized. Following U2's sterilization and the completion of U1's fermentation, a centrifugal pump (U2a.p in U2a) will transfer the fermentation broth to the 100 L bioreactor, U2. This series of pumping in water, adding in media and glucose, sterilizing, and then adding in the previous reactors' fermentation broth will be the order of operations in all the following upstream bioreactors. The fermentation broth of U2 will be pumped in (U3a.p in U3a) to U3, a 1,000 L reactor, filled with media, glucose, and water (U3b.p in U3b). The

final step of the seed train will be a production scale 10,000 L bioreactor, U4. It will be filled via streams U4a (pump U4a.p) and U4b (pump U4b.p). After completion of the fermentation, stream U5a (pump U5a.p) will be split into streams U5b.1-9 to begin the first production cycle. The seed train will be run only once at the beginning of the production year.

Next, a production step is run to produce the enzyme needed to run the cell-free reaction in 2 reactors. This includes 101 fermentation cycles per cell-free reactor, or 202 cycles to seed the 2 reactors. Additionally, once cell-free production part of the year begins, 2 replenishment cycles will run per cell-free reaction to replenish purged enzymes. All bioreactors in this production cascade are 10,000 L. U4 from the seed train and will always act as a cell culture reactor, where its fermentation broth is recycled back into the inoculation streams, U5b.1-9. After U4 is emptied in stream U6a.1, it will be pumped (U6a.p1) into a storage tank (S5) as the next batch of broth (media, glucose, and water) is sterilized in place. To begin the next cycle, water is pumped (U5c.p) into the bioreactor, and media and glucose are added from the solid storage silos, then sterilized. The inoculation broth storage tank is pumped (S3.p) and split into the 9 inoculation streams, U5b.1-9, and added to the 9 production bioreactors (U4 and U5.2-9). After the fermentation is complete, the broth from streams U6a.2-9 is merged into one stream U6b (pumped by U6b.p) that goes to purification.

The disk stack centrifuge (U6) will take the fermentation broth from U6b and separate 100% of the cell mass out. It will complete the separation in 1 hour and yield 63.7% of the enzymes produced from the upstream fermentations. The centrifuge will have 50 disks, an outer radius of 0.5 m, and an angular velocity of 894.5 RPM. The cell mass waste will be pumped out in stream U7b (pump U7b.p) and sent to an incinerator (S6) before being disposed of as non-hazardous solid waste. The supernatant containing the desired enzymes and some glucose will be pumped (U7a.p) in stream U7a to the ultrafiltration unit, U7. The membrane will retain 100% of the enzymes and concentrate them from 63 g/L to 176 g/L in stream U8a. The membrane will have a molecular weight cut off of 150-300 Da, an area of 534.64 m^2, operate at 30 bar, and have a pressure drop of 3 bar. The concentrated enzyme solution will be pumped (U8a.p) via stream U8a to the holding tank CF3 before entering the cell-free reactor. The wastewater, containing some glucose, will be disposed of as non-hazardous liquid waste pumped (U8b.p) out in stream

U8b.

4.1.0.2 Cell-Free Reaction

To allow for near-continuous operation of the cell-free reactors, two reactors will be operated in parallel. While one reactor is running, the other will be drained for downstream filtration through stream D1a. Each reactor will be fed through two main streams CF1b/CF2b and S7a/S8a. The CF1b and CF2b streams fill each reactor with the enzymes and water needed for the batch reactions to occur, while streams S7a and S8a feed solid glucose to each reactor directly through screw conveyors.

During the course of one batch reaction, the CF1d and CF2d streams circulate the contents of the reactor through jet nozzles to allow continuous mixing. To maintain the reactor at a pH of 7, NaOH is added directly to the CF1d and CF2d streams through a computer-controlled valve operating in a feedback loop with a pH probe present at the inlets of CF1d and CF2d. Temperature control in the reactors will be achieved in a similar way with a second control loop that consists of a temperature probe and an electric heater in line with streams CF1d and CF2d.

The overall flow diagram of the cell-free reactors is shown in Figure 14, and additional details regarding the design of each component can be found in Section 3.2

4.1.0.3 Downstream

The product from the cell-free reactor then goes through four stages of nanofiltration. Each membrane will have a 44,600 m^2 and an average permeate flux of 1.473 $L/m^2/hr$. Every membrane will operate at 30 bar and have a pressure drop of 3 bar. Each stream being fed (D1a, D2a, D3a, D4a) into a membrane will be mixed with makeup water (D1b, D2b, D3b, D4b). All permeate streams (D5a.1, D5a.2, D5a.3, D5a.4) will be merged into one stream (D5a.1-4) and sent to the flash drum. The retentate stream (D5b) will be split into a purge stream and a recycle stream. The purge stream (D5c) will be disposed of as waste and the recycle stream (D5d) will be sent through another nanofiltration membrane. This membrane has an area of 18,530 m^2 and an average permeate flow rate of 2.443 $L/m^2/hr$. The permeate stream (D12b) is disposed of as waste. The retentate stream (D12a) is sent to a tank for temporary storage.

The combined permeate stream (D5a.1-4) from the nanofiltration membrane system is then compressed to 2 atm. Once pressurized, the stream goes through a heat exchanger and is heated to 122 degrees Celsius. The stream is then fed into the flash drum, separating into a distillate and bottom stream. The liquid volume of the flash drum is 107 m^3. The diameter is 7.16 meters, and the tangent to tangent height is 3.66 meters. The design gauge pressure is 2.43 barg. The design temperature is 150 degrees Celsius, and the operating temperature is 122 degrees Celsius. The distillate (D6b) is put through a heat exchanger, condensed, cooled to 50 degrees Celsius, and depressurized to 0.123 bar. The distillate is then split into a recycle and a waste stream. The recycle stream (D6d) will be sent to the nanofiltration membrane system as makeup water and the waste stream (D6c) will be disposed of.

The bottoms product (D11a) of the flash drum is cooled using a heat exchanger to 33 degrees Celsius. Sulfuric acid (D11b) is added to the stream to lower the pH and protonate the lactic acid. This creates sodium bisulfate, some of which precipitates as a solid. The stream is sent through the sedimentation tank, resulting in a sludge and product stream. The tank is 6.18 meters long, 1.55 meters wide, and 3.5 meters deep. The volume of the sedimentation tank is 33.45 m^3, and the surface area is 9.56 m^2. The flow-through velocity is 0.000429 m/s. The weir length is 1.07 meters. The sludge stream (D11c) is then put into a storage tank through a screw conveyor and disposed of as a byproduct.

The sedimentation tank's product stream (D11d) is then combined with makeup water (D11e). The resulting stream is then fed into the liquid-liquid extractor. The extractor has a diameter of 1.57 meters and a height of 4.97 meters. Makeup solvent for the extractor (D6e) is pumped from a storage silo and then combined with the distillation recycle stream (D6f). This merged stream is also fed into the liquid-liquid extractor. Two streams leave the extractor. The first stream is the aqueous stream (D7b), which is treated and disposed of as waste. The second stream is the organic stream (D7a), which is heated up to 50 degrees Celsius by a heat exchanger.

4.1.0.4 Distillation Cascade

The heated-up stream (D7a) is then fed into the water separation column (D7) which separates all of the water into the distillate (stream D10a) along with a small quantity of octanol and the

remaining material flows out the bottoms (D8a). D7 operates at a pressure of 0.1 atm and a range of operating temperatures, dependent on stage, as seen in 17. D7 is 10.72 meters in diameter and 10.97 meters tall. Stream D10a is fed into the decanter (D10) at 58 degrees Celsius and stream D8a is fed into the octanol separation column (D8) at 155 degrees Celsius. The condenser (D7.c) has a heat exchange area of 889 square meters and a heat duty of 35340 kilowatts. The reboiler (D7.r) has a heat exchange area of 4,976 square meters and a heat duty of 36,017 kilowatts.

Stream D8a is fed into the octanol separation column (D8) to separate the remaining octanol as a distillate (stream D6f.2) along with trace amounts of lactic acid and the remaining material flows out the bottoms (D9a). D8 operates at a pressure of 0.1 atm and a range of operating temperatures, dependent on stage, as seen in 17. D8 is 3.04 meters in diameter and 28.65 meters tall. Stream D6f.2 is a recycle stream that is fed into a mixer with other recycle streams in the cascade at 142 degrees Celsius and stream D9a is fed into the trioctylamine (TOA) separation column (D9) at 171 degrees Celsius. The condenser (D8.c) has a heat exchange area of 40.7 square meters and a heat duty of 3382 kilowatts. The reboiler (D8.r) has a heat exchange area of 414 square meters and a heat duty of 3,384 kilowatts.

Stream D9a is fed into the TOA separation column (D9) to separate the trioctylamine through the bottoms (stream D6f.3) along with trace amounts of lactic acid while the remaining material flows into the distillate (S10a). D9 operates at a pressure of 0.1 atm and a range of operating temperatures, dependent on stage, as seen in 17. D9 is 2.85 meters in diameter and 13.41 meters tall. Stream D6f.3 is a recycle stream that is fed into a mixer with other recycle streams in the cascade at 182 degrees Celsius and stream S10a is fed into the product storage tank (S10). The condenser (D9.c) has a heat exchange area of 24.3 square meters and a heat duty of 4,773 kilowatts. The reboiler (D9.r) has a heat exchange area of 244 square meters and a heat duty of 4,588 kilowatts.

Stream D10a is fed into the decanter (D10) to separate the octanol through the bottoms (stream D6f.1) along with trace amounts of water while the remaining water flows into the bottoms (D6i). D10 operates at a pressure of 0.1 atm and a temperature of 115 degrees Celsius as seen in 17. D10 is 0.91 meters in diameter and 3.66 meters tangent to the height. Stream D6f.1 is a recycle

stream fed into a mixer with other recycle streams in the cascade at 115 degrees Celsius and stream D6g is treated as hazardous wastewater.

The recycle streams (streams D6f.1-3) running into the mixer combine (stream D6f) before they are cooled from 125 degrees Celsius to 22 degrees Celsius in a heat exchanger (D6f.h) using cooling water at 15 degrees Celsius over a heat exchange area of 29.18 square meters. Stream D6f is then pressurized from 0.1 atm to 1 atm in a centrifugal pump (D6f.p). D6f.p pumps stream D6f back into the LLE for reuse.

The product storage tank is 2,000 cubic meters tank allowing the storage of one month's worth of product before packaging the product in 55 gallon drums and shipping it out to our customers.

4.2 Production Schedule

This process ties together an upstream batch operation and continuous downstream processing. To achieve this, there is first a start-up phase where the enzymes used in the cell-free reactor will be produced. As described in the upstream discussion, 2 rounds of 101 production fermentation cycles will be used to produce the desired 450,000 kg of enzymes needed for both cell-free reactors. This start-up phase will take roughly 73 days with each fermentation needing 5.6 hours to complete along with 3 hours between cycles for processing.

After this start-up phase, the cell-free reactor and downstream operations will run for the remaining 292 days in a year. With each cell-free reaction taking 22.5 hours to complete, this allows for 311 cycles or roughly 155 cycles per cell-free reactor. Each of these reactions will have an associate enzyme purge, which requires the production fermentation unit to be run for 2 cycles per cell-free reaction, or 622 cycles during the second lactic acid production part of the year. The purifying steps (centrifuge and ultrafiltration steps) will be run directly following the fermentation cycles.

Maintenance of the upstream portion of the process will be completed once a year during various times. The seed train will be maintained during the lactic acid production phase, while the production reactors can only be completely shut down during the initial seed train step.

The disk stack centrifuge and ultrafiltration membrane can be worked on in between production cycles, but can only be fully shut down during the initial seed train step. Smaller maintenance operations will be carried out in the 3 hours of downtime between fermentations.

Maintenance of the downstream portion of the process will occur during the plant's 71 days of downtime. The nanofiltration membranes will be back washed and thoroughly cleaned. The flash drum and liquid-liquid extractor will be checked for any leaks. The bottom of the sedimentation tank will be thoroughly cleaned to remove residual solids.

4.3 Equipment Tables and Specifications

4.3.1 Upstream Equipment Tables

The equipment for the major upstream unit operations consists of various-sized bioreactors, a disk stack centrifuge, and an ultrafiltration membrane which is summarized in Table 14 and described in detail in Section 3.1. All other equipment is outlined in Section 3.4.

Table 14: Upstream equipment for major unit operations

Operation	Equipment	Identifier	Size	Temperature [°C)]	Pressure [bar]
Seed Train	Bioreactor	U1	2 L	37	1.01
Seed Train	Bioreactor	U2	100 L	37	1.01
Seed Train	Bioreactor	U3	1,000 L	37	1.01
Seed Train	Bioreactor	U4	10,000 L	37	1.01
Production Fermentation	Bioreactor	U5.2-9	10,000 L	37	1.01
Purification	Disk Stack Centrifuge	U6	Inner Radius: 0.45 m Outer Radius: 0.50 m 50 Stacks	-	1.01
Purification	Ultrafiltration Membrane	U7	Area: 534.64 m^2	-	30

4.3.2 Cell-Free Equipment Tables

Table 15: Major unit operations used for the cell-free synthesis of lactic acid

Operation	Equipment	Id	Volume (m^3)	Temperature (°C)	Pressure (atm)	pH	Batch Time (h)
Lactate Production	Cell-free Reactor	CF1	1,500	50	1	7	22.5
Lactate Production	Cell-free Reactor	CF2	1,500	50	1	7	22.5

4.3.3 Downstream Equipment Tables

Table 16 shows the equipment for the major unit operations in the downstream portion of our process, except for the distillation cascade.

Table 16: Downstream Equipment

Unit Operation	Unit Name	Temperature (°C)	Pressure (bar)	Size
Nanofiltration Membrane	D1	50	30	A = 44,625 m^2
Nanofiltration Membrane	D2	50	30	A = 44,625 m^2
Nanofiltration Membrane	D3	50	30	A = 44,625 m^2
Nanofiltration Membrane	D4	50	30	A = 44,625 m^2
Flash Drum	D5	102	2.03	D = 7.16 m h = 3.66 m
LLE	D6	22 - 32	1	D = 1.57 m h = 4.97 m
Sedimentation Tank	D11	33	1	V = 33.45 m^3
Nanofiltration Membrane	D12	50	30	A = 18,530 m^2

Table 17 shows the major unit operations for the distillation cascade.

Table 17: Distillation Cascade Equipment

Unit Operation	Unit Name	Temperature (°C)	Pressure (bar)	Size
Water Separation Column	D7	58-155	0.101	D = 10.72m H = 10.97m
D7 Condenser	D7.c	58	0.101	A = 889sqm
D7 Reboiler	D7.r	155	0.101	A = 4976sqm
Octanol Separation Column	D8	142-171	0.101	D = 3.04m H = 28.65m
D8 Condenser	D8.c	142	0.101	A = 40.7sqm
D8 Reboiler	D8.r	171	0.101	A = 414sqm
TOA Separation Column	D9	103-182	0.101	D = 2.85m H = 13.41m
D9 Condenser	D9.c	103	0.101	A = 24.3sqm
D9 Reboiler	D9.r	182	0.101	A = 244sqm
Decanter	D10	115	0.101	D = 0.91m H = 3.66m

4.3.4 Ancillary Equipment Tables

Aside from major unit operations, there will also be various ancillary equipment to assist in the smooth operation of the process. Table 19 summarizes all pumps in each area of the plant. Table 18 summarizes all true heat exchangers in the process. This does exclude electric heaters which are included in specific operations as described in the design portion of this design. Table 20 summarizes all storage tanks and miscellaneous equipment throughout the process.

Table 18: Summary of all heat exchangers for the process.

Identifier	Equipment Use	Quanity	Utility	Utility Flow Rate [kg/hr]	Heat Duty (kW)	Temperature of Stream In (C)	Temperature of Stream Out (C)
Downstream							
D6f.h	Cooling stream D6f	1	Cooling Water	558	517.0	15.0	100.0
D5a.1-4.p	Heating stream D5a.1-4	1	Steam	300,000	183,307	190.0	148.3
D6b.h	Condensing stream D6b	1	Cooling Water	14,140,323	182,582	22.0	33.3
D7.c	Condensor for D7	1	Steam	3,622	35,340	30.0	45.0
D7.r	Reboiler for D7	1	Steam	7,986	36,346	190.0	136.3
D8.c	Condensor for D8	1	Steam	4,058	3,511	30.0	45.0
D8.r	Reboiler for D8	1	Steam	3,928	3,513	190.0	159.2
D9.c	Condensor for D9	1	Steam	3,370	3,962	30.0	45.0
D9.r	Reboiler for D9	1	Steam	558	4,596	190.0	140.7
D11a.h	Cooling stream D11a	1	Cooling Water	11,000	930	22.0	93.2
D7a.h	Heating stream D7a	1	Cooling Water	11,000	230	93.2	76.3

Table 19: Summary of all pumps for the process.

Identifier	Equipment Use	Quanity	Pump Type	Flow Rate [m^3/s]	Power Annually [kWh]
Upstream					
U2a.p	U1 to U2	2	Centrifugal	0.000002	0.00003
U2b.p	Water to U2	2	Centrifugal	0.00011	0.0013
U3a.p	U2 to U3	2	Centrifugal	0.00012	0.0013
U3b.p	Water to U3	2	Centrifugal	0.00105	0.01
U4a.p	U3 to U4	2	Centrifugal	0.00117	0.01
U4b.p	Water to U4	2	Centrifugal	0.0105	0.12
U5a.p	U4 into production splitter	2	Centrifugal	0.01167	0.13
U5c.p	Water to production	2	Centrifugal	0.01	93.4
U6a.p	U4 to holding S5	2	Centrifugal	0.01167	109
U6b.p	Production merge to U6	2	Centrifugal	0.01167	654.1
S3.p	S5 to production splitter	2	Centrifugal	0.01167	109
U7a.p	U6 to U7	2	Centrifugal	0.06366	594.9
U7b.p	U6 to waste (incinerator)	2	Centrifugal	0.00106	59.2
U8a.p	U7 to CF3 holding	2	Centrifugal	0.00352	12,206
U8b.p	U7 to waste (water)	2	Centrifugal	0.00709	24,776
Cell Free Reactor					
CF1d.p	CFR1 Jet Mixing Pump	1	Centrifugal	57.83	529875
CF2d.p	CFR2 Jet Mixing Pump	1	Centrifugal	57.83	529875
CF1b.p	Pump to fill CFR from upstream holding tank	1	Centrifugal	0.6	9014.61
Downstream					
D6f.p	Distillation Recycle to D6	2	Centrifugal	6.70	1,618
D7.p	D7 Reflux Pump	2	Centrifugal	67.69	248,089
D8.p	D8 Reflux Pump	2	Centrifugal	42.91	202,789
D9.p	D9 Reflux Pump	2	Centrifugal	21.10	168,286
D1c.p	Feed Pump for D1	1	Centrifugal	0.0188	1,227,744
D2c.p	Feed Pump for D2	1	Centrifugal	0.0188	1,227,744
D3c.p	Feed Pump for D3	1	Centrifugal	0.0188	1,227,744
D4c.p	Feed Pump for D4	1	Centrifugal	0.0188	1,227,744
D5d.p	Feed Pump for D12	1	Centrifugal	0.0157	52,779
D5a.1-4.p	Feed Turbine for D5	1	Turbine	0.0791	882,000
D12a.p	Feed Turbine for CF3	1	Turbine	0.013	149,587
D6b.p	Pump to Pressurize D6b	1	Centrifugal	0.0759	74,794
D11a.h.1.p	Feed Pump for D11a.h	1	Centrifugal	0.00306	7,691
D11b.p	Feed Pump for D12	1	Centrifugal	0.000545	7,056
D11e.p	Feed Pump for D6	1	Centrifugal	0.0000632	7,056
D6e.p	Feed Pump for D6	1	Centrifugal	0.0000172	7,056

Table 20: Summary of all tanks and other miscellaneous equipment for the process.

Identifier	Equipment Use	Quantity	Power Annually [kWh]	Sizing
Upstream				
S1	Glucose Storage	1	--	10,000 L
S1a	Screw Conveyor	1	~138,333	10 ft
S2	Glucose Storage	1	--	10,000 L
S2a	Screw Conveyor	1	~138,333	10 ft
S3	Media Storage	1	--	10,000 L
S3a	Screw Conveyor	1	~138,333	10 ft
S4	Media Storage	1	--	10,000 L
S4a	Screw Conveyor	1	~138,333	10 ft
S5	Temporary Innoculum Storage	1	--	8,000 L
S6	Incinerator	1	~39,803	out of scope
Cell Free Reactor				
CF3	Recyle Enzyme Storage	1	--	150,000 L
CF4	NaOH Storage	1	--	2,000,000L
S7	Glucose Storage	1	--	10,000 L
S7a	Screw Conveyor	1	~138,333	10 ft
S8	Glucose Storage	1	--	10,000 L
S8a	Screw Conveyor	1	~138,333	10 ft
CF1.h	Electric Heater	1	~1960537	--
CF2.h	Electric Heater	1	~1960537	--
Downstream				
S9	Solvent Storage	1	--	50,000 L
S10	Product Storage	1	--	2,000,000 L
S11	Sodium Bisulfate Storage	1	--	700,000 L
S11a	Screw Conveyor	1	2132	10 ft

4.4 Material and Energy Balances

Individual mass balances can be found in the Appendix listed as Figure A20 and Tables A13 through A18.

4.5 Plant Location

The Acellular Lactic Acid Production Plant will be located outside of Detroit, Michigan. This location was selected for several reasons. Michigan is centrally located allowing two-day shipping by road to every major city in the continental United States which decreases transportation costs for both raw material inputs and the plant's product. Additionally, access to the

Great Lakes allows for shipping by sea both nationally and internationally.[69] Secondarily, the Detroit area currently has an increasing demand for work in the chemical and manufacturing sectors with a 2.5 percent decrease in jobs over the last year. The average employee compensation is approximately $41.90 per hour (or around $84,000 annually).[70] This production plan sets employee compensation at $105,000 annually, making our employee highly lucrative to a local workforce with experience in manufacturing and chemical production.[69] The state corporate tax rate, at 6 percent, is low compared to other industrialized states in the region such as Wisconsin, Illinois, and Minnesota making it a preferable production site.[71] Finally, the Detroit area offers ready access to large amounts of water removing many of the utility concerns that may plague locations without ready access to water.[72] Although the Detroit area has many benefits, there is a major hindrance to productivity. Detroit has a high annual snowfall, averaging above 40 inches per year since 2000,[73] which could cause product export to be delayed. It also has temperatures with lows below 25°F four months of the year[74] which may cause additional maintenance and repair costs over the life of the plant, especially when coupled with the snow and ice mitigation measures.

4.6 Process Economics

4.6.1 Plant Capital Costing

The plant total equipment cost is $60.8 million. As seen in Table 21, the downstream process costs approximately $57.9 million with the four-stage nanofiltration membranes costing $42.8 million and the distillation cascade costing $6.5 million. All equipment was modeled as stainless steel to mitigate the damage caused by the acidic, basic, and enzymatic reagents reacting throughout the process. This assumption allowed a maintenance cost within the fixed capital investment in Peters and Timmerhaus's *Plant Design and Economics for Chemical Engineers*.[75] The Marshall and Swift Equipment Cost Indexes were used to adjust the equipment costs over time. Initial equipment cost approximations were made using Capcost and ASPEN Plus. The complete equipment list with costing is listed below. Because this plant has the majority of its upfront and operating expenses during downstream processing, plant costs were approximated by treating the entire process as a fluid-processing plant. Using a Lang Factor of 5 for the fixed

Table 21: Process Economic Overview

TEC	$61,682,586
Upstream	$2,378,866
Cell Free Reactor	$895,900
Downstream	$57,888,521

capital investment (FCI),[75] the plant's calculated FCI was $304.2 million. Incorporating the additional investment of working capital which was approximately one-fifth of the FCI, or the same value as the total equipment cost (TEC),[75] the total capital investment (TCI) was $365.1 million. This cost is fronted over a two-year plant start-up period with half of the FCI being spent in the first start-up year and the remaining FCI and working capital being spent in the second start-up year.

The upstream portion of the process is outlined in Table 22. All bioreactors, pumps (priced including spares), and storage tanks were priced from sizing in CAPCOST.[76] The disk stack centrifuge cost was estimated based on its 50,000 L/hr capacity.[77] The ultrafiltration membrane pricing was scaled linearly from the membrane pricing from the work of Woods et al.[78] The solid storage silos were priced based on the going prices for galvanized corrugated steel silos.[79] The screw conveyors were estimated off of 2023 market prices.[67] Finally, the incinerator was estimated from quote estimates.[80]

Table 22: Upstream Equipment Fixed Cost. Note pump pricing includes a spare pump.

Large Unit Operations			
Identifier	**Equipment**	**Sizing Parameter**	**Price**
U1	Bioreactor	2 L	$ 7,530
U2	Bioreactor	100 L	$ 7,530
U3	Bioreactor	1,000 L	$ 25,700
U4	Bioreactor	10,000 L	$ 87,300
U5.2	Bioreactor	10,000 L	$ 87,300
U5.3	Bioreactor	10,000 L	$ 87,300
U5.4	Bioreactor	10,000 L	$ 87,300
U5.5	Bioreactor	10,000 L	$ 87,300
U5.6	Bioreactor	10,000 L	$ 87,300
U5.7	Bioreactor	10,000 L	$ 87,300
U5.8	Bioreactor	10,000 L	$ 87,300
U5.9	Bioreactor	10,000 L	$ 87,300
U6	Disk Stack Centrifuge	50,000 L/hr capacity	$ 175,000
U7	Ultrafiltration Membrane	534.64 m^2	$ 137,306

Pumps			
Identifier	**Equipment**	**Sizing Parameter**	**Price**
U2a.p	Centrifugal Pump	0.2 W	$ 22,500
U2b.p	Centrifugal Pump	7.7 W	$ 22,500
U3a.p	Centrifugal Pump	7.9 W	$ 22,500
U3b.p	Centrifugal Pump	71 W	$ 22,500
U4a.p	Centrifugal Pump	79 W	$ 22,500
U4b.p	Centrifugal Pump	709 W	$ 22,500
U5a.p	Centrifugal Pump	788 W	$ 22,500
U5c.p	Centrifugal Pump	701 W	$ 22,500
U6a.p	Centrifugal Pump	788 W	$ 22,500
S3.p	Centrifugal Pump	1,051 W	$ 241,000
U6b.p	Centrifugal Pump	788 W	$ 22,500
U7a.p	Centrifugal Pump	4,019 W	$ 28,100
U7b.p	Centrifugal Pump	14,883 W	$ 22,500
U8a.p	Centrifugal Pump	5,770 W	$ 7,300
U8b.p	Centrifugal Pump	26,839 W	$ 100,000

Storage Silos			
Identifier	**Equipment**	**Sizing Parameter**	**Price**
S1	Silo	100,000 L	$17,000.00
S2	Silo	100,000 L	$17,000.00
S3	Silo	100,000 L	$17,000.00
S4	Silo	100,000 L	$17,000.00

Storage Tanks			
Identifier	**Equipment**	**Sizing Parameter**	**Price**
S5	Storage Tank	8,000 L	$85,200.00
CF3	Storage Tank	150,000 L	$224,000.00

Miscellaneous			
Identifier	**Equipment**	**Sizing Parameter**	**Price**
S1a	Screw Conveyor	10 ft	$40,000.00
S2a	Screw Conveyor	10 ft	$40,000.00
S3a	Screw Conveyor	10 ft	$40,000.00
S4a	Screw Conveyor	10 ft	$40,000.00
S6	Incinerator	-	$79,000.00

CFR equipment was priced using CAPCOST. The reactors were not insulated allowing them to be approximated as tanks for pricing purposes.

Table 23: Cell Free Reactor Equipment Costs

Unit Operation	Volume [m^3]	Cost [$]
CF1	1500	$224,000
CF2	1500	$224,000
Heat Exchangers	Cost [$]	
CF1.h	$55,900	
CF2.h	$55,900	
Pumps	Power [kW]	Cost [$]
CF1d.p	174	$39,500
CF1d.p2	174	$39,500
CF2d.p	174	$39,500
CF2d.p2	174	$39,500
CF1b.p	174	$39,050
CF1b.p2	174	$39,050
Miscalleneous Equipment	Measurement	Cost [$]
S7	1000 m^3	$10,000
S8	1000 m^3	$10,000
S7a	10 ft	$40,000
S8a	10 ft	$40,000

Table 24: Nanofiltration Membrane System Equipment Costs

Unit Operation	Membrane Area [m^2]	Cost [$]
D1	44,625	$10,710,000
D2	44,625	$10,710,000
D3	44,625	$10,710,000
D4	44,625	$10,710,000
D12	18,530	$4,447,200
Pumps	Power [kW]	Cost [$]
D1c.p	174	$127,500
D2c.p	174	$127,500
D3c.p	174	$127,500
D4c.p	174	$127,500
D5d.p	7.48	$9,300
D12a.p	21.3	$10,300

Table 25: Flash Drum Equipment Costs

Unit Operation	Cost [$]	
D5	367,500	
Heat Exchangers	Cost [$]	
D5a.1-4.h	863,000	
D6b.h	1,461,700	
Pumps	Power [kW]	Cost [$]
D5a.1-4.p	125.0	$33,400

Table 26: Sedimentation Tank Equipment Costs

Unit Operation	**Tank Floor Area [ft^2]**	**Cost [$]**
D11	9.56	$202,721
Heat Exchangers	**Cost [$]**	
D11a.h	40,500	
Pumps	**Power [kW]**	**Cost [$]**
D11a.h.1.p	1.09	$22,600
D11b.p	1.00	$22,500
D11e.p	1.00	$22,500
Miscalleneous Equipment	**Measurement**	**Cost [$]**
S11	700 m^3	$156,000
S11a	10 ft	$40,000

Table 27: Liquid-Liquid Extractor Equipment Costs

Unit Operation	**Cost [$]**	
D6	$168,000	
Heat Exchangers	**Cost [$]**	
D7a.h	$13,800	
Pumps	**Power [kW]**	**Cost [$]**
D6e.p	1.00	$22,500
Miscalleneous Equipment	**Measurement**	**Cost [$]**
S9	50 m^3	$98,000

The equipment costs for the downstream processes are shown in Table 24 to Table 28. The cost of a nanofiltration membrane is \$240/m^2.[78] The cost of the flash drum was calculated in ASPEN Plus. The cost of the sedimentation tank is \$21,000/ft^2.[81] The cost of the liquid-liquid extractor was calculated using Capcost.[76]

Table 28: Distillation Cascade Equipment Costs

Unit Operation	Equipment Cost
D7	$2,446,200.00
D7.c	$217,100.00
D7.ca	$38,900.00
D7.r	$1,729,500.00
D7.p	$11,500.00
D8	$946,300.00
D8.c	$23,100.00
D8.ca	$30,200.00
D8.r	$150,500.00
D8.p	$9,300.00
D9	$474,900.00
D9.c	$18,400.00
D9.ca	$25,000.00
D9.r	$92,900.00
D9.p	$8,100.00
D10	$22,700.00
Total	$6,244,600.00

All equipment costing for the distillation cascade was found using ASPEN Plus including the towers and their component parts (condensers, reboilers, reflux pumps, and accumulators).

4.6.2 Operating Expenses

The utility costs are shown in Appendix A19 to Appendix A24. Three main utilities are used in our plant: electricity, steam, and cooling water. For our plant in Michigan, electricity will cost 8.45 cents per kilowatt hour.[82] Cooling water will cost 0.00608 cents per liter.[83] The cost of steam and condenser cooling water was calculated from ASPEN Plus. The condenser cooling water costs \$0.0264 per m^3. 100 psi steam costs \$0.0179 per m^3. 165 steam costs

0.02151711682 per m^3. The total utility cost is $20.5 million.

The raw materials costs are shown in Appendix A25 to Appendix A27. Six different raw materials are used in our plant: water, sulfuric acid, octanol, trioctylamine, glucose, and media. Process water costs 3 cents per kilogram.[84] Sulfuric acid costs 11 cents per kilogram.[85] Octanol costs $2.54 per kilogram.[86] Trioctylamine costs $2 per kilogram.[87] Glucose costs 30 cents per kilogram.[88] Media costs $1.22 per kilogram, as summarized in Appendix A7. The total raw material is $26.6 million.

The waste stream costs are shown in Appendix A28 to Appendix A29. There are three types of waste streams: solid sludge, liquid waste, and inert solids. Disposing of post-incineration solid sludge costs 3.6 cents per kilogram.[75] Treating and disposing of liquid waste costs 0.159 cents per liter.[68] Disposing of inert solids in a landfill costs 50 dollars per ton.[68] The total waste cost is $1.69 million.

The cost to run the sedimentation tank is a miscellaneous operating cost that is not categorized as a utility, raw material, or waste stream expense. It is calculated based on the volume of liquid treated per year. In this case, it is $479 per million gallons.[89] For our process, 15.6 million gallons need to go through the sedimentation tank per year, which means the operating cost of the sedimentation tank is $7468 per year.

Labor is largely based on the annual production, number of independent unit operations, and how the location of the plant impacts individual wages. The amount of labor was the first value calculated. Acting as a fluid processing plant and producing roughly 77.3 metric tons of lactic acid each day, Figure 25 indicates that roughly 30 operating hours are needed per day per major unit operation.[75] Not every major unit operation needs an operator,[75] so based on duplicates, 21 individual process focuses are necessary during operation. Over the course of 294 days of annual operation, a total of 185,220 employee hours are needed for operation. Equation 71 shows the multiplication used to calculate this value.

$$\frac{\text{operator hours}}{\text{year}} = \left(\frac{\text{operator hours}}{\text{day} \times \text{operating step}}\right) \times (\text{\# of days}) \times (\text{\# of processing steps}) \qquad (71)$$

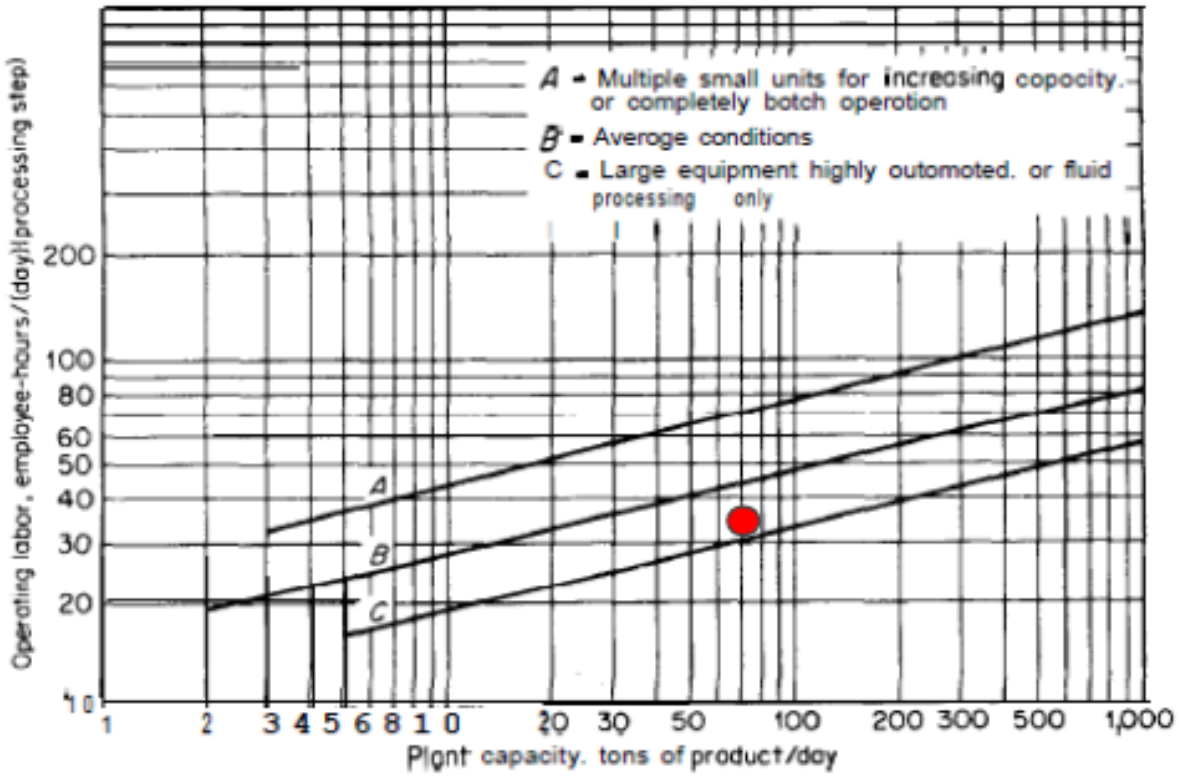

Figure 25: Estimate of Necessary Employee-Hours per Day per Processing Step

Using a standard 40-hour work week over the 294-day (42-week) operating year, employees would work 1680 hours per year. Using Equation 72, the total number of operators, 111, is calculated. Based on wage estimates in Detroit in 1989[75] and the average rise in wages from 1989 to 2024,[90] the average operator costs $105,000 per year. Equation 73 shows the operator compensation calculation. Multiplying operator compensation and the number of operators together, the total operator cost is found to be $11.6 million per year.

$$\#\text{ of operators} = \frac{\text{total operator hours}}{\text{weekly hours} \times \text{annual weeks worked}} \tag{72}$$

$$\text{Operator Compensation} = \#\text{ of Operators} \times (\text{Hourly Wage in 1989}) \times (\text{Wage Adjustment Factor}) \tag{73}$$

The supervisor wage adjustment over time is the same as the operator wage adjustment but at a higher initial wage.[75] Assuming the same annual hour estimates, the annual supervisor

salary is estimated at $140,000 per year. Assuming that one supervisor is needed for every ten operators and using the same equations above, supervisor compensation will amount to $1.55 million per year. The administrative staff was estimated as 10 percent of the operating staff with the same wages and hours as the operators. They amount to $1.16 million per year in labor costs. Summing the three working categories together, the total labor cost is approximately $14.4 million per year.

Various other miscellaneous charges appear annually that must also be accounted for. Chapter six of Peters and Timmerhaus's *Plant Design and Economics for Chemical Engineers*[75] provided the estimations for each of the following expenses. Annual maintenance and repairs are estimated at 6 percent of FCI amounting to $18.3 million per year. Operating supplies are estimated at 15 percent of maintenance and repair costs resulting in $2.8 million of expenses per year. Lab costs are estimated at 10 percent of the operating labor cost amounting to $1.44 million per year. Insurance is approximately 1 percent of the FCI and local property taxes are approximately 2 percent of the FCI costing $3.04 million and $6.2 million respectively. These miscellaneous operating expenses consume $32 million per year. Table A30 shows the starting values used to estimate miscellaneous and operating labor costs. All operating sectors summed together, operating costs amount to $94.8 million as seen in Table 29.

Table 29: Operating Costs Summary

Operating Cost	$94,767,287
Raw Material	$26,619,118
Utilities	$20,474,401
Waste Stream	$1,687,203
Labor	$14,424,508
Miscellaneous	$31,562,056

4.6.3 Economic Analysis (Discounted Cash Flow)

Lactic acid is typically sold in 55 gallon drums. 55 gallon drums contain 251.7 kilograms of lactic acid based on the unit conversions in Figure A21. Producing 3221 kilograms of lactic acid per hour, or 22.7 million kilograms per year, results in 90296 drums being filled. Wholesale pricing in the middle of the American market is $2,800 per drum[91] which equates to $253 million

per year as shown in Figure A22. Subtracting the $94.4 million in annual operating costs from the $252 million revenue results in a gross profit of $158 million annually. This plant will use an eight-year straight-line depreciation on the TCI which comes to $46.3 million of the gross profit annually exempt from taxation for the first eight years (year one to year eight). Combining the 21 percent federal corporate tax and the 6 percent Michigan state corporate tax for a total of 27 percent results in a $30.3 million loss annually in the first eight years and $42.7 million from year nine through year nineteen. Cumulatively, $797 million will be taxed from this process. The annual net profit is $127.7 million during the years with straight-line depreciation and reduces to $115.4 million when the full gross profit is taxed at 27 percent. Year twenty has a moderately higher gross and net profit because of the use of working capital ($54.8 million approximated as 90 percent of TEC), equipment resale ($6.1 million approximated as 10 percent of TEC), and land sale ($608,000 approximated as 1 percent of TEC)[75] which nets extra income and costs additional taxes for the process in that year. Figure 26 shows the annual profit difference before and after taxes every year. The complete data set is shown in Table A32.

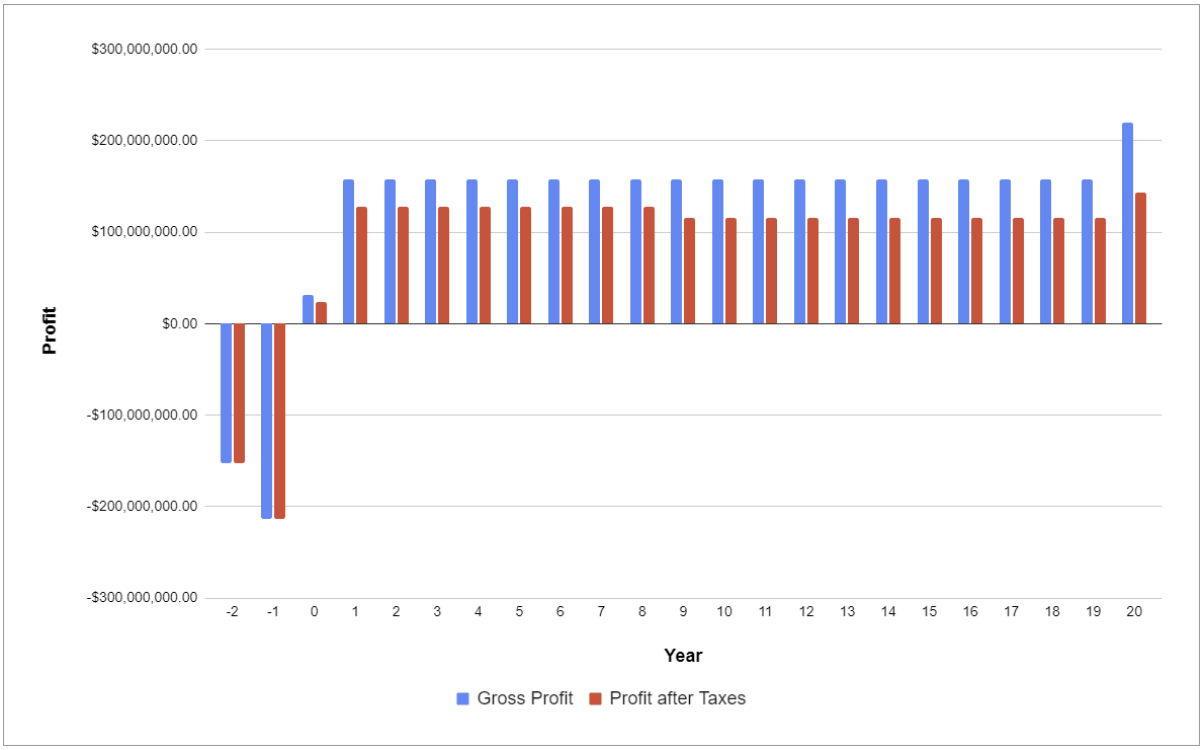

Figure 26: Annual Profit Before and After Taxes

The cumulative position, illustrated on a per-year basis in Figure 27, is evaluated by summing the profit after taxes from year negative two to the present year. The plant is modeled to have a

two-year start-up to account for the weather conditions in Michigan and operate at half capacity in year zero to act as a training year for the operators and supervisors. The plant life is forecasted to be 20 years. As Figure 27 shows, the plant is projected to have a positive cumulative cash flow by year three, accumulate over a $1 billion by year eleven, and be sold with a net profit of $2.1 billion after twenty years of operation.

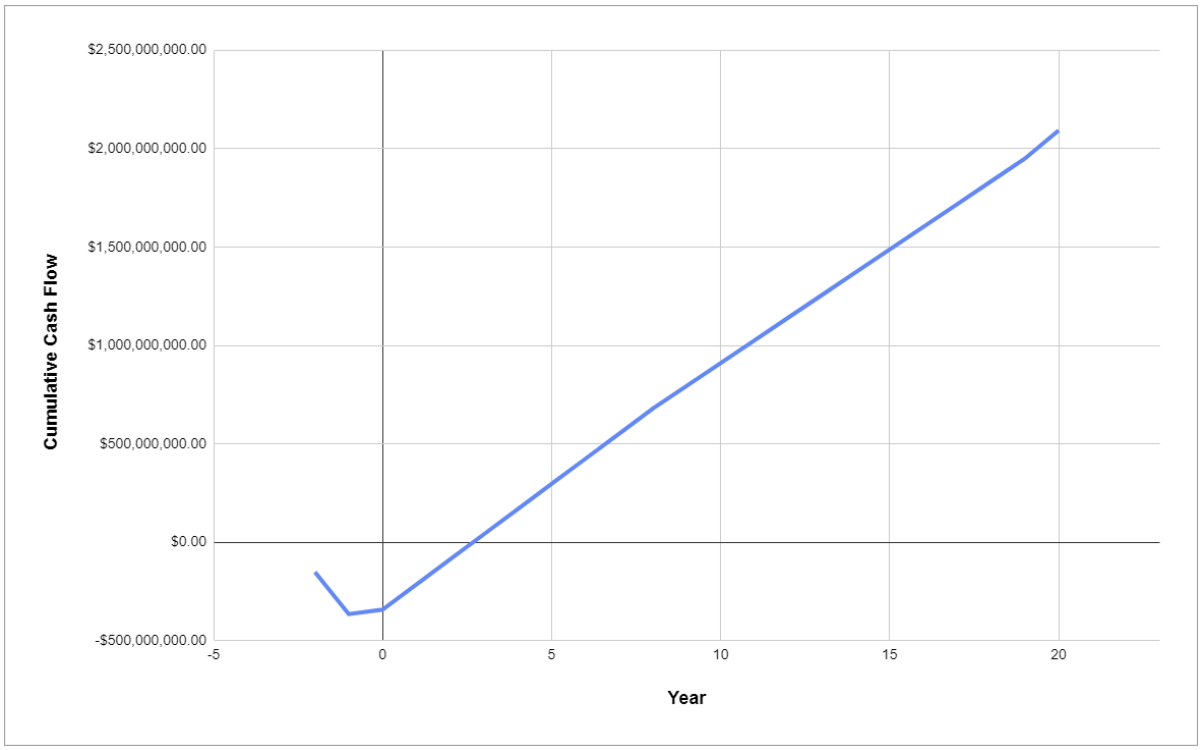

Figure 27: Cumulative Cash Flow

A better way to measure the economic performance of a chemical plant is the present value each year. The present value was based on an eight percent interest rate meaning that the cumulative cash flow of a given year had to exceed an eight percent growth to maintain an increasing present value. As Table A32 shows, the present value becomes positive in year three. Unlike the cumulative cash flow, the present value shows when the plant may meet its maximum utility and profitability. Figure 28 shows a dip in year sixteen that continues through the life of the plant. The annual present value was found using Equation 74.

$$\text{Present Value} = \frac{\text{Cumulative Position}}{(1 + \text{Rate of Return})^{\text{Year}}} \tag{74}$$

The sum of the annual present value to date is known as the net present value. After 20 years

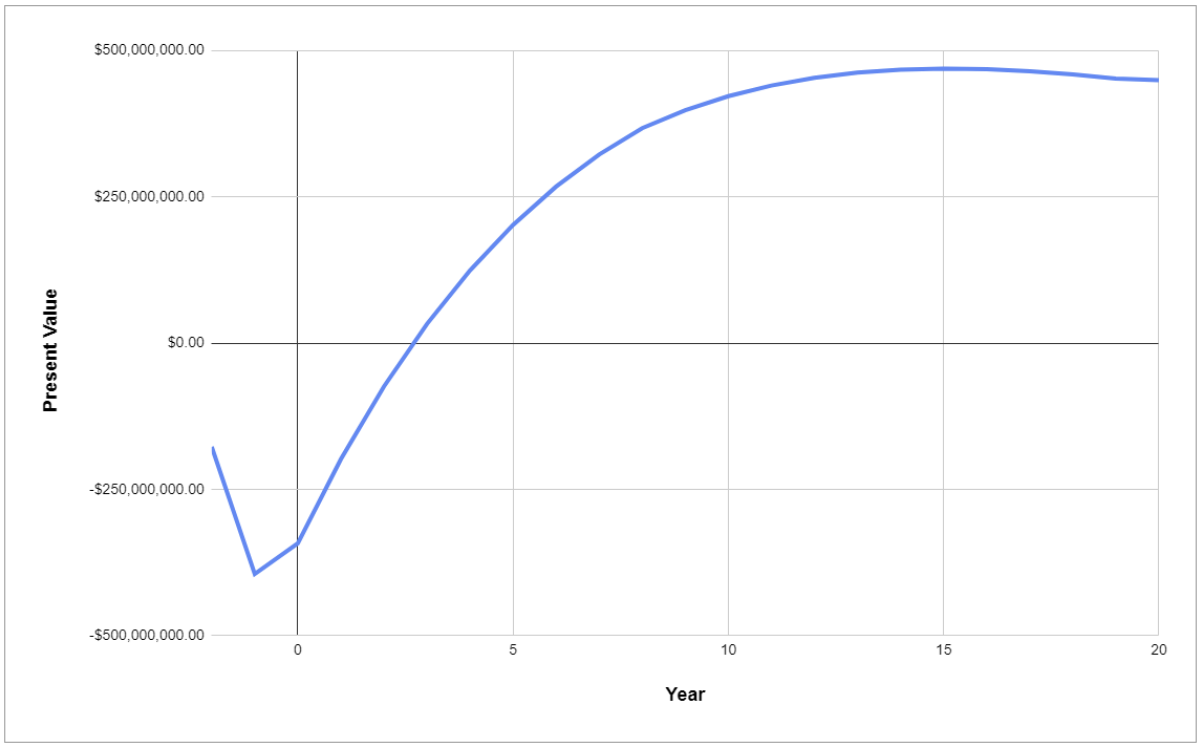

Figure 28: Present Value as a Function of Year

of operation, this plant has a net present value of $5.5 billion. The best evaluation, however, of the plant's return on investment is the internal rate of return (IRR). Using the IRR function in Excel, the IRR of this process over the twenty-year operating period was found to be 25 percent. This is on the lower end of acceptable returns for high-risk plant projects.

4.6.4 Risk Analysis

This plant has a lot of potential in terms of raw cash flow, but it also has lots of risk factors. The first set of risks has to do with market assumptions around lactic acid. While wholesale lactic acid, at 95 percent purity, in the United States is priced at $2,800 per drum,[91] 88 percent purity lactic acid can be as low as $1,500 per drum[92] which reduces competitiveness in the market because 88 percent is food grade lactic acid. While buyers may begin seeking higher purities as regulations increase food purity standards in both foreign and domestic markets, there is a significant risk that the chosen price point will not be preferable for the increase in purity. If this plant's lactic acid price point were dropped to the lowest available wholesale, cumulative revenue would be reduced to $332 million, the present value would be negative for nine years of operation against an eight percent interest rate and the IRR would drop from 25 percent to

negative three percent definitely suggesting the plan be scrapped (at an annual revenue of $135 million).

While the production of this plant only accounts for four percent of the current global market and will likely be reduced to one percent of the market by 2032[93] and will therefore not likely impact market price in the near future, the projected market growth could cause a drop in product pricing, especially if global supply chains continue to operate normally. As more companies sell wholesale lactic acid at 88 percent or higher purities, cheaper processes will likely be developed and the product price will drop which would have detrimental effects on the economic viability of this process. In addition to potential market losses, increases in operating labor costs look likely based on a worker loss rate of over five percent in 2023,[94] a hiring rate that exceeds the layout rate[94] indicating employee leverage in compensation negotiations, and rates increasing between two and eight percent annually.[90] The rise in cost annually could raise operating costs and decrease the IRR which is already at the low end for novel chemical production methods.

The largest risk in the process is the novelty of the cell-free catalysis of glucose into lactic acid. The reactor model details have already been discussed, but the scalability unknown due to estimated kinetic information, the viscosity issue surrounding the enzyme concentration needed to operate the reactor, and the ability to recover the enzymes at large quantities make this process extremely risky. This makes sense considering that lab testing proved this potential process possible less than fifteen years ago.[1] The lack of optimization within the system is also of high concern, namely the upfront cost of downstream filtration and the utilities needed for the separation of water in the distillation cascade and flash drum. Many assumptions were made throughout this process which were oversimplified and maximized the productivity of the plant, likely further decreasing the profits and increasing the risk.

Based on these considerations, this project is not recommended to proceed from a cost perspective. While the potential to reduce enzyme production costs was realized in the process, enzyme recovery has proven to be extremely expensive and the number of filtration steps necessary to recover the necessary enzymes increases annual operating costs significantly. With an IRR of 25 percent including optimistic pricing assumptions for a novel and highly risky pro-

cess, the return is not high enough to certify the risk. Until the enzyme recovery and cell-free enzymatic pathways can be replicated on a larger scale, this project is too risky to invest in.

5 Regulatory, Safety, and Environmental Considerations

Several chemicals are used in this plant that must be treated with special care. Sulfuric acid, sodium hydroxide, dissolved sodium bisulfate, and lactic acid are corrosive due to their acidity or basicity.[95–97] To prevent corrosion, the equipment used in this process will be made of stainless steel. Operators working with or around equipment that contains these chemicals will wear gloves, safety glasses, and long clothing. A spill kit will also be located nearby in case of an emergency. Waste streams containing these chemicals must be neutralized before they are disposed of. Trioctylamine and octanol are both irritants.[98,99] Operators working with or around equipment that contains these chemicals will wear gloves, safety glasses, and long clothing to prevent irritation. Waste streams containing these chemicals must be properly treated before being disposed of because they are environmental hazards.[98,99] Additionally, further investigation into chemical compatibility for bulk storage of chemicals will need to be considered in the placement of these storage vessels.

Another hazard to consider is the storage and use of dry powders/solids in various unit operations, namely glucose and media. Dry powders can result in dust explosions if not properly handled. One way to address this could be through keeping the solids in a slightly more humid storage unit and storing the solids in non-confined spaces. Furthermore, regular cleaning of storage areas and their associated screw conveyors will be key in reducing the risk of dust explosions. Several thermal hazards are also present in our process. The cell-free reactor, flash drum, and distillation cascade all operate at elevated temperatures. To address this, the following precautions will be taken. The temperature of these processes will be actively monitored to ensure they do not reach temperatures that may cause chemicals to catch on fire or explode. Maintenance will be done on these processes to prevent electrical or mechanical errors that could cause rapid temperature increases. Everything made out of stainless steel will be grounded to prevent the buildup of static electricity. Sprinkler systems and fire extinguishers will be installed so that when a fire occurs, there are measures to stop it. The final precaution is that workers

and supervisors will be properly trained and wear appropriate PPE when operating near these processes.

Finally, with such a large-scale operation, there will be many moving parts, requiring coordination of shipments, deliveries, and movement around the plant. All levels of staff will have regular hazard training to understand how to identify the risks around the plant. In addition to training, they will also have high-visibility vests and clearly marked areas of danger where heavy machinery often crosses their paths.

6 Social and Ethical Considerations

Lactic acid is considered a generally recognized safe (GRAS) microbial-derived ingredients product, so there are relatively few social and ethical concerns regarding the plant's main product.[7] However, it is worth noting the impact of building a new plant on the surrounding community and environment. The release of genetically modified bacteria can disrupt the local ecosystem they are released into. It will be extremely important to ensure the incineration of the modified bacteria is effective in destroying them. Aside from the modified bacteria, the safety of the surrounding community will be of the utmost importance. The safety measure previously mentioned will be in place to protect the community, but creating a culture in the workforce that values upholding a high standard of safety will keep the surrounding community safe. Finally, continuous improvement of the process will allow the company to minimize its environmental impact on the community.

7 Conclusions and Recommendations

This plant has a lot of potential in terms of raw cash flow, but it also has lots of risk factors. In order to make the total capital investment worth the many risks discussed in the economic risk section and further discussed throughout the conclusion, an IRR of 40 percent would be required. This high IRR recommendation is due to the novelty of the process, potential complications arising from lack of optimization, location risks, and market constraints. At our current price point in the middle of the American market, $2,800 per 55 gallon drum, 95 percent lactic acid produces $253 million annually and a projected cumulative cash flow of $2.1 billion. That

produces an IRR of 25 percent. In order to meet the 40 percent IRR goal expected to make this project viable, the Total Equipment Cost (TEC) would need to be reduced to $34 million from a current cost of $61.7 million (or a TCI reduction to $200 million from the current TCI of $370 million) or a twenty-year cumulative cash flow increase from $2.1 billion to $4 billion would be needed. Based on the risks involved and projected IRR falling short of the 40 percent threshold set, the long-term economic plan recommends that this project design should be rejected until either production can be increased or TEC and operating costs can be decreased.

One of the most promising areas for future work seems to be in increasing the volumetric yield of the cell-free reactor, which could simultaneously reduce the TEC and operating costs. As discussed in section 3.2.3, the main reason for low volumetric yields appears to be rate imbalances between the GDH and L-LDH enzymes, causing almost all of the NAD to be pushed to its reduced or oxidized state. With the enzyme ratios used herein, the rate of glucose consumption is much less than the maximum rate that GDH can catalyze, even in excess of glucose. If GDH and L-LDH were not limited by the NAD/NADH concentrations, rates more similar to those seen in Figure 11 would be expected, resulting in a 10-fold increase in volumetric yield. In addition, these increased rates would allow much higher concentrations of glucose to be fed, which should increase the volumetric yields by one or two additional orders of magnitude. Unfortunately, there is not enough data in the literature to properly fine-tune the enzyme ratios and fix this problem. These issues are not present in cellular lactic acid synthesis due to the tight regulation of coenzyme levels in the cells, and as such a similar approach could also be taken in the cell-free reactors, in addition to better tuning of the enzyme ratios.

Finally, with downstream filtration once again being the largest contributor to TEC, finding a more efficient way to separate the enzymes from the lactic acid product is another area of future work. The problem in this stage of the process is the amount of water used in the filtration steps to remove enzymes. The amount of filtration that must be conducted in order to meet the needed protein recycle quantities also imposes a high initial fixed cost. This recycling has the aim of reducing the upstream cost by lowering enzyme production and removing enzymes from the feed, but in many ways, it is the most expensive part of the cell-free process (equipment cost, utility cost, solvent/filter liquid cost, etc.). In addition to the expense of water used in the

process and the initial costs of the filters, the most expensive stage on an annual basis is the removal of water in the distillation cascade. In a $20 million annual utility budget, almost $8 million is needed to power the water separation reboiler. Finding an alternate enzyme separation method is imperative to reduce the cost of this process and make it economically viable. One suggestion is to adhere the enzymes to either the walls of the cell-free reactor or polymer beads, which could be mechanically separated from the reactor outlet stream. This mechanical method would reduce the water needs, subtract the cost of the filter membranes altogether from the fixed cost, and reduce the utility cost necessary to continuously remove water from the product streams in the flash drum and water separation column.

In addition to economic and novelty risks, this plant also faces weather risks, namely cold temperatures and an excess of snow and other precipitation.[74] This increases the risk of disaster should additional precautions in accordance with state and federal regulations along with good manufacturing processes not be followed. Namely the potential for plant failures due to freezing in a process that is based on fluids with freezing points in the single-digit negative degrees Celsius, a common occurrence in Michigan during the winter. Plant equipment may also need replacement more frequently due to the weather.[100] Weather issues to mitigate disasters will include additional utility costs to minimize the effects of the winter. Besides plant management and process upkeep, the potential for poor weather may affect shipping times with high variability and low predictability likely costing customers.

Together, these limitations prevent the current design from being economically viable due to the risks associated with the process's novelty, but these insights have revealed some of the key design challenges that still need to be overcome to make cell-free systems utilizable in practice.

8 Acknowledgements

This team would like to thank those who helped us complete this project with their time, effort, and expertise. Firstly, thank you to our capstone advisor, Eric Anderson, for his advice through all aspects of this project. Additionally, in no particular order, thank you to Nick Vecchiarello, Blair Okita, Bob Davis, and George Prpich for their expertise on the various design problems and their willingness to help us navigate through many details of this project.

References

(1) Zhang, Y.-H. P. *Biotechnology and Bioengineering* **2010**, n/a–n/a.
(2) Datta, R.; Henry, M. *Journal of Chemical Technology & Biotechnology* **2006**, *81*, 1119–1129.
(3) Datta, R.; Tsai, S.-P.; Bonsignore, P.; Moon, S.-H.; Frank, J. R. *FEMS Microbiology Reviews* **1995**, *16*, 221–231.
(4) Wee, Y.-J.; Ryu, H.-W. *Bioresource Technology* **2009**, *100*, 4262–4270.
(5) Alves de Oliveira, R.; Komesu, A.; Vaz Rossell, C. E.; Maciel Filho, R. *Biochemical Engineering Journal* **2018**, *133*, 219–239.
(6) Bapat, S. S.; Aichele, C. P.; High, K. A. *Sustainable Chemical Processes* **2014**, *2*, 3.
(7) Nutrition, C. f. F. S. a. A. Microorganisms & Microbial-Derived Ingredients Used in Food (Partial List), en, Publisher: FDA, 2023.
(8) Kwan, T. H.; Hu, Y.; Lin, C. S. K. *Journal of Cleaner Production* **2018**, *181*, 72–87.
(9) Manandhar, A.; Shah, A. *Processes* **2020**, *8*, DOI: 10.3390/pr8020199.
(10) Kawabata, Y.; Kimura, K.; Funane, K. *Applied Microbiology and Biotechnology* **2012**, *93*, 1877–1884.
(11) Stamenković-Stojanović, S.; Karabegović, I.; Beškoski, V.; Nikolić, N.; Lazić, M. *Advanced Technologies* **2020**, *9*, 44–49.
(12) Stamenkovic-Stojanovic, S.; Karabegovic, I.; Danilovic, B.; Mancic, S.; Lazic, M. *Journal of the Serbian Chemical Society* **2023**, *88*, 1103–1117.
(13) Salvador Pinos, C.; Pérez Navarro, O.; Albernas Carvajal, Y.; Mesa Garriga, L.; Jácome Navarrete, J.; González Suárez, E. *Afinidad. Journal of Chemical Engineering Theoretical and Applied Chemistry* **2022**, *79*, DOI: 10.55815/400724.
(14) McNulty, C. *Pharmaceutical Technology* **2016**, *40*, Publisher: MJH Life Sciences, 46–48.
(15) CDC Steam Sterilization — Disinfection & Sterilization Guidelines — Guidelines Library — Infection Control — CDC, en-us, 2019.
(16) OMEGA Engineering How to Calculate your Heater Wattage (Get your target temperature), 2019.
(17) My Engineering Tools Tank heating / cooling time : step by step calculation guide.
(18) Shonnard, D. Chapter 10: Sterilization and Bioreactor Operation.
(19) Engineers Edge Convective Heat Transfer Coefficients Table Chart.
(20) Alexandri, M.; Schneider, R.; Venus, J. *Membranes* **2018**, *8*, DOI: 10.3390/membranes8040094.
(21) Xie, L.; Wei, X.; Zhou, X.; Meng, D.; Zhou, R.; Zhang, Y.-H. P. J.; Xu, S.; You, C. *Synthetic and Systems Biotechnology* **2018**, *3*, 204–210.
(22) Cornish-Bowden, A., *Fundamentals of Enzyme Kinetics*, Google-Books-ID: _3fqaYnrdosC; John Wiley & Sons: 2013.
(23) Mitchell, D. A.; Krieger, N. *Biochemical Engineering Journal* **2022**, *178*, 108276.
(24) POCKER, Y.; E, G. *HYDROLYSIS OF D-GLUCONO-DELTA -LACTONE. I. GENERAL ACID-BASE CATALYSIS, SOLVENT DEUTERIUM ISOTOPE EFFECTS, AND TRANSITION STATE CHARACTERIZATION* **1973**.
(25) Kroll, A.; Rousset, Y.; Hu, X.-P.; Liebrand, N. A.; Lercher, M. J. *Nature Communications* **2023**, *14*, Number: 1 Publisher: Nature Publishing Group, 4139.
(26) Maeda, K.; Hatae, A.; Sakai, Y.; Boogerd, F. C.; Kurata, H. *BMC Bioinformatics* **2022**, *23*, 455.

(27) Giardina, P.; de Biasi, M. G.; de Rosa, M.; Gambacorta, A.; Buonocore, V. *Biochemical Journal* **1986**, *239*, 517–522.
(28) Wang, J.; Qu, G.; Xie, L.; Gao, C.; Jiang, Y.; Zhang, Y.-H. P. J.; Sun, Z.; You, C. *Applied Microbiology and Biotechnology* **2022**, *106*, 3625–3637.
(29) Wrba, A.; Jaenicke, R.; Huber, R.; Stetter, K. O. *European Journal of Biochemistry* **1990**, *188*, _eprint: https://onlinelibrary.wiley.com/doi/pdf/10.1111/j.1432-1033.1990.tb15388.x, 195–201.
(30) Foster, J. W.; Park, Y. K.; Penfound, T.; Fenger, T.; Spector, M. P. *Journal of Bacteriology* **1990**, *172*, Publisher: American Society for Microbiology, 4187–4196.
(31) Kumari, S.; Beatty, C. M.; Browning, D. F.; Busby, S. J. W.; Simel, E. J.; Hovel-Miner, G.; Wolfe, A. J. *Journal of Bacteriology* **2000**, *182*, 4173–4179.
(32) Zhou, Y.; Wang, L.; Yang, F.; Lin, X.; Zhang, S.; Zhao, Z. K. *Applied and Environmental Microbiology* **2011**, *77*, 6133–6140.
(33) Hong, T.; Iwashita, K.; Shiraki, K. *Current Protein & Peptide Science* **2018**, *19*, 746–758.
(34) Mooney, M. *Journal of Colloid Science* **1951**, *6*, 162–170.
(35) Faroughi, S. A.; Huber, C. *Physical Review E* **2014**, *90*, Publisher: American Physical Society, 052303.
(36) *Metabolic Engineering* **2016**, *35*, Publisher: Academic Press, 114–120.
(37) Hall, S. Rules of Thumb: Jet Mixing.
(38) gdh - Glucose 1-dehydrogenase - Saccharolobus solfataricus (Sulfolobus solfataricus) — UniProtKB — UniProt.
(39) 2-dehydro-3-deoxy-phosphogluconate/2-dehydro-3-deoxy-6-phosphogalactonate aldolase - Sulfolobus acidocaldarius (strain ATCC 33909 / DSM 639 / JCM 8929 / NBRC 15157 / NCIMB 11770) — UniProtKB — UniProt.
(40) ilvD - Dihydroxy-acid dehydratase - Saccharolobus solfataricus (strain ATCC 35092 / DSM 1617 / JCM 11322 / P2) (Sulfolobus solfataricus) — UniProtKB — UniProt.
(41) ldh - L-lactate dehydrogenase - Thermotoga maritima (strain ATCC 43589 / DSM 3109 / JCM 10099 / NBRC 100826 / MSB8) — UniProtKB — UniProt.
(42) Ross, P. D.; Minton, A. P. *Biochemical and Biophysical Research Communications* **1977**, *76*, 971–976.
(43) Fleming, P. J.; Fleming, K. G. *Biophysical Journal* **2018**, *114*, 856–869.
(44) Mirdita, M.; Schütze, K.; Moriwaki, Y.; Heo, L.; Ovchinnikov, S.; Steinegger, M. *Nature Methods* **2022**, DOI: 10.1038/s41592-022-01488-1.
(45) Jumper, J. et al. *Nature* **2021**, DOI: 10.1038/s41586-021-03819-2.
(46) Evans, R. et al. Protein complex prediction with AlphaFold-Multimer, biorxiv, 2021.
(47) Steinegger, M.; Söding, J. *Nature Biotechnology* **2017**, *35*, 1026–1028.
(48) Neurosnap Inc. Computational Biology Platform for Research Accessed: Insert the date you accessed this resource, https://neurosnap.ai/.
(49) Detroit, Michigan, United States, Average Monthly Weather.
(50) Miedama, S. A. 4.4: Terminal Settling Velocity Equations, en, 2020.
(51) Knueven, C. J. Sodium bisulfate as acidulant in foods, EP1104245A1.
(52) Sodium Bisulfate Chemical Information – Jones Hamilton, en-US.
(53) Hess, A. MECC ENV115: Sedimentation Tank Calculations.
(54) Nazaroff, W. W.; Alvarez-Cohen, L., *Environmental Engineering Science*, 1st Edition; Wiley: 2000.

(55) Din, N. A. S.; Lim, S. J.; Maskat, M. Y.; Mutalib, S. A.; Zaini, N. A. M. *Bioresources and Bioprocessing* **2021**, *8*, 31.
(56) Lan, K.; Xu, S.; Li, J.; Hu, C. *ACS Omega* **2019**, *4*, Publisher: American Chemical Society, 10571–10579.
(57) Seader, J. D.; Henley, E. J.; Roper, D. K., *Separation Process Principles with Applications Using Process Simulators*, 3rd; John Wiley & Sons, Inc.: 2011.
(58) PubChem Water (Compound), en.
(59) Demond, A. H.; Lindner, A. S. *Environmental Science & Technology* **1993**, *27*, Publisher: American Chemical Society, 2318–2331.
(60) Lamm, M. H.; Jarboe, L. R., *Chemical Engineering Separations: A handbook for students*; Iowa State University Digital Press: Ames, Iowa, 2021.
(61) Sandtorv, A. 2.3: Liquid-Liquid Extraction, en, 2019.
(62) Alan S. Foust, e. a., *Principles of Unit Operations*; John Riley and Sons, Inc.: 1980.
(63) DISTILLATION/ABSORPTION COLUMN TRAY DESIGN, University of Oklahoma, 2010.
(64) Taguchi, H. PreFEED Solutions for R and D to Design PreFEED Corporation Calculation of Minimum Number of Theoretical Stages using Fenske Equation Solutions for R and D to Design PreFEED Solutions for R and D to Design, 2010.
(65) Lamm, M.; Jarboe, L., *CHEMICAL ENGINEERING SEPARATIONS: A HANDBOOK FOR STUDENTS*; Iowa State Pressbooks: 2022.
(66) Shell and Tube Heat Exchangers, Standard XChange, 2013.
(67) How Much Does a Screw Conveyor Cost? ¡ Screw Conveyor Parts, en-US.
(68) Towler, G.; Sinnott, R., *Chemical Engineering Design: Principles, Practice and Economics of Plant and Process Design*, 2nd Edition; Butterworth-Heinemann: 2012.
(69) Des Chenes, J. About Michigan's Chemical Industry, www.michiganchemistry.com, 2024.
(70) McEntarfer, E. Detroit Area Economic Summary, Bureau of Labor Statistics, 2024.
(71) Fritts, J. State Corporate Income Tax Rates and Brackets for 2023, Tax Foundation, 2023.
(72) Authority, G. L. W. Michigan's source for water, Great Lakes Water Authority, 2023.
(73) US Department of Commerce, N. Snow Breakout By Season, www.weather.gov, 2021.
(74) US Department of Commerce, N. Southeast Michigan Climate Information, www.weather.gov, 2021.
(75) Peters, M.; Timmerhaus, K.; West, R., *Plant Design and Economics for Chemical Engineers*, 5th Edition; McGraw Hill: 2002.
(76) Turton, R. Analysis Synthesis and Design of Chemical Processes 5th Edition, en, 2019.
(77) 50000LPH Automatic Disc Stack Food Centrifuge for Algae Concentration.
(78) Woods, D. R. In *Rules of Thumb in Engineering Practice*, _eprint: https://onlinelibrary.wiley.com/doi/pdf/10.1002/9783527611119.app4; John Wiley & Sons, Ltd: 2007, pp 376–436.
(79) [Hot Item] 100m3 Farm Used Feed Grain Storage Silo for Sale, en.
(80) Mfg, F. Pet Incinerator Questions - Costs, Laws, Maintenance & More - Firelake Mfg. en-US, 2021.
(81) DiGregorio, D. Cost of Wastewater Processes, 1968.
(82) Electric Power Monthly - U.S. Energy Information Administration (EIA).
(83) Cooling Water Costs — Current and Forecast.
(84) New Water Service Rate Information, en-US, 2023.
(85) Sulfuric Acid Prices — Historical and Current, en-gb.

(86) High Quality 1-Octanol/Octan-1-Ol CAS No. 111-87-5 with Best Price, en.
(87) Trioctylamine Toa Cas 1116-76-3 - Buy Trioctylamine,Toa,1116-76-3 Product on Alibaba.com.
(88) Wholesale Price Xiwang Glucose Dextrose Monohydrate Powder CAS 5996-10-1, en.
(89) Chamblee, J. Analysis of Operations and Maintenance Costs for Municipal Wastewater Treatment Systems, 1978.
(90) Administration, S. S. Average Wage Index, Social Security Administration, 2023.
(91) MoreBeer! Five Star Lactic Acid 88 Percent, MoreBeer!, 2024.
(92) Supplier.com, I. Lactic Acid 88 Percent, Ingredient Supplier.com, 2024.
(93) Insights, F. B. Lactic Acid Market Size, 2023-2032, Fortune Business Insights, 2023.
(94) Of Labor Statistics, B. JOB OPENINGS AND LABOR TURNOVER – FEBRUARY 2024, Bureau of Labor Statistics, 2024.
(95) PubChem Sodium hydrogen sulfate, en.
(96) PubChem Sodium Hydroxide, en.
(97) PubChem Sulfuric Acid, en.
(98) 1-Octanol SDS (Safety Data Sheet) — Flinn Scientific.
(99) PubChem Trioctylamine, en.
(100) Burgess, H. Winter is Coming. Is Your Facility Protected?, NFPA, 2022.
(101) Hu, J.; Lei, P.; Mohsin, A.; Liu, X.; Huang, M.; Li, L.; Hu, J.; Hang, H.; Zhuang, Y.; Guo, M. *Microbial Cell Factories* **2017**, *16*, 150.
(102) Feso4 — Sigma-Aldrich, en.
(103) Magnesium Sulfate, USP Grade, en.
(104) Mncl2 — Sigma-Aldrich.
(105) Potassium Chloride USP/FCC Grade, en.
(106) Calcium Nitrate Tetrahydrate Crystal Lab Grade, en.
(107) Animal Extract Beef/Cattle Bone Ash/Calcined Bone Ash - China Ash and Bone Ash.
(108) Top Quality Food Additive Nutritional Fortifier Yeast Extract CAS 8013-01-2, en.
(109) Industrial Collagen Peptone Good Solubility in Water Used in Feed, en.
(110) Errington, J.; Aart, L. T. V. D. *Microbiology* **2020**, *166*, 425–427.
(111) Harrison, R. G.; Todd, P. W.; Rudge, S. R.; Petrides, D. P., *Bioseparations science and engineering*, Second edition; Topics in chemical engineering: a series of textbooks and monographs; Oxford University Press: Oxford New York Aukland, 2015.
(112) Poon, C. Measuring the density and viscosity of culture media for optimized computational fluid dynamics analysis of *in vitro* devices, en, 2020.
(113) Carta, G., *Heat and mass transfer for Chemical Engineers: Principles and applications*; McGraw-Hill Education: 2021.
(114) Ambrose, D.; Sprake, C. *The Journal of Chemical Thermodynamics* **1970**, *2*, 631–645.
(115) Liu, C.-T.; Lindsay, W. T. *Journal of Chemical and Engineering Data* **1970**, *15*, 510–513.
(116) Lactic Acid Properties, CHEMICALBOOK, 2024.
(117) PubChem Trioctylamine, pubchem.ncbi.nlm.nih.gov, 2024.

A Appendix

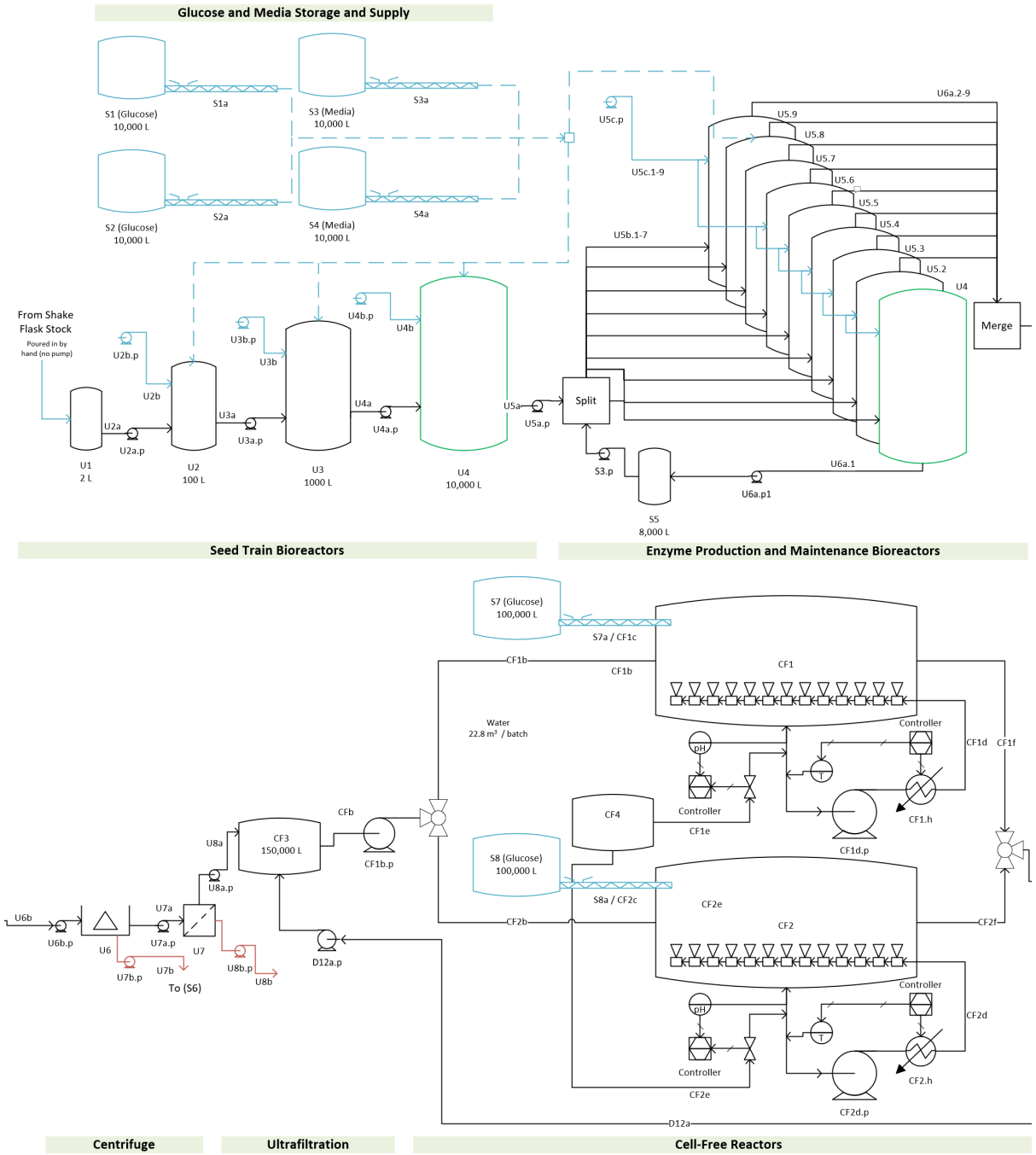

Figure A1: Overall Process Flow Diagram of the Acellular Lactic Acid Plant

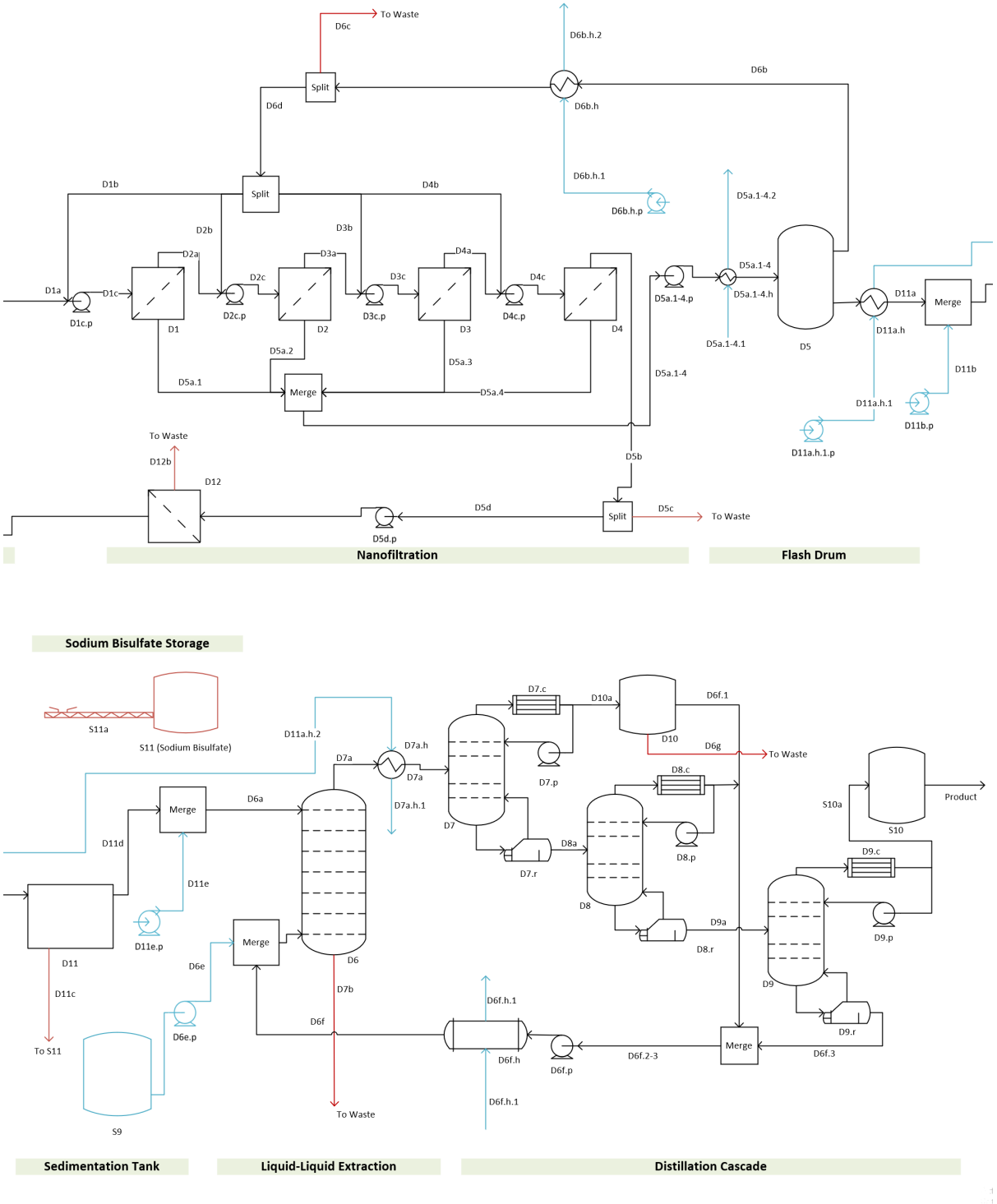

Figure A2: Overall Process Flow Diagram of the Acellular Lactic Acid Plant (cont.)

Unit Operations: CF1
(U - upstream, CF - cell-free , S - storage, D - downstream)
Streams: D3b or U5b.1-7
Pumps: U6b.p
Heat Exchangers: D11a.h
Heat Exchange Streams: D11a.h.1
Condensers and Reboilers: D7.c or D7.r

Figure A3: Examples of the naming scheme used in the process flow diagrams. The naming scheme used for the streams in this process is not necessarily conventional and warrants explanation. The general format is shown above. The unit operation will be denoted in red and has the noted 4 abbreviations. Streams will be indexed alphabetically as shown in green. If there are multiple identical streams, they will be followed by a ".#" suffix. Pumps, heat exchangers, condensers, and reboilers will be denoted by adding a ".p", ".h", ".c", and ",r" after the stream index, respectively. Heat exchangers may also be followed by a ".#" to signify the order in the stream that appears in the heat exchanger path.

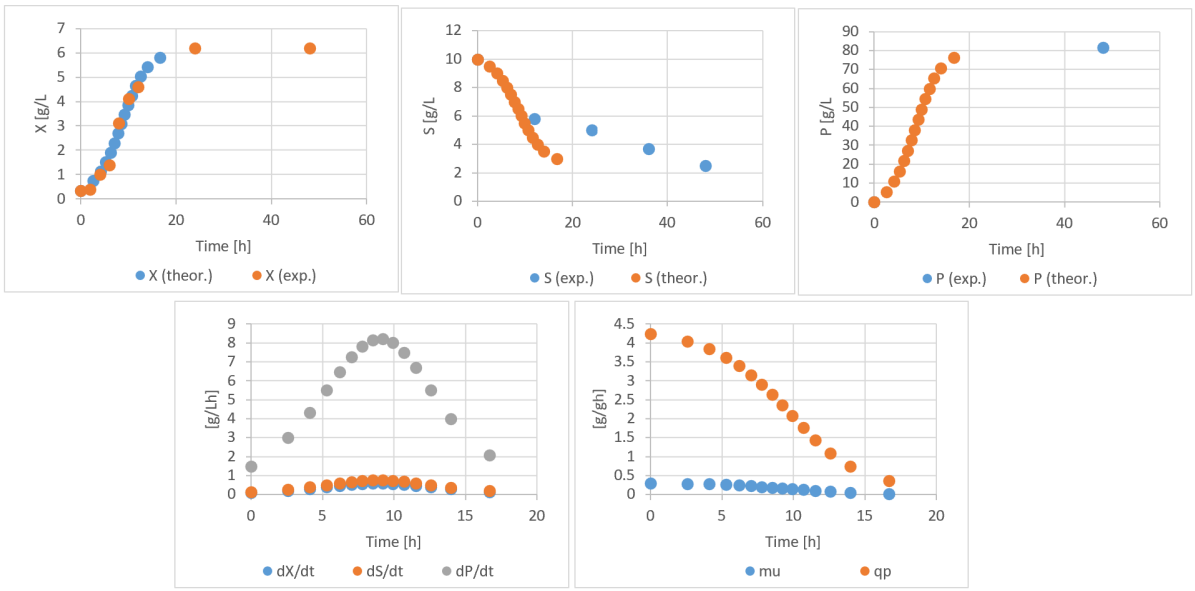

Figure A4: Theoretical and fit curve comparisons, productivity graphs, and cell-specific productivity.

Mass Balance w/ Media				
In	g/L		**In**	g/L
Glucose	80		Glucose	80
Cells	2.59308		Cells	2.59308
Oxygen	0.263		Oxygen	0.263
Protein	6.89422		Protein	6.89422
Media	80		Media	80
sum	170		sum	170
Out	g/L		**Out**	g/L
Protein	62.7832		Protein	62.7832
Glucose	3		Glucose	3
Cells	23.6141	adjusted ->	Cells	104
CO2	0.353		CO2	0.353
Media	0		Media	0
sum	89.7503		sum	170
Difference	80		Difference	0

$$RQ = \frac{moles\ of\ CO_2}{moles\ of\ O_2}\ goal = 98\%$$

$$RQ = \frac{0.353\ \frac{g\ of\ CO_2}{L}\left(\frac{1\ mole}{44\ g\ of\ CO_2}\right)}{0.263\ \frac{g\ of\ O_2}{L}\left(\frac{1\ mole}{32\ g\ of\ O_2}\right)} = 0.976\ or\ 97.6\%$$

Figure A5: Mass balance around production scale reactor to determine protein production. First, using the respiratory quotient (RQ) estimate, the ideal amount of CO_2 was calculated.[101] Next, the enzyme production was optimized to balance the bioreactor. Note that media was not initially included in this material balance, this was due to the protein production being modeled as dependent on glucose concentration as we did not find media yield coefficients in the literature. To combat this, the remaining difference was added back into the cell mass. This additional cell mass has no impact on protein yield.

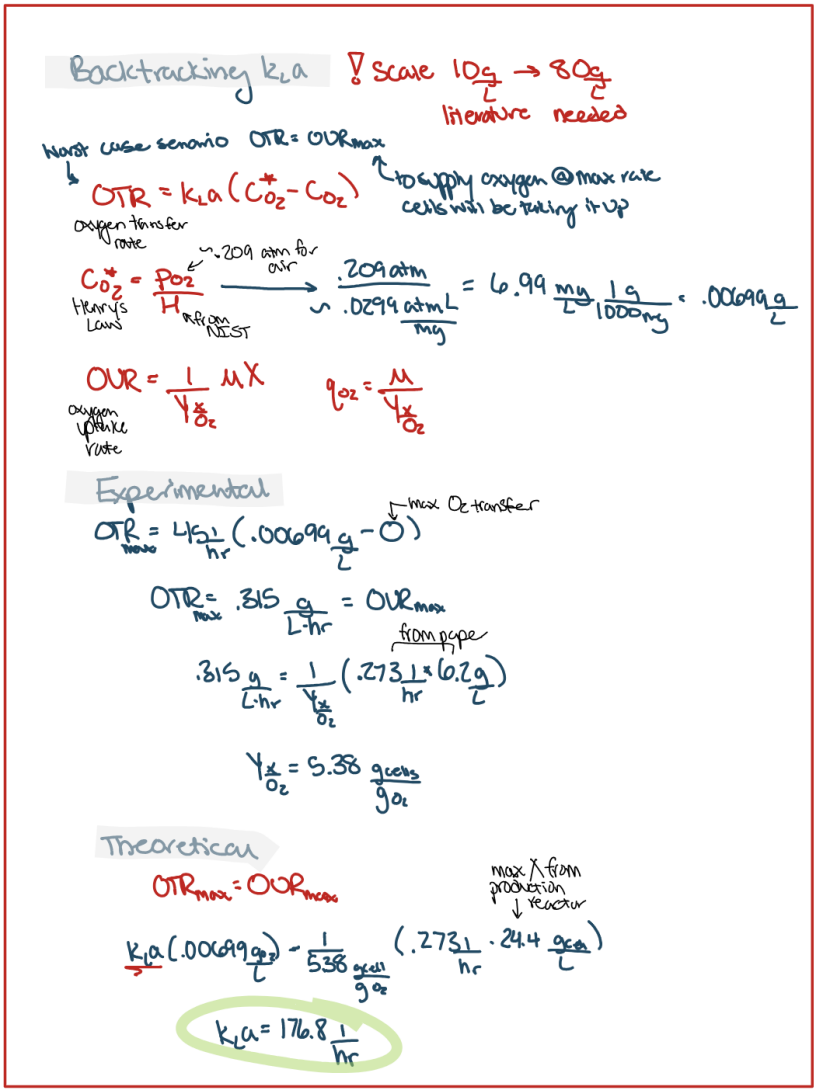

Figure A6: Scaling the k_La from a 10 g/L to 80 g/L glucose growth model.

Trace (1 container per year)			price per container
KCl	25 kg		$506.00
MgSO4	25 kg		$412.00
Ca(NO3)2	25 kg		$702.00
MnCl2	25 g		$ 41.60
FeSO4	25 g		$377.00
Bulk Media Recipe			
Item…	g/L	fraction	price per kg
Beef extract	1	0.07692	$ 1.00
Yeast extract	2	0.15385	$ 1.00
Peptone	5	0.38462	$ 2.50
NaCl	5	0.38462	$ 0.06

Figure A7: The breakdown of media components. The trace components will be purchased once a year from Lab Alley and Sigma Aldrich.[102–106] The bulk of the media will be beef extract,[107] yeast extract,[108] peptone,[109] and NaCl[105] bought wholesale. Using the fractions noted in the figure, the price of the media is estimated to be $1.22 per kg.

Standard Geometry Equations:

$$D_{tank} = \left(\frac{4V_{tank}}{\pi}\right)^{\frac{1}{3}}$$

$$D_{tank} = H_{tank}$$

$$A_{tank} = \frac{\pi}{4}D^2_{tank}$$

$$D_{impeller} = \frac{D_{tank}}{3}$$

Bioreactor Design Rules:

to prevent cell lysis…

$$tip\ velocity\ of\ v_{impeller\ tip} = \pi N D_{impeller} < 2.5\frac{m}{s}$$

to prevent slugging…

$$superficial\ velocity\ of\ v_s = \frac{Q_g}{A_{tank}} < 125\ [\frac{m}{hr}]$$

to prevent flooding…

$$air\ volumetric\ flow\ rate\ of\ Q_g < \frac{0.6D^5_{impeller}N^2}{D^{1.5}_{tank}}\ [\frac{m^3}{s}]$$

$$Power{:}\ volume\ ratio = \frac{P_g}{V_{tank}} < 15{,}000\ \frac{W}{m^3}$$

Reynold's Number: $R_e = \frac{ND^2_{impeller}\rho}{\eta}$

Power Number: $N_p = \frac{P}{\rho N^3 D^5_{impeller}}$

Aeration Number: $N_a = \frac{Q_g}{ND^3_{impeller}}$

$$power\ [W] = P = N_p \rho N^3 D^5_{impeller}$$

$$power\ gassed\ [W] = P_{gassed} = PN_{impellers}(P_{gas\ decrease})$$

$$k_l a_{predicted} = \frac{0.0333}{D^4_{tank}}\left(\frac{P_g}{V_{tank}}\right)^{0.541} Q_g^{\frac{0.541}{\sqrt{D_{tank}}}}$$

Variables:

D_{tank} = *tank diameter* $[m]$

V_{tank} = *tank volume* $[m^3]$

H_{tank} = *tank height* $[m]$

A_{tank} = *tank cross sectional area* $[m^2]$

$D_{impeller}$ = *impeller diameter* $[m]$

ρ = *density of broth* $[\frac{kg}{m^3}]$

η = *viscosity of broth* $[\frac{kg}{m*s}]$

N = *rotation speed of impeller* $[\frac{rad}{s}]$

$N_{impellers}$ = *number of impellers*

$P_{gas\ decrease}$ = *power reduction from gas usage (from aeration curve)*

$k_l a_{predicted}$ = *volumetric mass transfer coefficient* $[\frac{1}{s}]$

Figure A8: Equations utilized in bioreactor design. Note Appendix A9 contains the charts used to find the Reynold's number and power gas decrease.

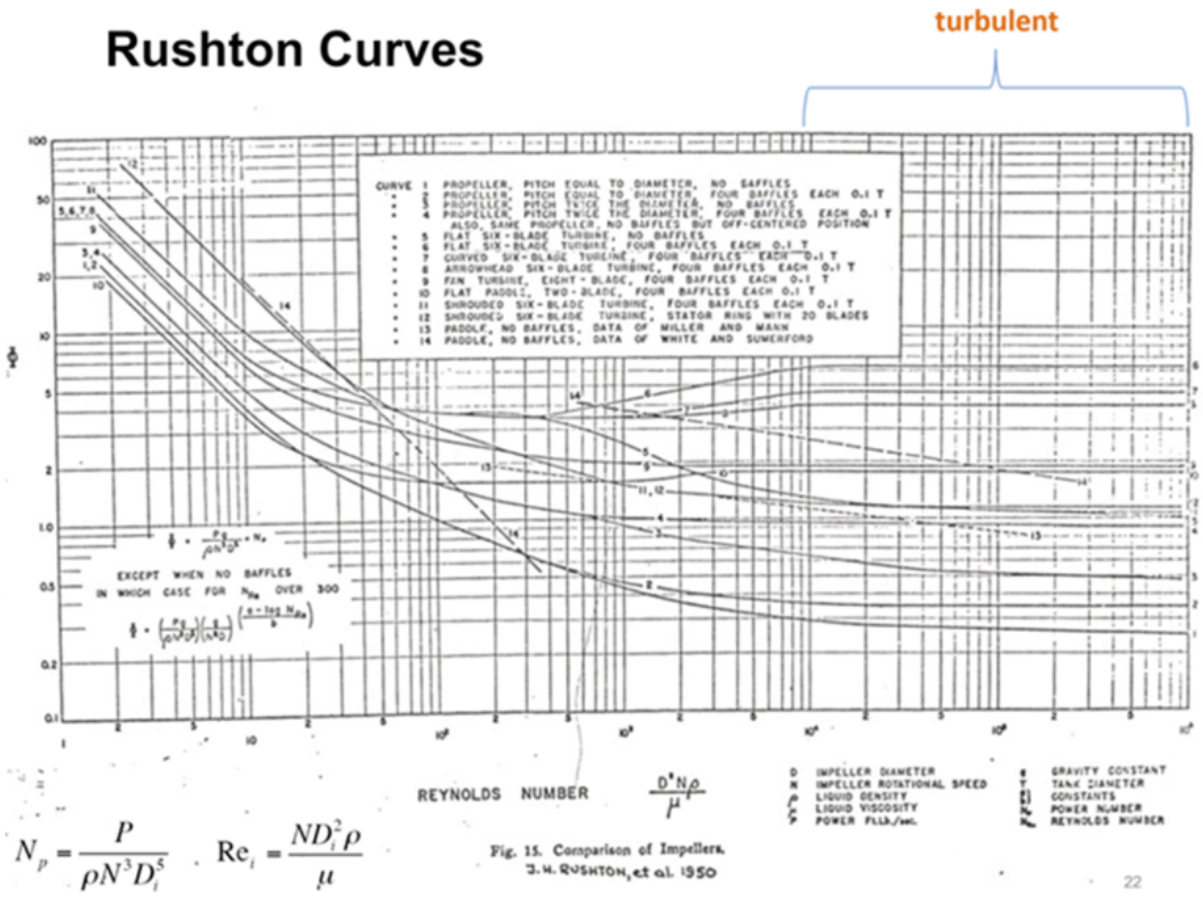

Accounting for Aeration

$$N_a = \frac{Q_g}{ND_i^3}$$

A: Flat-blade turbine (n_p=8)
B: Vaned disk (n_p=8)
C: Vaned disk (n_p=6)
D: Vaned disk (n_p=16)
E: Vaned disk (n_p=4)
F: Paddle
D_t/D_i=3
W_b/D_t=0.1
D_t/H_1=3

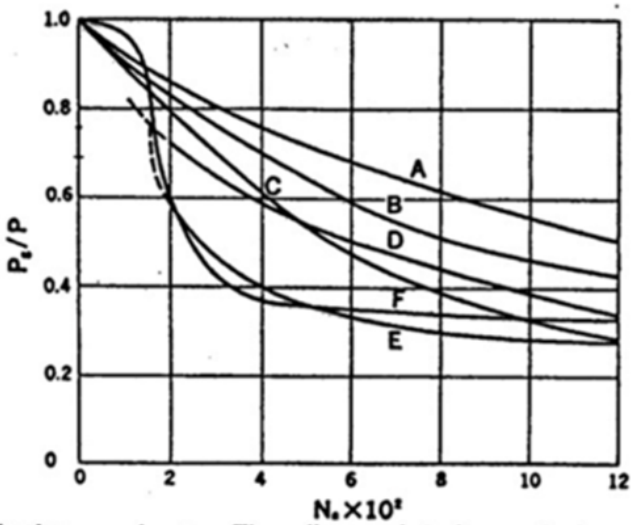

Fig. 6.6. Power requirements for agitation in a gassed system. The ordinate and abscissa are the degree of power decrease, P_g/P, and the aeration number, N_a. Parameters are the types of impellers, whose representative geometrical ratios in agitated vessels are also shown in the figure.[38]

Figure A9: Charts utilized to determine Reynold's number and power decrease from gas.

Table A1: Breakdown of mass and volume balance for the seed train streams U1a-U5a.

U1a											
Mass			Volume from Mass			Concentration			Volume Composition		
Water	1,248	g	Water	1.25	L	Water	892	g/L	Water	0.894377	L/L
Cell	1.40	g	Cell	0.00	L	Cell	1	g/L	Cell	0.002975	L/L
Product	0.00	g	Product	0.00	L	Product	0	g/L	Product	0	L/L
Media	112.00	g	Media	0.07	L	Media	80	g/L	Media	0.051324	L/L
Substrate	112.00	g	Substrate	0.07	L	Substrate	80	g/L	Substrate	0.051324	L/L
total =	1,474	g	Total	1.40	L						

U2a											
Mass			Volume from Mass			Concentration			Volume Composition		
Water	1,297	g	Water	1.30	L	Water	926	g/L	Water	0.92893	L/L
Cell	30.83	g	Cell	0.04	L	Cell	22	g/L	Cell	0.027621	L/L
Product	78.24	g	Product	0.06	L	Product	56	g/L	Product	0.041525	L/L
Media	0.00	g	Media	0.00	L	Media	0	g/L	Media	0	L/L
Substrate	4.20	g	Substrate	0.00	L	Substrate	3	g/L	Substrate	0.001925	L/L
total =	1,410	g	Total	1.40	L						

U2b											
Mass			Volume from Mass			Concentration			Volume Composition		
Water	61,434	g	Water	61.62	L	Water	896	g/L	Water	0.898228	L/L
Cell	0	g	Cell	0.00	L	Cell	0	g/L	Cell	0	L/L
Product	0	g	Product	0.00	L	Product	0	g/L	Product	0	L/L
Media	5,600	g	Media	3.59	L	Media	82	g/L	Media	0.052372	L/L
Substrate	5,282	g	Substrate	3.39	L	Substrate	77	g/L	Substrate	0.0494	L/L
total =	72,316	g	Total	68.6	L						

U3a											
Mass			Volume from Mass			Concentration			Volume Composition		
Water	62,244	g	Water	62	L	Water	889	g/L	Water	0.891883	L/L
Cell	1,502	g	Cell	4	L	Cell	21	g/L	Cell	0.063838	L/L
Product	3,990	g	Product	3	L	Product	57	g/L	Product	0.042355	L/L
Media	0	g	Media	0	L	Media	0	g/L	Media	0	L/L
Substrate	210	g	Substrate	0	L	Substrate	3	g/L	Substrate	0.001925	L/L
total =	67,947	g	Total	70	L						

U3b											
Mass			Volume from Mass			Concentration			Volume Composition		
Water	561,262	g	Water	563	L	Water	891	g/L	Water	0.893573	L/L
Cell	0	g	Cell	0	L	Cell	0	g/L	Cell	0	L/L
Product	0	g	Product	0	L	Product	0	g/L	Product	0	L/L
Media	56,000	g	Media	36	L	Media	89	g/L	Media	0.057027	L/L
Substrate	48,510	g	Substrate	31	L	Substrate	77	g/L	Substrate	0.0494	L/L
total =	665,772	g	Total	630	L						

U4a											
Mass			Volume from Mass			Concentration			Volume Composition		
Water	616,527	g	Water	618	L	Water	881	g/L	Water	0.883404	L/L
Cell	16,217	g	Cell	48	L	Cell	23	g/L	Cell	0.068911	L/L
Product	43,113	g	Product	32	L	Product	62	g/L	Product	0.04576	L/L
Media	0	g	Media	0	L	Media	0	g/L	Media	0	L/L
Substrate	2,100	g	Substrate	1	L	Substrate	3	g/L	Substrate	0.001925	L/L
total =	677,957	g	Total	700	L						

U4b											
Mass			Volume from Mass			Concentration			Volume Composition		
Water	5,612,622	g	Water	5630	L	Water	891	g/L	Water	0.893573	L/L
Cell	0	g	Cell	0	L	Cell	0	g/L	Cell	0	L/L
Product	0	g	Product	0	L	Product	0	g/L	Product	0	L/L
Media	560,000	g	Media	359	L	Media	89	g/L	Media	0.057027	L/L
Substrate	485,100	g	Substrate	311	L	Substrate	77	g/L	Substrate	0.0494	L/L
total =	6,657,722	g	Total	6300	L						

U5a											
Mass			Volume from Mass			Concentration			Volume Composition		
Water	6,159,358	g	Water	6,178	L	Water	880	g/L	Water	0.882556	L/L
Cell	163,364	g	Cell	486	L	Cell	23	g/L	Cell	0.069419	L/L
Product	434,336	g	Product	323	L	Product	62	g/L	Product	0.046101	L/L
Media	0	g	Media	0	L	Media	0	g/L	Media	0	L/L
Substrate	21,000	g	Substrate	13	L	Substrate	3	g/L	Substrate	0.001925	L/L
total =	6,778,057	g	Total	7,000	L						

Table A2: Breakdown of mass and volume balance for the production bioreactor streams.

U5b.1-9											
Mass			Volume from Mass			Concentration			Volume Composition		
Water	498,785	g	Water	500	L	Water	641	g/L	Water	0.643225	L/L
Cell	80,589	g	Cell	240	L	Cell	104	g/L	Cell	0.308203	L/L
Product	48,831	g	Product	36	L	Product	63	g/L	Product	0.046647	L/L
Media	0	g	Media	0	L	Media	0	g/L	Media	0	L/L
Substrate	2,333	g	Substrate	1	L	Substrate	3	g/L	Substrate	0.001925	L/L
total =	630,539	g	Total	778	L						

U5c.1-9											
Mass			Volume from Mass			Concentration			Volume Composition		
Water	5,538,908	g	Water	5,556	L	Water	890	g/L	Water	0.89286	L/L
Cell	0	g	Cell	0	L	Cell	0	g/L	Cell	0	L/L
Product	0	g	Product	0	L	Product	0	g/L	Product	0	L/L
Media	560,000	g	Media	359	L	Media	90	g/L	Media	0.05774	L/L
Substrate	479,111	g	Substrate	307	L	Substrate	77	g/L	Substrate	0.0494	L/L
total =	6,578,019	g	Total	6,222	L						

U6a.1											
Mass			Volume from Mass			Concentration			Volume Composition		
Water	4,489,067	g	Water	4,503	L	Water	641	g/L	Water	0.643225	L/L
Cell	725,299	g	Cell	2,157	L	Cell	104	g/L	Cell	0.308203	L/L
Product	439,483	g	Product	327	L	Product	63	g/L	Product	0.046647	L/L
Media	0	g	Media	0	L	Media	0	g/L	Media	0	L/L
Substrate	21,000	g	Substrate	13	L	Substrate	3	g/L	Substrate	0.001925	L/L
total =	5,674,848	g	Total	7,000	L						

U6a.2-9											
Mass			Volume from Mass			Concentration			Volume Composition		
Water	4,489,067	g	Water	4,503	L	Water	641	g/L	Water	0.643225	L/L
Cell	725,299	g	Cell	2,157	L	Cell	104	g/L	Cell	0.308203	L/L
Product	439,483	g	Product	327	L	Product	63	g/L	Product	0.046647	L/L
Media	0	g	Media	0	L	Media	0	g/L	Media	0	L/L
Substrate	21,000	g	Substrate	13	L	Substrate	3	g/L	Substrate	0.001925	L/L
total =	5,674,848	g	Total	7,000	L						

U6b											
Mass			Volume from Mass			Concentration			Volume Composition		
Water	35,912,534	g	Water	36,021	L	Water	641	g/L	Water	0.643225	L/L
Cell	5,802,388	g	Cell	17,259	L	Cell	104	g/L	Cell	0.308203	L/L
Product	3,515,860	g	Product	2,612	L	Product	63	g/L	Product	0.046647	L/L
Media	0	g	Media	0	L	Media	0	g/L	Media	0	L/L
Substrate	168,000	g	Substrate	108	L	Substrate	3	g/L	Substrate	0.001925	L/L
total =	45,398,783	g	Total	56,000	L						

Centrifuge Design Equations:

$$V_g = \frac{4r_p^2(\rho_p - \rho_f)g}{18\eta}$$

Variables:

V_g = *settling velocity* $[\frac{m}{s}]$

r_p = *cell radius* $[m]$

ρ_p = *cell density* $[\frac{kg}{m^3}]$

ρ_f = *broth density* $[\frac{kg}{m^3}]$

g = *gravity* $[\frac{m}{s^2}]$

η = *broth viscosity* $[\frac{kg}{m*s}]$

$$Q_g = V_g \varepsilon_T$$

Variables:

Q_g = *volumetric flow rate* $[\frac{m^3}{s}]$

V_g = *settling velocity* $[\frac{m}{s}]$

$$P = \rho_p Q_g \omega^2 R_o^2$$

Variables:

P = *power* $[W]$

ρ_p = *cell density* $[\frac{kg}{m^3}]$

Q_g = *volumetric flow rate* $[\frac{m^3}{s}]$

ω = *angular velocity* $[\frac{rad}{s}]$

R_o = *outer radius* $[m]$

$$\varepsilon_T = \frac{2\pi(n-1)\omega^2}{3g} cot\theta (R_o^3 - R_i^3)$$

Variables:

ε_T = *sigma value* $[m^2]$

n = *number of stacks*

ω = *angular velocity* $[\frac{rad}{s}]$

g = *gravity* $[\frac{m}{s^2}]$

θ = *half cone angle* $[deg]$

R_o = *outer radius* $[m]$

R_i = *inner radius* $[m]$

Figure A10: Equations utilized in disk stack centrifuge design. Independent variables are: r_p= 0.000006 m,[110] ρ_p= 1,100 kg/m^3,[111] ρ_f= 1,014 kg/m^3,[112] g= 9.8 m/s^2, η= 0.00083 kg/ms**, R_o= 0.50 m, R_i= 0.45 m, θ= 45 deg, and n=50 stacks. The calculation method is derived from Harrison et al.[111] **Note: η was determined using the viscosity model described in Section 3.2.5

.

Table A3: Breakdown of mass and volume balance for the disk stack centrifuge, specifically the output streams U7a and U7b.

Supernatant (to ultrafiltration) U7a											
Mass			Volume from Mass			Concentration			Volume Composition		
Water	33,859,403	g	Water	33,961	L	Water	949	g/L	Water	0.606	L/L
Cell	0	g	Cell	0	L	Cell	0	g/L	Cell	0.000	L/L
Product	2,241,050	g	Product	1,665	L	Product	63	g/L	Product	0.030	L/L
Substrate	107,085	g	Substrate	69	L	Substrate	3	g/L	Substrate	0.001	L/L
total =	36,207,539	g	Total	35,695	L						

Sludge (out) U7b											
Mass			Volume from Mass			Concentration			Volume Composition		
Water	2,053,131	g	Water	2,059	L	Water	101	g/L	Water	0.101	L/L
Cell	5,802,388	g	Cell	17,259	L	Cell	286	g/L	Cell	0.850	L/L
Product	1,274,810	g	Product	947	L	Product	63	g/L	Product	0.047	L/L
Substrate	60,915	g	Substrate	39	L	Substrate	3	g/L	Substrate	0.002	L/L
total =	9,191,244	g	Total	20,305	L						

Table A4: Breakdown of mass and volume balance for the ultrafiltration membrane, specifically the output streams U8a and U8b.

Retentate (U8a)											
Mass			Volume from Mass			Concentration			Volume Composition		
Water	11,009,659	g	Water	11,043	L	Water	865	g/L	Water	0.867	L/L
Cell	0	g	Cell	0	L	Cell	0	g/L	Cell	0.000	L/L
Product	2,241,050	g	Product	1,665	L	Product	176	g/L	Product	0.131	L/L
Substrate	39,571	g	Substrate	25	L	Substrate	3	g/L	Substrate	0.002	L/L
total =	13,290,281	g	Total	12,733	L						

Waste Water (U8b)											
Mass			Volume from Mass			Concentration			Volume Composition		
Water	22,849,744	g	Water	22,918	L	Water	995	g/L	Water	0.998	L/L
Cell	0	g	Cell	0	L	Cell	0	g/L	Cell	0.000	L/L
Product	0	g	Product	0	L	Product	0	g/L	Product	0.000	L/L
Substrate	67,514	g	Substrate	43	L	Substrate	3	g/L	Substrate	0.002	L/L
total =	22,917,258	g	Total	22,962	L						

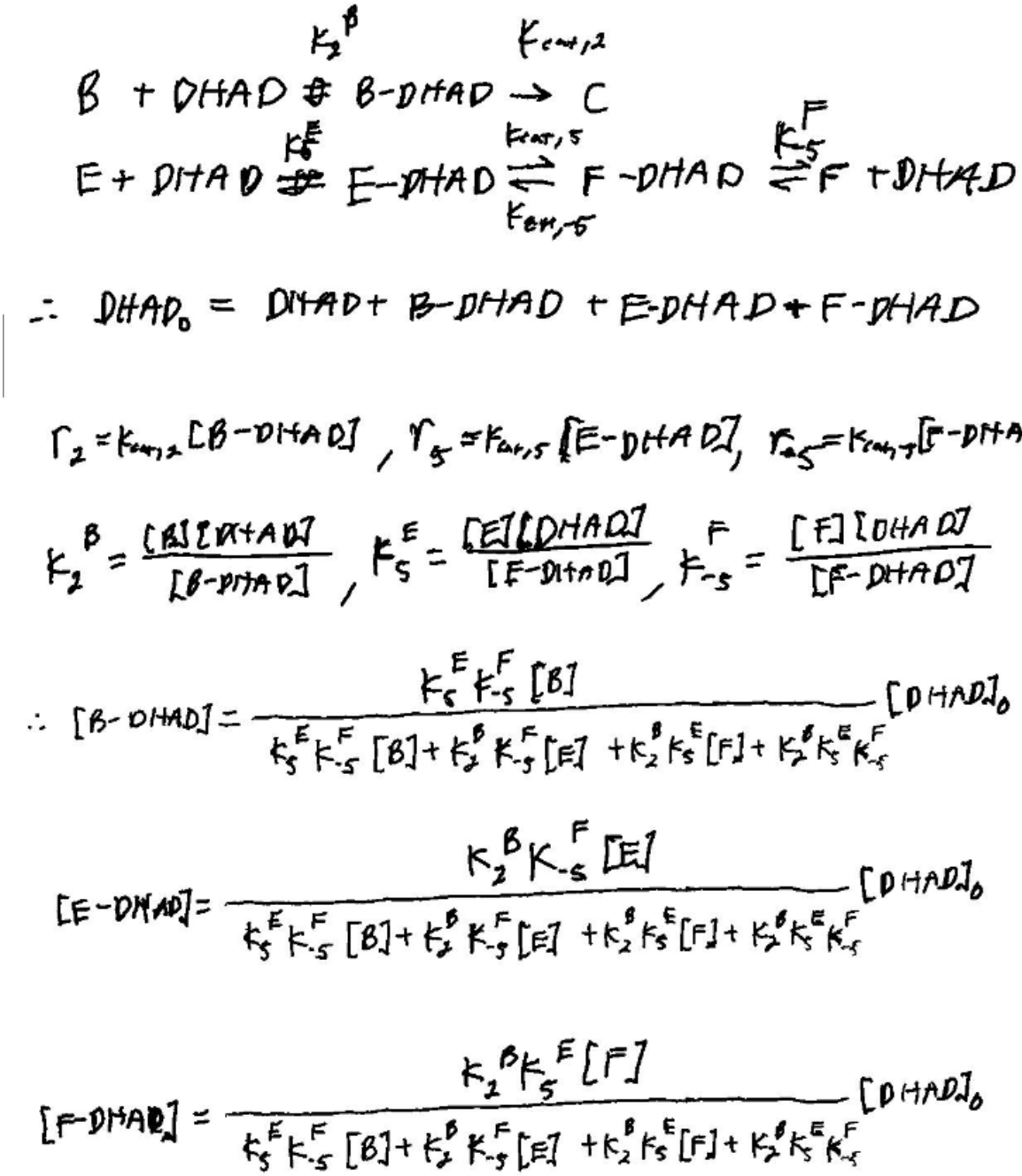

Figure A11: Derivation of equations 25 and 28. The model assumes that both substrates bind the same active site. This is very likely, as the enzyme catalyzes the same reaction on both substrates (oxidation of the carboxylic acid's β-hydroxy group).

$$Rate = \frac{k_{cat}\,[A]}{K_{M,A} + [A]}\,[E]_0 \qquad Rate = \frac{k_{cat}\,[B]}{K_{M,B} + [B]}\,[E]_0$$

$$\downarrow$$

$$Rate = \frac{k_{cat}\,[A]\,[B]}{K_{M,B}\,[A] + K_{M,A}\,[B] + [A]\,[B]}\,[E]_0$$

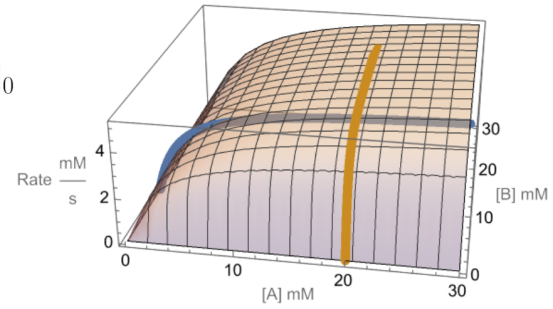

Figure A12: Method used to convert effective Michaelis-Menten parameters to true bi-molecular kinetic parameters. The Michaelis-Menten plots were moved into 3-dimensions and plotted along the line of constant substrate concentration that was reported in the assay. Points were then sampled along these plots and non-linear regression was used to fit the new model parameters to the reported effective Michaelis-Menten parameters

Table A5: Alpha Fold Results for the top 5 tetrameter structures of DHAD

Model Rank	Mean pLDDT	Max PAE	pTM	ipTM	Uncertainty	Overall Quality
1	95.16	29.98	0.96	0.95	N/A	Very High
2	95.51	28.52	0.96	0.95	N/A	Very High
3	95.19	29.98	0.96	0.95	N/A	Very High
4	94.67	31.03	0.95	0.95	N/A	Very High
5	94.02	29.86	0.95	0.95	N/A	Very High

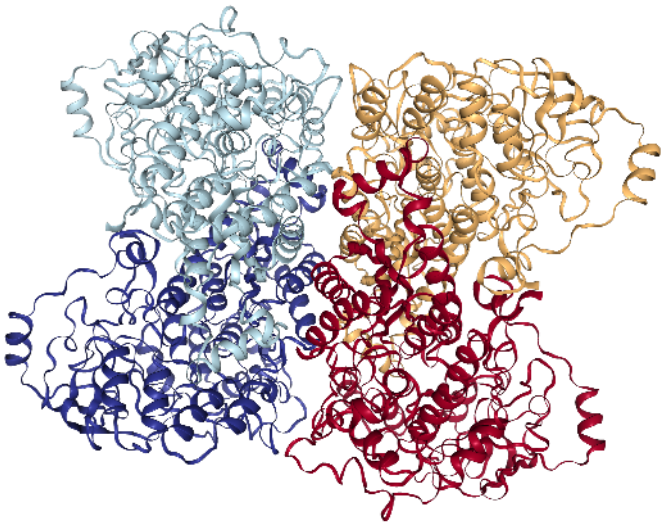

Figure A13: Highest ranking AlphaFold2 predicted structure of a DHAD tetramer.

Table A6: HullRad results for the 5 cell-free pathway enzymes.

Property	GDH	DHAD	KDGA	ALDH	LLDH
#Amino Acids	724	2232	576	1968	312
M (g/mol)	80938	237667	65022	218464	34233
v_bar (mL/g)	0.748	0.744	0.752	0.740	0.748
Ro(Anhydrous) (Å)	28.85	41.23	26.86	40.02	21.65
Rg(Anhydrous) (Å)	27.53	38.14	25.24	50.35	19.90
Dmax (Å)	89.43	136.27	84.25	158.44	61.19
Axial Ratio	1.41	1.61	1.56	1.85	1.26
f/fo	1.25	1.23	1.20	1.36	1.22
Dt (cm^2/s)	5.93e-07	4.21e-07	6.66e-07	3.93e-07	8.11e-07
R(Translation) (Å)	36.16	50.90	32.20	54.56	26.42
s (sec)	4.98e-13	1.06e-12	4.42e-13	9.19e-13	2.89e-13
Int. Viscosity (mL/g)	4.101	3.819	3.853	6.676	3.659
ks(non-ideal) (mL/g)	5.847	5.516	5.116	7.313	5.419
Asphericity	0.12	0.10	0.20	0.42	0.08
Dr (s^-1)	2.90e+06	1.02e+06	3.94e+06	7.84e+05	7.42e+06
R(Rotation) (Å)	38.12	53.95	34.42	58.97	27.88
tauC (ns)	57.41	162.79	42.29	212.61	22.46

The following are the equations used to solve for the k_{cat} values in terms of the associated K values and the measurements of enzyme activity.[21] Here, a is the measured activity with units of $\frac{\mu mol}{\text{min mg}}$ (not to be confused with thermodynamic activity), and [A] and [B] are the concentrations of the substrates used in the activity assay. For two-substrate enzymes, Equation A1 was used while Equation A2 was used for single-substrate enzymes.

$$k_{cat} = \frac{aMM}{\frac{[A][B]}{K_A[B]+K_B[A][A][B]}} \tag{A1}$$

$$k_{cat} = \frac{aMM}{\frac{[A]}{K_A+[A]}} \tag{A2}$$

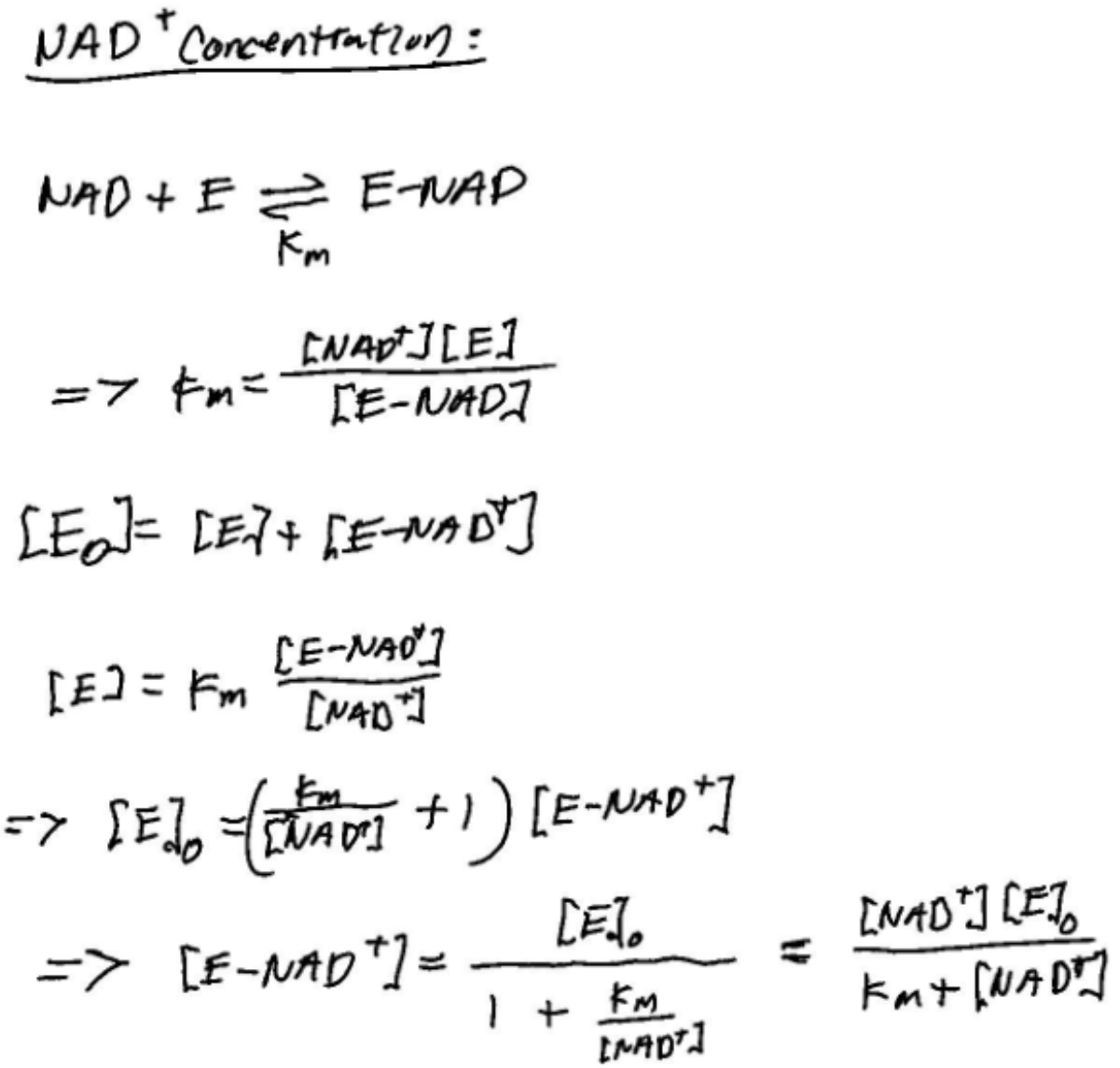

Figure A14: Derivation of equations 30 and 31. The general case is derived here showing the amount of coenzyme that will be bound to an enzyme. Equations 30 and 31 are the sum of this derived for for all coenzyme binding enzymes in the pathway.

$$m_i = c_i \cdot V_{tot}$$

$$V_{tot} = \sum V_p + V_S$$

$$V_p = \bar{V} c_i V_{tot}$$

$$\therefore V_{tot} = \sum_i \bar{V}_i c_i V_{tot} + V_S$$

$$\Rightarrow V_{tot} \left(1 - \sum_i \bar{V}_i c_i\right) = V_S$$

$$m_S = \rho_S V_S$$

$$\rho_{tot} = \frac{\sum c_i V_{tot} + \rho_S V_S}{V_{tot}}$$

$$\boxed{\rho = \sum c_i + \rho_S \left(1 - \sum \bar{V}_i c_i\right)}$$

Figure A15: Derivation of equation 43.

$$Tw = 50\,\overset{\circ}{\Delta}C;$$

$$Ta = 18\,\overset{\circ}{\Delta}C;$$

$$\mu = \text{ThermodynamicData}\left["Air", "DynamicViscosity", \{"Temperature" \to 18\,°C\}\right];$$

$$\rho = \text{ThermodynamicData}\left["Air", "Density", \{"Temperature" \to 18\,°C\}\right];$$

$$k = \text{ThermodynamicData}\left["Air", "ThermalConductivity", \{"Temperature" \to 18\,°C\}\right];$$

$$Cp = \text{ThermodynamicData}\left["Air", "MolarIsochoricHeatCapacity", \{"Temperature" \to 18\,°C\}\right];$$

$$L = 54\,m;$$

$$W = 8.5\,m;$$

$$A = 2\,W\,L;$$

$$V = 18\,mi/h;$$

$$RE = \frac{\rho\,V\,L}{\mu};$$

$$REcr = 5 * 10^5;$$

$$Pr = 1;$$

$$Nu = 0.664\,REcr^{\frac{1}{2}}\,Pr^{\frac{1}{3}} + 0.036\,RE^{0.8}\,Pr^{0.43}\left(1 - \left(\frac{REcr}{RE}\right)^{0.8}\right);$$

$$h = k\,Nu\,/\,L;$$

$$Q = \text{UnitConvert}[A\,h\,(Tw - Ta), "Kilowatts"] + \frac{555\,h\,kW}{22.5\,h}\ //\ \text{Framed}$$

$$\boxed{484.394\,kW}$$

Figure A16: Calculation of the total heat duty of the cell-free reactor. It is assumed that the primary heat duty is needed to make up for convective heat transfer to the surroundings along the largest 2 faces of the reactor. The semi-empirical correlations used are from Table 6.1 of Heat and Mass Transfer for Chemical Engineers by Giorgio Carta[113]

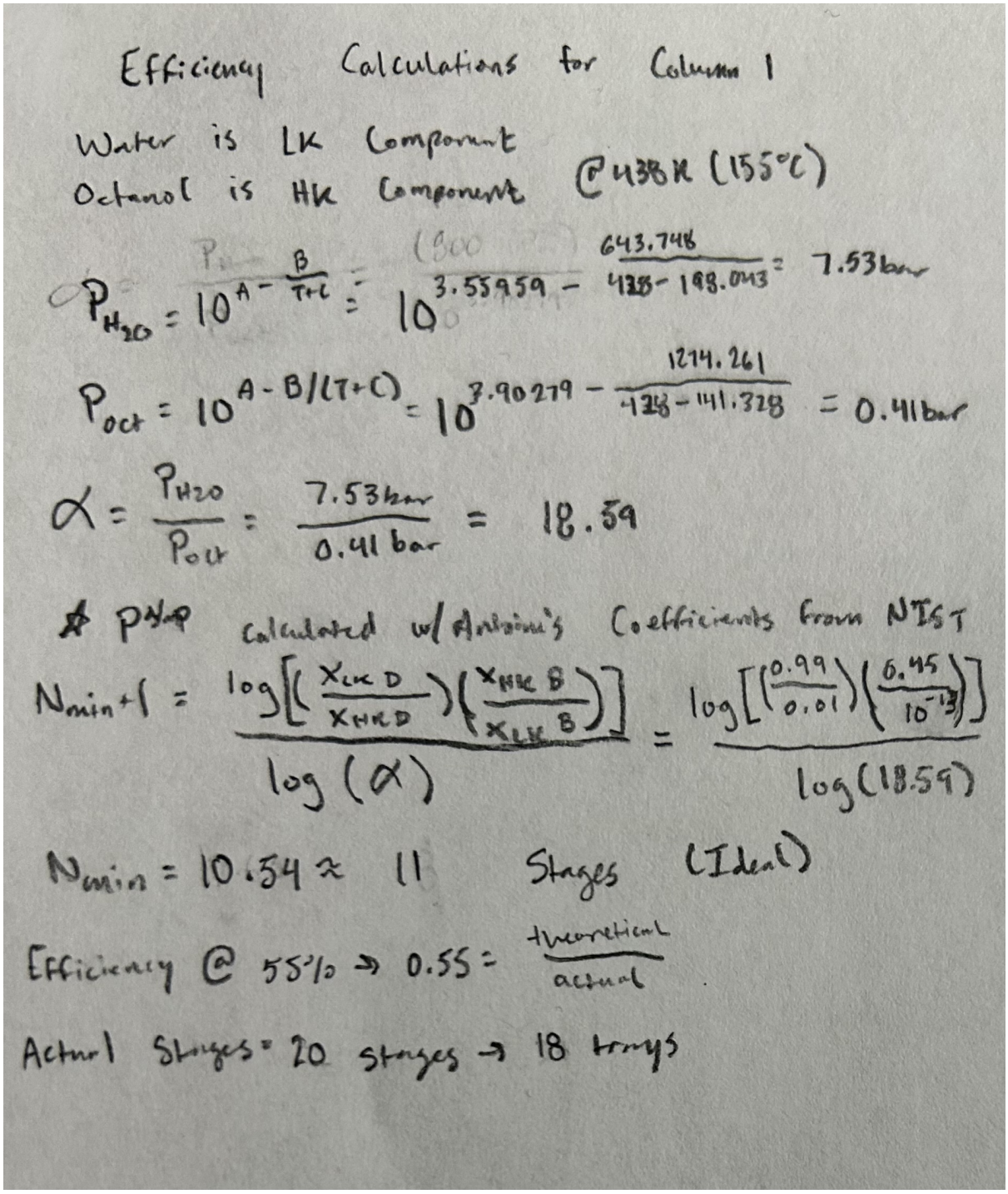

Figure A17: D7 Ideal Stage Number Calculations. The individual vapor pressures were found on NIST and adjusted to column temperature using Antoine's Equation. The vapor pressures were then used to compute the relative volatility between octanol[114] and water.[115] The minimum number of stages was found using the Fenske Equation.[64] Two stages were subtracted to find trays because the top and bottom trays serve as the condenser and reboiler respectively. Based on the calculations, 11 stages were ideal and 20 stages were needed.

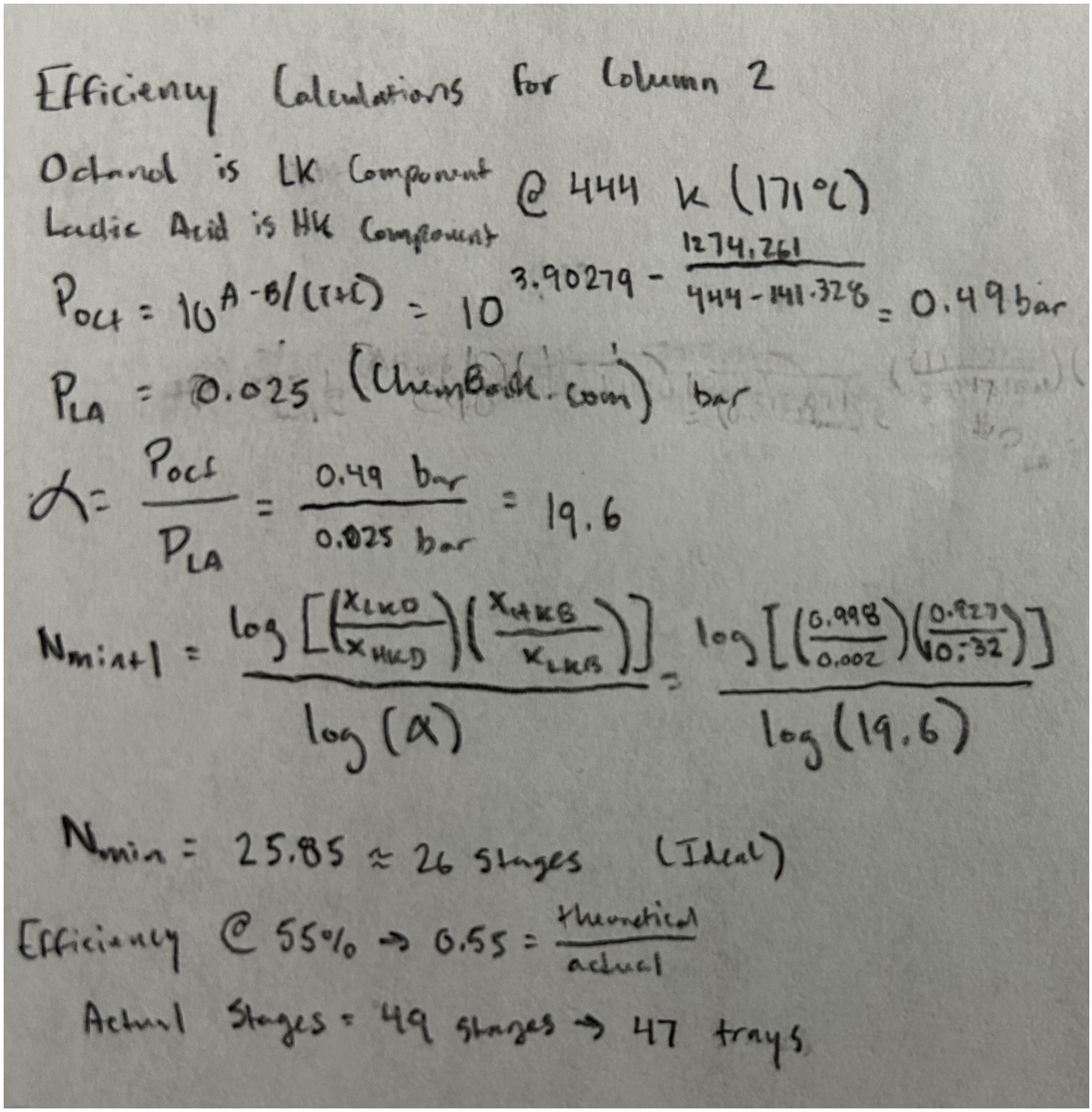

Figure A18: D8 Ideal Stage Number Calculations. The octanol vapor pressure was found on NIST[114] and adjusted to column temperature using Antoine's Equation and the lactic acid vapor pressure was approximated using ChemBook.[116] The vapor pressures were then used to compute the relative volatility between octanol and lactic acid. The minimum number of stages was found using the Fenske Equation.[64] Two stages were subtracted to find trays because the top and bottom trays serve as the condenser and reboiler respectively. Based on the calculations, 26 stages were ideal and 49 stages were needed.

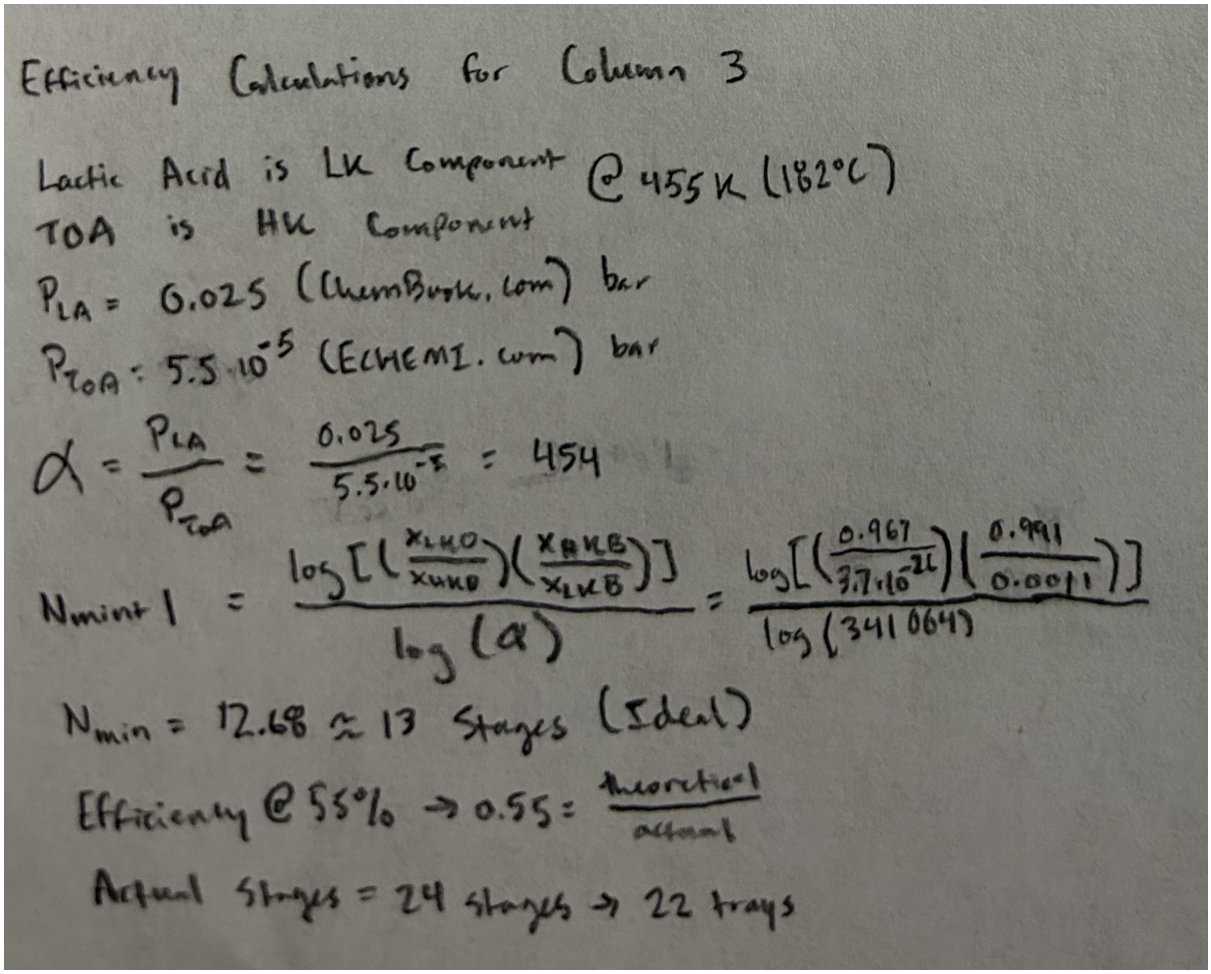

Figure A19: D9 Ideal Stage Number Calculations. The trioctylamine vapor pressure was approximated using EChemi[117] and the lactic acid vapor pressure was approximated using Chemical Book.[116] The vapor pressures were then used to compute the relative volatility between lactic acid and trioctylamine. The minimum number of stages was found using the Fenske Equation.[64] Two stages were subtracted to find trays because the top and bottom trays serve as the condenser and reboiler respectively. Based on the calculations, 13 stages were ideal and 24 stages were needed.

Table A7: D7 Mass and Molar Flows

	Feed			Distillate			Bottoms		
	Mass Flow (kg/h)	Mass Percent	Molar Percent	Mass Flow (kg/h)	Mass Percent	Molar Percent	Mass Flow (kg/h)	Mass Percent	Molar Percent
Water	3263	0.281	0.714	3263	0.901	0.985	0	0	0
Octanol	4367	0.379	0.133	345	0.095	0.014	4052	0.507	0.446
Lactic Acid	3228	0.278	0.141	0	0	0	3228	0.404	0.514
Trioctylamine	557	0.048	0.006	0	0	0	557	0.07	0.022
Glycerate	149	0.013	0.005	0	0	0	149	0.019	0.018
Glyceraldehyde	14	0.001	0.001	14	0.004	0.001	0	0	0

Table A8: Column Diameter Calculations Using Single Chemical Property Assumptions

	Column 1 Top	Column 2 Top	Column 3 Top	Column 1 Bottom	Column 2 Bottom	Column 3 Bottom
L (kg/h)	278148.00	15683.00	185.00	291841.00	16899.00	192.00
V (kg/h)	280523.00	20660.00	222.00	296227.00	20819.00	220.00
L/V	0.99	0.76	0.83	0.99	0.81	0.87
Pressure (atm)	0.10	0.10	0.10	0.10	0.10	0.10
MW (kg/mol)	0.13	0.13	0.09	0.13	0.09	0.09
R (m3*atm/mol/K)	0.00	0.00	0.00	0.00	0.00	0.00
Temperature (K)	410.00	436.00	442.00	414.00	443.00	442.00
pV (kg/m3)	0.39	0.36	0.25	0.38	0.25	0.25
Specific G	0.83	0.83	1.25	0.83	1.25	1.25
Density of Water (kg/m3)	1000.00	1000.00	1000.00	1000.00	1000.00	1000.00
pL (kg/m3)	829.00	829.00	1249.00	829.00	1249.00	1249.00
F_lv	0.02	0.02	0.01	0.02	0.01	0.01
C_sb	0.39	0.38	0.39	0.39	0.39	0.39
surf_tens (dyne)	27.60	27.60	54.00	27.60	54.00	54.00
U_flood (ft/s)	19.26	19.35	33.73	19.36	33.77	33.73
U_flood (m/h)	21130.47	21231.73	36999.56	21233.34	37041.40	36999.56
efficiency	0.55	0.55	0.58	0.55	0.55	0.58
f	0.80	0.80	0.80	0.80	0.80	0.80
D (kg/h)	3555.00	4185.00	3360.00	3555.00	4185.00	3360.00
V (kg/h)	419898.64	17372.33	20160.00	240101.91	22226.41	26400.00
V (mol/h)	3229989.52	133633.33	223751.39	1846937.78	246685.98	293007.77
Diameter (m)	12.20	2.55	2.45	9.25	2.64	2.80

Table A9: Condenser and Reboiler Sizing Calculations Using ASPEN Surface Area and Pipe Sizing Data

	C1 - Condenser	C2 - Condenser	C3 - Condenser	C1 - Reboiler	C2 - Reboiler	C3 - Reboiler
A (m^2)	889.037	40.7257	24.305	4975.66	414.196	243.865
OD, tubes (m)	0.0254	0.0254	0.0254	0.0254	0.0254	0.0254
Spacing (m)	0.03175	0.03175	0.03175	0.03175	0.03175	0.03175
Tube Length (m)	6.096	6.096	6.096	6.096	6.096	6.096
SA per tube (m)	0.48643918	0.48643918	0.48643918	0.48643918	0.48643918	0.48643918
Number of Tube	1827.642667	83.72208013	49.96513645	10228.74021	851.4856884	501.3268052
Shell I Diameter (m)	1.426943311	0.665064944	0.537517545	1.852492617	1.238208439	1.107313515

Table A10: D8 Mass and Molar Flows

	Feed			Distillate			Bottoms		
	Mass Flow (kg/h)	Mass Percent	Molar Percent	Mass Flow (kg/h)	Mass Percent	Molar Percent	Mass Flow (kg/h)	Mass Percent	Molar Percent
Octanol	4052	0.507	0.446	4052	0.998	0.998	0	0	0
Lactic Acid	3228	0.404	0.514	6	0.002	0.002	3222	0.82	0.927
Trioctylamine	557	0.07	0.022	0	0	0	557	0.142	0.041
Glycerate	149	0.019	0.018	0	0	0	149	0.038	0.032

Table A11: D9 Mass and Molar Flows

	Feed			Distillate			Bottoms		
	Mass Flow (kg/h)	Mass Percent	Molar Percent	Mass Flow (kg/h)	Mass Percent	Molar Percent	Mass Flow (kg/h)	Mass Percent	Molar Percent
Lactic Acid	3222	0.82	0.927	3221	0.956	0.967	1	0.002	0.009
Trioctylamine	557	0.142	0.041	0	0	0	557	0.998	0.991
Glycerate	149	0.038	0.032	149	0.044	0.033	0	0	0

Table A12: D10 Mass and Molar Flows

	Feed			Distillate			Bottoms		
	Mass Flow (kg/h)	Mass Percent	Molar Percent	Mass Flow (kg/h)	Mass Percent	Molar Percent	Mass Flow (kg/h)	Mass Percent	Molar Percent
Water	3263	0.901	0.985	25	0.068	0.345	3238	0.995	0.999
Octanol	345	0.095	0.014	341	0.931	0.653	4	0.001	0
Glyceraldehyde	14	0.004	0.001	1	0.001	0.002	13	0.004	0.001

Mass [kg]	U1a	U2a	U2b	U3a	U3b	U4a	U4b	U5a	U5b.1-9*	U5c.1-9*
Water	1.248	1.297	61.434	62.244	561.262	616.527	5,613	6,159	3,698,991	41,076,542
Cell	0.001	0.031	-	1.502	-	16.217	-	163	597,646	-
Product	-	0.078	-	3.990	-	43.113	-	434	362,134	-
Media	0.112	-	5.600	-	56.000	-	560	-	-	4,152,960
Substrate	0.112	0.004	5.282	0.210	48.510	2.100	485	21	17,304	3,553,088
Total	1.474	1.410	72.316	67.947	665.772	677.957	6,658	6,778	4,676,075	48,782,590

Mass [kg]	U6a.1	U6a.2-9*	U6b	U7a	U7b	U8a	U8b
Water	3,698,991	29,591,928	29,591,928	27,900,148	1,691,780	9,071,959	18,828,189
Cell	597,646	4,781,168	4,781,168	-	4,781,168	-	-
Product	362,134	2,897,069	2,897,069	1,846,625	1,050,444	1,846,625	-
Media	-	-	-	-	-	-	-
Substrate	17,304	138,432	138,432	88,238	50,194	32,607	55,631
Total	4,676,075	37,408,597	37,408,597	29,835,012	7,573,585	10,951,192	18,883,820

Mass balance before media correction. (above)

Material Balance Check

In (sum of U1a, U2b, U3b, U4b, and U5c.1-9):
48,789,987 kg yearly

Out (sum of U7b, U8b, U8a):
37,408,597 kg yearly

Difference:
11,381,390 kg extra biomass yearly
^^ This is the additional cell mass due to media

The yearly mass needed to correct for media. (above)

Mass [kg]	U1a	U2a	U2b	U3a	U3b	U4a	U4b	U5a	U5b.1-9*	U5c.1-9*
Water	1.248	1.297	61.434	62.244	561.262	616.527	5,613	6,159	3,698,991	41,076,542
Cell	0.001	0.031	-	1.502	-	16.217	-	163	597,646	-
Product	-	0.078	-	3.990	-	43.113	-	434	362,134	-
Media	0.112	-	5.600	-	56.000	-	560	-	-	4,152,960
Substrate	0.112	0.004	5.282	0.210	48.510	2.100	485	21	17,304	3,553,088
Total	1.474	1.410	72.316	67.947	665.772	677.957	6,658	6,778	4,676,075	48,782,590

Mass [kg]	U6a.1	U6a.2-9*	U6b	U7a	U7b	U8a	U8b
Water	3,698,991	29,591,928	29,591,928	27,900,148	1,691,780	9,071,959	18,828,189
Cell	597,646	16,162,558	16,162,558	-	16,162,558	-	-
Product	362,134	2,897,069	2,897,069	1,846,625	1,050,444	1,846,625	-
Media	-	-	-	-	-	-	-
Substrate	17,304	138,432	138,432	88,238	50,194	32,607	55,631
Total	4,676,075	37,408,597	37,408,597	29,835,012	18,954,975	10,951,192	18,883,820

Figure A20: Yearly mass used in the upstream process before correction for media. (Corrected masses are shown in the blue table entries where media has been added as cell mass) *The table shows the sum of each identical stream (U5b.1 + U5b.2 + ...).

Table A13: Mass balances surrounding the cell-free reactors. The stream labels represent the sums of the streams for each of the two duplicate reactors. For instance, a value in CFc represents the sum of the values in streams CF1c and CF2c. It is assumed that all annual mass flows are split evenly between the two reactors, with each reactor being used to produce 157 batches a year.

Mass [kg/hr]	CFc	CFb	CFe	CFf
Water	0	319336880	42193780	367122520
Na+	0	114080	7275820	7389900
OH-	0	0	5382320	0
Glucose	25565260	24810	0	0
D-Gluconate	0	950	0	1840
Glyceraldehyde	0	7430	0	127580
Glycerate	0	51670	0	1116350
L-Lactate	0	1559710	0	25754500
Protein	0	68453120	0	68453120
Total	25565260	389548650	54851920	469965810

Table A14: Overall Mass Balance for Water Separation Column(D7)

Material	D7a: Feed	D10a: Decanter	D8a: Column 2
Water	3,262.63	3,262.63	0.00
Glyceric acid	135.38	0.00	135.38
Glyceraldhyde	13.91	13.91	0.00
D-Gluconic acid	13.09	0.00	13.09
Lactic Acid	3,227.87	0.00	3,227.87
Glucose	0.14	0.00	0.14
Trioctylamine	557.27	0.00	557.27
Octanol	4,396.69	345.06	4,051.63
Total	11,606.98	3,621.60	7,985.38

Table A15: Overall Mass Balance for Octanol Separation Column (D8)

Material	D8a: Feed	D6f.2: Octanol Recycle	D9a: Column 3
Glycerate	135.38	0.25	135.13
D-Gluconate	13.09	0.00	13.09
Lactic Acid	3,227.87	6.17	3,221.70
Glucose	0.14	0.00	0.14
Trioctylamine	557.27	0.00	557.27
Octanol	4,051.63	4,051.63	0.00
Total	7,985.38	4,058.05	3,927.33

Table A16: Overall Mass Balance for Trioctylamine (D9)

Material	D9a: Feed	D10a: Product	D6f.3: TOA Recycle
Glycerate	135.13	134.94	0.19
D-Gluconate	13.09	13.09	0.00
Lactic Acid	3,221.70	3,220.62	1.08
Glucose	0.14	0.14	0.00
Trioctylamine	557.27	0.00	557.27
Total	3,927.33	3,368.79	558.54

Table A17: Overall Mass Balance for the Decanter (D10)

Material	D9a: Feed	D6g.1: Octanol Recycle	D6i: Wastewater
Water	3,262.63	24.93	3,237.70
Glyceraldhyde	13.91	0.52	13.39
Octanol	345.06	340.95	4.11
Total	3,621.60	366.40	3,255.20

Table A18: Overall Mass Balance for Combined Recycle Stream (D6f)

Material	D6f.1: Octanol Recycle	D6f.2: Octanol Recycle	D6f.3: TOA Recycle	D6f: LLE Solvent Merge
Water	24.93	0.00	0.00	24.93
Glycerate	0.00	0.25	0.19	0.44
Glyceraldhyde	0.52	0.00	0.00	0.52
Lactic Acid	0.00	6.17	1.08	7.25
Trioctylamine	0.00	0.00	557.27	557.27
Octanol	340.95	4,051.63	0.00	4,392.58
Total	366.40	4,058.05	558.54	4,982.99

Table A19: Upstream Electricity Costs

Large Unit Operations			
Identifier	**Equipment**	**Yearly Utility [kWh]**	**Yearly Cost**
U1	Bioreactor	2	$0.19
U2	Bioreactor	125	$10.56
U3	Bioreactor	942	$79.56
U4	Bioreactor	1,324,909	$111,954.83
U5.2	Bioreactor	1,324,909	$111,954.83
U5.3	Bioreactor	1,324,909	$111,954.83
U5.4	Bioreactor	1,324,909	$111,954.83
U5.5	Bioreactor	1,324,909	$111,954.83
U5.6	Bioreactor	1,324,909	$111,954.83
U5.7	Bioreactor	1,324,909	$111,954.83
U5.8	Bioreactor	1,324,909	$111,954.83
U5.9	Bioreactor	1,324,909	$111,954.83
U6	Disk Stack Centrifuge	17,524	$1,480.78
U7	Ultrafiltration Membrane	-	-

Pumps			
Identifier	**Equipment**	**Yearly Utility [kWh]**	**Yearly Cost**
U2a.p	Centrifugal Pump	0.00003	$0.00
U2b.p	Centrifugal Pump	0.0013	$0.00
U3a.p	Centrifugal Pump	0.0013	$0.00
U3b.p	Centrifugal Pump	0.0100	$0.00
U4a.p	Centrifugal Pump	0.0100	$0.00
U4b.p	Centrifugal Pump	0.12	$0.01
U5a.p	Centrifugal Pump	0.13	$0.01
U5c.p	Centrifugal Pump	96	$8.13
U6a.p	Centrifugal Pump	108	$9.14
S3.p	Centrifugal Pump	866	$73.16
U6b.p	Centrifugal Pump	108	$9.14
U7a.p	Centrifugal Pump	549	$46.42
U7b.p	Centrifugal Pump	317	$26.75
U8a.p	Centrifugal Pump	12,206	$1,031.39
U8b.p	Centrifugal Pump	22,011	$1,859.90

Storage Silos			
Identifier	**Equipment**	**Yearly Utility [kWh]**	**Yearly Cost**
S1	Silo	-	$0.00
S2	Silo	-	$0.00
S3	Silo	-	$0.00
S4	Silo	-	$0.00

Storage Tanks			
Identifier	**Equipment**	**Yearly Utility [kWh]**	**Yearly Cost**
S5	Storage Tank	-	$0.00
CF3	Storage Tank	-	$0.00

Miscellaneous			
Identifier	**Equipment**	**Yearly Utility [kWh]**	**Yearly Cost**
S1a	Screw Conveyor	138,333	$11,689.17
S2a	Screw Conveyor	138,333	$11,689.17
S3a	Screw Conveyor	138,333	$11,689.17
S4a	Screw Conveyor	138,333	$11,689.17
S6	Incinerator	39,803	$3,363.33

The bioreactor energy is based on sterilization and agitation power requirements. The disk stack centrifuge is based on the power required to reach the design RPM. The ultrafiltration

membrane will be pressure-driven, so all costs are incorporated into pump power. All pumps are based on the flowrate they are designed to pump as well as accommodating for any pressure differential. The silos and storage tanks require no power. The screw conveyors and incinerator utilities are based on an allowance, though the design of their power consumption was not included in this project design, rather is an estimate.

Table A20: Cell Free Reactor Utility Costs

Equipment Name	Annual Power Use [kWh]	Annual Cost [$]
CF1d.p	614,655	$51,938
CF2d.p	614,655	$51,938
CF1b.p	211,950	$35,820
CF1a.p	3,533	$299
CF2a.p	3,533	$299
CF1.h	1,960,538	$165,665
CF2.h	1,960,538	$165,665

Table A21: Downstream Electricity Costs

Equipment Name	Annual Power Use [kWh]	Annual Cost [$]
D10	2,096,714	$146,625
D1c.p	1,479,261	$103,449
D2c.p	1,479,261	$103,449
D3c.p	1,479,261	$103,449
D4c.p	1,479,261	$103,449
D5d.p	63,792	$4,461
D5a.1-4.p	1,061,692	$74,245
D6b.h.p	3,016,393	$210,940
D6e.p	8,526	$596
D11a.h.1.p	9,293	$650
D5a.1-4.h	22,935	$1,604
D11a.h	550,353	$38,487
D7a.h	446,080	$31,195
D6b.h	668,694	$46,762
D7.p	299,774	$20,964
D8.p	245,037	$17,136
D9.p	203,345	$14,220
D6f.p	1,961	$137
D11b.p	8,526	$596
D11e.p	8,526	$596
S11a	2,132	$151
D12a.p	181,178	$12,670

Table A22: Downstream Condenser Water Utility Costs

Equipment Name	Volume [m^3]	Annual Cost [$]
D7.c	251,609,904	$605,591
D8.c	24,773,616	$59,609
D9.c	33,720,624	$81,217

Table A23: Downstream Cooling Water Utility Costs

Equipment Name	Volume [m^3]	Annual Cost [$]
D11a.h	77,616	$4,719
D6b.h	99,774,122	$6,066,267
D6f.h	35,280,000	$2,145,024

Table A24: Downstream Steam Utility Costs

Equipment Name	Volume [m^3]	Pressure [psi]	Annual Cost [$]
D7.r	256,457,376	100	$7,963,026
D5a.1-4.h	2,116,800	165	$45,547
D8.r	24,787,728	165	$401,273
D9.r	32,429,376	165	$524,858

Table A25: Upstream Raw Material Costs

Material	Annual Mass Needed [kg]	Annual Cost [$]
Glucose	2,684,759	$805,428
Water	33,045,144	$991,354
Media	3254222	$3,953,902

Table A26: Cell Free Reactor Material Costs

Material	Annual Mass Needed [kg]	Annual Cost [$]
Glucose	27,000,000	$8,100,000
Water	6,910,000	$207,300

Table A27: Downstream Raw Material Costs

Material	Annual Mass Needed [kg]	Annual Cost [$]
Water	7,921,675	$237,651
Sulfuric Acid	25,333,487	$2,424,518
Octanol	52,073	$319,874
Trioctylamine	364,913	$284,573

Table A28: Upstream Waste Costs

Stream Name	Annual Mass Disposed [kg]	Annual Cost [$]
U7b	16,870,393	$607,334
Stream Name	**Annual Volume Disposed [L]**	**Annual Cost [$]**
U8b	18,831,043	$29,847

Table A29: Downstream Waste Costs

Stream Name	Annual Volume Disposed [L]	Annual Cost [$]
D5c	10,026,576	$15,892.12
D6c	35,978,544	$57,026.0
D6g	26,008,416	$41,223.3
D7b	7,897,075	$12,517
D12b	67,531,565	$107,038
Stream Name	**Annual Mass Disposed [kg]**	**Annual Cost [$]**
D11c	16,320,528	$816,026

Table A30: Labor and Miscellaneous Operating Expenses

Labor Cost	$14,424,508.16
Operator-Hours/Day/Processing	30
# of Steps	21
Operator-Hours/Year	185220
Hours/Employee	1680
Cost/Operator	$105,313.32
Operator Cost	$11,610,793.53
Cost/Supervisor	$140,346.66
Supervisor Cost	$1,547,321.95
Admin Cost	$1,161,079.35

Miscellaneous	$31,975,331.41
Maintenance & Repairs	$18,504,776.12
Operating Supplies	$2,775,716.42
Lab Costs	$1,442,450.82
Insurance	$3,084,129.35
Local Land Taxes	$6,168,258.71

Table A31: Estimations of salaries from 1989[75] and their adjustments to the present using the 3.174 average wage adjustment from 1989 to 2023

Cost of Operator (1989)	$19.75
Cost of Operator	$62.69
Cost of Supervisor (1989)	$26.32
Cost of Supervisor	$83.54

$$251.7\,\mathrm{kg/drum} = (55\,\mathrm{gal/drum}) \times (3.785\,\mathrm{L/gal}) \times (1.21\,\mathrm{kg/L})$$

Figure A21: Conversion of 55 Gallon drums into Kilograms of Lactic Acid

$$\$253,000,000/\mathrm{year} = (\$2,800/\mathrm{drum}) \times (22,700,000\,\mathrm{kg/year})/(251.7\,\mathrm{kg/drum})$$

Figure A22: Annual Revenue Production Calculations

Table A32: Economic Data for Lifetime of the Plant

Year	Revenue	Operating Cost	Resale	Gross Profit	Depreciation	Taxes	Profit after Taxes	Cumulative Position	Present Value
-2	$0.00	$154,206,467.63	-	-$154,206,467.63	$0.00	$0.00	-$154,206,467.63	-$154,206,467.63	-$179,866,423.84
-1	$0.00	$215,889,054.68	-	-$215,889,054.68	$0.00	$0.00	-$215,889,054.68	-$370,095,522.30	-$399,703,164.08
0	$126,413,692.49	$94,370,535.95	-	$32,043,156.54	$0.00	$8,651,652.27	$23,391,504.27	-$346,704,018.03	-$346,704,018.03
1	$252,827,384.98	$94,370,535.95	-	$158,456,849.03	$46,261,940.29	$30,292,625.36	$128,164,223.67	-$218,539,794.36	-$202,351,661.44
2	$252,827,384.98	$94,370,535.95	-	$158,456,849.03	$46,261,940.29	$30,292,625.36	$128,164,223.67	-$90,375,570.69	-$77,482,485.16
3	$252,827,384.98	$94,370,535.95	-	$158,456,849.03	$46,261,940.29	$30,292,625.36	$128,164,223.67	$37,788,652.98	$29,997,851.08
4	$252,827,384.98	$94,370,535.95	-	$158,456,849.03	$46,261,940.29	$30,292,625.36	$128,164,223.67	$165,952,876.65	$121,980,318.49
5	$252,827,384.98	$94,370,535.95	-	$158,456,849.03	$46,261,940.29	$30,292,625.36	$128,164,223.67	$294,117,100.32	$200,171,156.44
6	$252,827,384.98	$94,370,535.95	-	$158,456,849.03	$46,261,940.29	$30,292,625.36	$128,164,223.67	$422,281,323.99	$266,108,864.38
7	$252,827,384.98	$94,370,535.95	-	$158,456,849.03	$46,261,940.29	$30,292,625.36	$128,164,223.67	$550,445,547.65	$321,179,690.17
8	$252,827,384.98	$94,370,535.95	-	$158,456,849.03	$46,261,940.29	$30,292,625.36	$128,164,223.67	$678,609,771.32	$366,631,744.16
9	$252,827,384.98	$94,370,535.95	-	$158,456,849.03	$0.00	$42,783,349.24	$115,673,499.79	$794,283,271.11	$397,339,385.98
10	$252,827,384.98	$94,370,535.95	-	$158,456,849.03	$0.00	$42,783,349.24	$115,673,499.79	$909,956,770.91	$421,486,050.72
11	$252,827,384.98	$94,370,535.95	-	$158,456,849.03	$0.00	$42,783,349.24	$115,673,499.79	$1,025,630,270.70	$439,875,243.12
12	$252,827,384.98	$94,370,535.95	-	$158,456,849.03	$0.00	$42,783,349.24	$115,673,499.79	$1,141,303,770.49	$453,227,430.06
13	$252,827,384.98	$94,370,535.95	-	$158,456,849.03	$0.00	$42,783,349.24	$115,673,499.79	$1,256,977,270.28	$462,187,933.64
14	$252,827,384.98	$94,370,535.95	-	$158,456,849.03	$0.00	$42,783,349.24	$115,673,499.79	$1,372,650,770.07	$467,334,110.61
15	$252,827,384.98	$94,370,535.95	-	$158,456,849.03	$0.00	$42,783,349.24	$115,673,499.79	$1,488,324,269.86	$469,181,880.37
16	$252,827,384.98	$94,370,535.95	-	$158,456,849.03	$0.00	$42,783,349.24	$115,673,499.79	$1,603,997,769.65	$468,191,658.95
17	$252,827,384.98	$94,370,535.95	-	$158,456,849.03	$0.00	$42,783,349.24	$115,673,499.79	$1,719,671,269.44	$464,773,750.82
18	$252,827,384.98	$94,370,535.95	-	$158,456,849.03	$0.00	$42,783,349.24	$115,673,499.79	$1,835,344,769.23	$459,293,246.59
19	$252,827,384.98	$94,370,535.95	-	$158,456,849.03	$0.00	$42,783,349.24	$115,673,499.79	$1,951,018,269.03	$452,074,470.01
20	$252,827,384.98	$94,370,535.95	$62,299,412.92	$220,756,261.95	$0.00	$76,425,032.21	$144,331,229.73	$2,095,349,498.76	$449,553,478.84